Grand Unification in Heterotic $\mathbb{Z}_2 \times \mathbb{Z}_4$ Orbifold Compactifications

Masterarbeit in Physik
von
Paul-Konstantin Oehlmann

angefertigt im
Physikalischen Institut

vorgelegt der
Mathematisch- Naturwissenschaftlichen Fakultät
der
Rheinischen Friedrich-Wilhelms-Universität
Bonn

im September 2011

Referent: Prof. Dr. Hans Peter Nilles
Korrefent: Priv. Doz. Dr. Stefan Förste

Acknowledgements
First of all, I would like to thank Prof. Dr. Hans Peter Nilles for giving me the opportunity to work on this highly interesting topic. I also would like to thank PD. Dr. Stefan Förste for being my second assessor. Special thanks go to the whole research group for all the support and the great atmosphere. Especially, I would like to thank Michael Blaszczyk and Fabian Rühle for their supervision and all their time to proofread this thesis and to answer so many questions. Special thanks go also to Damián Kaloni Mayorga Peña without whose collaboration this thesis would not have been possible.
Though the greatest thanks go to my girlfriend Katja, my mother Illi and to my family for all their support and love throughout my life.

Contents

Chapter 1

Introduction

One of the strongest concepts in physics is the concept of symmetries. Following that concept allowed to explain seemingly disconnected phenomena in a unified and elegant way. This guideline led to two fundamental pillars of modern physics:

- **General Relativity** describes the weakest observed force, gravity. It is sourced by the curvature of the 4 dimensional space time that has local coordinate invariance as its underlying symmetry principle.

- **Yang-Mills Theory** describes the other three observed forces, the strong and the electro-weak, where the later is broken by the Higgs effect at a scale of 247 GeV [18]. The standard model is described by a $\mathbf{SU(3)}_C \times \mathbf{SU(2)}_L \times \mathbf{U(1)}_Y$ gauge group that is broken down to $\mathbf{SU(3)}_C \times \mathbf{U(1)}_Q$.

Although the Higgs particle is still not observed, the electro-weak unification and the particle *standard model* (SM) is in excellent agreement with experiments. However, it is very desirable to unify the three forces further to an $\mathbf{SU(5)}$ *grand unified theory* (GUT) or even to an SO(10) theory that also unifies all SM particles as well as a right handed neutrino into one group representation [22].
The concept of *super symmetry* (SUSY) could even relate bosonic and fermionic particles. Besides the adjustment of the running of the gauge couplings to meet (almost) exactly at one point arround 10^{16} GeV [19] , which is not the case in non-SUSY GUTs, it has a remarkable feature when promoted to a *local* symmetry: It naturally introduces *super symmetric gravity* (SUGRA) to the particle theory and though it is not renormalizable as a quantum field theory there is hope that SUSY is one key ingredient for a unified theory of all forces [20].
The most promising candidate to unify all forces is *super string theory* , in which particles are described by excitations of a fundamental string [21]. 10 space time dimensions are required by consistency of the theory and can be seen as a prediction of the theory. The phenomenological most promising fact however is, that it is possible to explain all SM constants like coupling constants, Yukawa couplings, the μ term and many more just by

its underlying geometrical properties and one constant: the string length.
There are five distinct string theories in ten dimensions, namely Type I, Type II A and B as well as the Heterotic $SO(32)$ and $E_8 \times E_8$. They are connected by a web of dualities in low dimensions and could be unified to *M-theory*. However, for phenomenology the heterotic theories are particularly interesting.
If we take string theory seriously we have to compactify six spatial dimensions which is best understood on an *orbifold*. In this way chiral matter is introduced and the gauge group is broken [8] [9]. This mechanism also provides a very natural explanation of R-symmetries, that are need to forbid operators that induce fast proton decay, as the residual Lorentz symmetry of the compactified space. Providing seemingly the possibility to address all questions of modern physics, the physical method is turned upside down since the task is know to break a very symmetric and mathematical rich theory, at best by a unique way mechanism, down to our asymmetric observed world.
In recent years many string vacua with properties of the *minimal super symmetric standard model* (MSSM) were found in $\mathbb{Z}_{6-II}$ [5] and $\mathbb{Z}_2 \times \mathbb{Z}_2$ [15] orbifolds. Motivated by this it is natural to assume that one can be similarly successful in the $\mathbb{Z}_2 \times \mathbb{Z}_4$ orbifolds because $\mathbb{Z}_4$ has also a $\mathbb{Z}_2$ subgroup. To suppress the μ term and forbid proton decay operators we have to look for an R-symmetry as well. A convenient one that commutes with GUT groups like SO(10) and SU(5) is the $\mathbb{Z}_4$ R-symmetry [16], [17] and it is reasonable to assume that this can be achieved in an orbifold with the same symmetry factor.

Outline

This thesis is structured as follows: In the second chapter we review the heterotic string and its construction as well as compactifications on orbifolds. In order to put us in a good starting position we provide a complete classification of all $\mathbb{Z}_2 \times \mathbb{Z}_4$ models in chapter three. To achieve this we make use of the internal symmetries of the E_8 root lattice and construct all *144* inequivalent models. Among them we find **35** $SO(10)$, **26** E_6 and **25** $SU(5)$ models. In chapter four we will then introduce the geometry of our orbifold models and look at features of them. At last we have a brief look at spectra of E_6 and $SO(10)$ models and introduce Wilson lines in order to break down to the SM gauge group and three families.

Chapter 2

The heterotic string in orbifold compactification

The idea of heterotic string theory is to combine the 26 dimensional bosonic string and the 10 dimensional super string to a hybrid theory of both[1] that lives in 10 space time dimensions.
The heterotic super string theory looks artificially at first sight, in contrast to Type I and Type II theories since it is constructed from two other string theories. However the heterotic string naturally comes with a big non-Abelian gauge group which makes it very interesting for phenomenology.
The two possibilities for these gauge groups are either SO(32) or $E_8 \times E_8$. Both gauge groups are very large but only the second one can incorporate the E_6 and all other common GUT gauge groups and provides a second E_8 as a hidden sector gauge group. Therefore this thesis will focus on the $E_8 \times E_8$ heterotic string.
To make contact with the observed world one needs to compactify 6 extra dimensions and make them small. To get phenomenologically favoured models that posses $\mathcal{N} = 1$ super symmetry the compact manifold has to be a Calabi-Yau threefold or an orbifold. As the metric on a Calabi-Yau threefold is unknown we stick to orbifold spaces. In recent years it was possible to achieve many MSSM like models out of the orbifolded heterotic string which reinforces the hope that string theory could be a description of our world.
In this chapter the basic concepts we use are reviewed, namely the heterotic string, orbifold compactifications and their consequences for the heterotic string.

2.1 Introduction to string theory

In contrast to a point particle has string theory the striking feature to describe our matter as a two dimensional object. Therefore, the world line of the particle becomes a world sheet that is embedded into the target space. The super string world sheet action is given

[1]There is also a fermionic construction but this thesis will focus on the bosonic one.

by [1]:

$$S = -\frac{1}{2\pi}\int d\sigma d\tau \left(\partial_\alpha X_\mu \partial^\alpha X^\mu + \bar{\psi}^\mu \rho^\alpha \partial_\alpha \psi_\mu\right) . \tag{2.1.1}$$

The world sheet coordinates σ and τ are mapped to the target space via the bosonic coordinates X^μ and the fermionic coordinates ψ^μ. The index $\mu = 0, \ldots, D-1$ runs over the D dimensional target space and $\alpha = 0, 1$ over the 2-world sheet coordinates and ρ^α are the two dimensional gamma matrices

$$\rho^0 = \begin{pmatrix} 0 & -1 \\ 1 & 0 \end{pmatrix} \quad \text{and} \quad \rho^1 = \begin{pmatrix} 0 & 1 \\ 1 & 0 \end{pmatrix} .$$

This action posses global world sheet super symmetry that maps the bosonic coordinates to the fermionic ones and vice versa under the transformations:

$$\begin{aligned} \delta X^\mu &= \bar{\epsilon}\psi^\mu , \\ \delta\psi^\mu &= \rho^\alpha \partial_\alpha X^\mu \epsilon . \end{aligned}$$

Leaving out the fermionic part of the action, gives the purely bosonic string theory. Both theories have a tachyonic ground state but can be removed from the spectrum in the super string case. Hence the bosonic string has not a stable vacuum and is not a consistent theory on its own but in the construction of the heterotic string it is of great importance. Further symmetries of the action are world sheet Weyl- and reparametrization invariance as well as target space Poincaré invariance given by the transformations:

$$\begin{aligned} h_{\alpha\beta} &\to e^{\phi(\sigma,\tau)} h_{\alpha\beta} , \\ \sigma^\alpha &\to f^\alpha(\sigma,\tau) , \\ X^\mu &\to a^\mu{}_\nu X^\nu + b^\mu . \end{aligned}$$

Since string theory is a conformal field theory on the world sheet one can use Weyl and reparametrization invariance to bring the metric into a locally flat form.
This freedom can be exploited to write the action in light cone coordinates $\sigma^\pm = \frac{1}{2}(\tau \pm \sigma)$, turning the worldsheet metric into

$$h_{\pm,\pm} = -\frac{1}{2}\begin{pmatrix} 0 & 1 \\ 1 & 0 \end{pmatrix}$$

and changing the action to

$$S = \frac{1}{\pi}\int d\sigma^+ d\sigma^- \left(2\partial_+ X^\mu \partial_- X_\mu + i\psi_+^\mu \partial_- \psi_{+,\mu} + i\psi_-^\mu \partial_+ \psi_{-,\mu}\right) . \tag{2.1.3}$$

To minimize the action one has to assign boundary conditions to the bosonic and fermionic coordinates and impose the equations of motions for the fields and the world sheet metric. In the further discussions we will only consider closed strings with boundary conditions

$$\begin{aligned} X^\mu(\sigma + \pi) &= X^\mu(\sigma) , \\ \psi_\pm(\sigma + \pi) &= \pm\psi_\pm(\sigma) . \end{aligned}$$

For the fermionic coordinates it is possible to assign positive Ramond (R) and negative Neveu-Schwarz (NS) boundary conditions.
The equations of motions for the fields in light cone gauge are

$$\partial_+\partial_- X^\mu = 0\,, \tag{2.1.4a}$$
$$\partial_+\psi_- = \partial_-\psi_+ = 0\,, \tag{2.1.4b}$$

implying that one can split up the real bosonic coordinates $X^\mu = X_+^\mu(\sigma^+) + X_-^\mu(\sigma^-)$ into left-and right-moving modes with respect to the light cone coordinates[2]. The general solution to the equations of motion can be written as a mode expansion,

$$X_\pm^\mu = \frac{1}{2}x^\mu + \frac{1}{2}p_\pm^\mu(\tau \pm \sigma) + \frac{i}{2}\sum_{n\in\mathbb{Z},n\neq 0}\frac{1}{n}\alpha_{n,\pm}^\mu e^{-2in(\tau\pm\sigma)}\,, \tag{2.1.5}$$

with a center of mass position x^μ, momentum $p^\mu = p_+^\mu = p_-^\mu$ and two distinct sets of oscillators $\alpha_{n,+}^\mu$ and $\alpha_{n,-}^\mu$for left and right-movers respecting the closed string boundary conditions.
The two different boundary conditions for the fermions results in two different mode expansions for each case

$$\psi_\pm^\mu(\sigma,\tau) = \sum_{n\in\mathbb{Z}} d_{n,\pm}^\mu e^{-2in(\tau\pm\sigma)} \qquad \text{R boundary conditions}\,,$$
$$\psi_\pm^\mu(\sigma,\tau) = \sum_{s\in\mathbb{Z}+\frac{1}{2}} b_{s,\pm}^\mu e^{-2is(\tau\pm\sigma)} \qquad \text{NS boundary conditions}\,.$$

Since we fixed the world sheet metric $h_{\pm,\pm}$, one has to demand that its equation of motion is still fulfilled. With

$$\frac{\delta S}{\delta h^{\pm,\pm}} \propto T_{\pm,\pm} = 0\,,$$

one has to impose the condition that the energy momentum tensor $T_{\pm,\pm}$ vanishes.
When one promotes super symmetry from a global to a local symmetry on the world sheet, one has to demand in addition that the super current J vanishes. The Fourier modes of the energy momentum tensor and the super current J are the super conformal generators L_n,$\tilde{L}_n$ and F_s in the R-sector and G_t in the NS-sector respectively.
When we quantise the theory, the coordinates have to fulfill the canonical (anti-)commutation relations and one can derive the following commutation relations for the modes:

$$\left[\alpha_{m,\pm}^\mu, \alpha_{n,\pm}^\nu\right] = m\delta_{m+n,0}\eta^{\mu\nu}\delta_{\pm,\pm}$$
$$\{d_{n,\pm}^\mu, d_{n,\pm}^\nu\} = \delta_{m+n,0}\eta^{\mu\nu}\delta_{\pm,\pm}.$$

[2]Including the reality constraint this implies that the fermions are Majorana-Weyl fermions as one would expect in a 2D theory.

Reality of the coordinates $X(\sigma,\tau)$ together with the Majorana-Weyl fermion $\psi^\mu_\pm(\sigma^\pm)$ imply the conditions

$$(\alpha^\mu_{n,\pm})^\dagger = \alpha^\mu_{-n,\pm}\,, \tag{2.1.8a}$$
$$(d^\mu_{n,\pm})^\dagger = d^\mu_{-n,\pm}\,, \tag{2.1.8b}$$
$$(b^\mu_{n,\pm})^\dagger = b^\mu_{-n,\pm}. \tag{2.1.8c}$$

The modes of the energy momentum tensor satisfy the Virasoro algebra

$$[L_{m,\pm}, L_{n,\pm}] = \left((m-n)L_{n+m} + f(m)\delta_{m+n,0}\right)\delta_{\pm,\pm}\,,$$

with a central extension $f(m)$, hinting at the quantum mechanical breaking of the conformal symmetry which is absent in the classical theory.
Imposing vanishing of the energy momentum tensor $T_{\pm,\pm}$ and the super current J translates into the condition that their positive modes annihilate a physical state:

$$L_{m,\pm}|\phi\rangle = 0 \text{ for } n > 0 \tag{2.1.9a}$$
$$F_s|\phi\rangle = 0 \text{ for } s > 0 \tag{2.1.9b}$$
$$G_t|\phi\rangle = 0 \text{ for } t > 0\,. \tag{2.1.9c}$$

The zero modes are problematic because they have a normal ordering ambiguity. This applies only to $L_{m,\pm}$ since F_s and G_t are fractional modes. Equation (2.1.9a) thus changes to

$$L_{0,\pm} - a_{R/NS}|\phi\rangle = 0\,, \tag{2.1.10}$$

so that the zero modes get a normal ordering constant $a_{R/NS}$ depending on the sector. Another constraint that has to be imposed on a physical state is

$$L_{0,+} - L_{0,-}|\phi\rangle = 0. \tag{2.1.11}$$

This condition is the level matching condition and has to be imposed since $L_{0,+} - L_{0,-}$ generates rigid world sheet translation along the σ direction under which a closed string must be invariant [2]. This condition is the only relation between left and right-moving modes.
The light cone gauge has not yet fixed all residual degrees of freedom of the conformal symmetry, such that many unphysical states appear in the spectrum. These 'spurious' states have zero norm and should decouple from the physical spectrum.
They do for appropriate values of the normal ordering constant $a_{R/NS}$ and the target space dimensionality that appears in the central extension of the Virasoro algebra.
Thus the normal ordering constant $a_{R/NS}$ can be evaluated to

$$a_R = \frac{1}{2} \qquad \text{R boundary condition}\,, \tag{2.1.12a}$$
$$a_{NS} = 0 \qquad \text{NS boundary condition}\,, \tag{2.1.12b}$$
$$a_b = 1 \qquad \text{purley bosonic string}\,. \tag{2.1.12c}$$

These consistency requirements lead to the astonishing result that string theory fixes its target space dimensionality to $d = 26$ for the purely bosonic string and $d = 10$ for the super string.
There is still a residual symmetry left that can be used to fix 2 bosonic and fermionic target space coordinates and their oscillators, such that the appearing oscillators are transverse, hence the name light cone coordinates.
Since the string was decomposed into left and right-moving modes, a physical state is recaptured by tensoring the left-and right-movers back together to form

$$|\phi\rangle = |\phi_+\rangle \otimes |\phi_-\rangle$$

respecting their mass equations given by

$$L_{0,-} - a_{R/NS} \;=\; L_{0,+} - a_{R/NS} \;=\; 0$$

and the level matching condition (2.1.11).[3]
In the bosonic and the super string there are tachyonic ground states. Thanks to the GSO projection [21] the tachyonic states are absent from the super string theory and fixes $\mathcal{N} = (1,0)$ target space super symmetry.

2.2 The heterotic string

The heterotic string is build up from the right-movers of the 10 dimensional super string and the 26 dimensions of the bosonic string. The heterotic string action is given by

$$S = \frac{1}{\pi}\int d^2\sigma \left(2\partial_+ X^\mu \partial_- X_\mu + i\psi_+^\mu \partial_- \psi_{r,\mu} + 2\partial_+ X_-^I \partial_- X_{-,I}\right) . \tag{2.2.1}$$

Hence, $X^\mu = X_+^\mu + X_-^\mu$ are recombined to a space time boson. Consequently, the index μ runs from 2 to 9 since the first two coordinates are fixed in the light cone gauge. What remains are the fermionic right-movers and the residual 16 dimensional bosonic left-movers labelled by the index I that runs from 1 to 16.

2.2.1 The right-mover

The right-mover is taken from the super string from the previous chapter. Its mass is given by the usual zero modes minus the normal ordering constant given by

$$\frac{M_+^2}{8} = N_{R/NS} - a_{R/NS}$$

[3]Space time bosons are made up of R-R and NS-NS and fermions of R-NS and NS-R left- and right-mover combinations.

with the oscillator number operators

$$N_R = \sum_{n=1}^{\infty} \alpha^{\mu}_{-n}\alpha_{n,\mu} + d^{\mu}_{-n}d_{n,\mu}\,,$$
$$N_{NS} = \sum_{n=1}^{\infty} \alpha^{\mu}_{-n}\alpha_{n,\mu} + b^{\mu}_{-n+1/2}b_{n-1/2,\mu}\,.$$

for the Ramond and Neveu-Schwarz sector respectively. The mass scale of the heterotic string is in the 10^{17}GeV regime [1], so we consider only massless strings. A ground state is defined as a state that is annihilated by all positive oscillators such that higher excitations are created by negative modes.
The massless state in the Ramond sector is its ground state. The ground state is also an eigenstate of the d_0^{μ} operator since this operator commutes with N_R. d_0^{μ} also fulfills the Clifford algebra

$$\{\sqrt{2}d_0^{\mu}, \sqrt{2}d_0^{\nu}\} = 2\eta^{\mu\nu} \tag{2.2.3}$$

up to a rescaling factor. Since two coordinates of d_0^{ν} are fixed in the light cone gauge, the ground state transforms under the little group SO(8). Additionally d_0^{ν} is also real, seen by equation eq:oszidagger, such that the ground state is a massless 10 dimensional Majorana-Weyl fermion.
The ground state of the Neveu-Schwarz sector is a tachyon with $\frac{M_+^2}{8} = -\frac{1}{2}$. Since there is no left-mover with the same mass, the level matching condition ensures that this state is removed from the spectrum. Thus the massless ground state is given by

$$b^{\mu}_{-1/2}|0\rangle. \tag{2.2.4}$$

This states transforms as a massless space time vector boson under SO(8).
One can shorten the notation by rewriting the mass equation for the two sectors as

$$\frac{M_+^2}{8} = \frac{q^2}{2} + N - \frac{1}{2} \tag{2.2.5}$$

with q being a weight vector of SO(8). The Ramond sector is encoded via the spinorial roots

$$q_s = \left(\pm\frac{1}{2}, \pm\frac{1}{2}, \pm\frac{1}{2}, \pm\frac{1}{2}\right) \tag{2.2.6}$$

with a positive number of minus signs yielding the spinor representation $\mathbf{8}_s$ of SO(8). The Neveu-Schwarz sector is given by the vectorial roots

$$q_v = \underline{(\pm 1, 0, 0, 0)}\,, \tag{2.2.7}$$

with the underline meaning all possible permutations of the entries yielding the $\mathbf{8}_v$ representation of SO(8).

2.2.2 The left-mover

The left-mover is given by the 26 dimensional bosonic string from the previous chapter. The first 10 coordinates are combined with the bosonic right-movers but there are 16 left-movers in the action given in equation (2.2.1). The concept that is used to get rid of them is also used in the next chapter: compactification.
The 16 dimensions are compactified by modding a 16 dimensional lattice out of $\mathbb{R}^{16}$

$$M_{16} \xrightarrow{\text{Compactification}} \frac{\mathbb{R}^{16}}{\Lambda_{16}} = T^{16} \,.$$

This is just the generalization of Kaluza and Klein's idea of compactification of a fifth dimension on a circle which is now a sixteen torus T^{16}.
An identification of space points means that the string can now close up to a lattice shift $X^I = X^I + \Lambda_{16}$. Due to the single-valuedness of the wave function that comes with a factor of e^{iPX} it is clear that the momentum in the compactified direction has to be quantized in the dual lattice Λ^*.
In fact modular invariance of the one-loop partition function requires the lattice to be unimodular, integral, even and self dual [2]. These are quiet many strong requirements on the lattice but luckily there are two lattices that fulfill these: The $SO(32)$ and the $E_8 \times E_8$ root lattice. Each of these lattices provides gauge degrees of freedom and builds up an own unique heterotic string theory. Getting non-Abelian gauge theories from compactification is thus a purely 'stringy' result and not possible for point-like particles as in the usual Kaluza-Klein theory. In the low energy effective super gravity limit, the modular invariance of the string partition function translates into absemce of anomalies such that string theory can naturally explain why only $E_8 \times E_8$ and SO(32) appear as anomaly free gauge groups! However we will concentrate on the $E_8 \times E_8$ heterotic string in this thesis.
The mass equation for the left-mover follows from equation (2.1.10)

$$\frac{M_-^2}{8} = \frac{P^2}{2} + N - 1 \,, \tag{2.2.8}$$

with the excitation number operator

$$N = \sum_{n=1}^{\infty} \alpha^{\mu}_{-n,-} \alpha^{\nu} - n, -\eta_{\mu,\nu} + \alpha^{I}_{-n,-} \alpha^{J}_{-n,-} \delta_{I,J} \,.$$

The ground state of the left-mover is again a tachyon and absent since its mass square is $M_-^2 = -8$ and the tachyon of the right-mover has mass square $M_+^2 = -4$ such that their masses do not match and the level matching condition ensures that this state is absent. The first excited modes that are also massless are given by

$$\begin{aligned} &|P\rangle \,, \\ \alpha^{I}_{-1,-}&|0\rangle \,, \\ \alpha^{\mu}_{-1,-}&|0\rangle \,. \end{aligned}$$

where the first two transform as a space time scalar and the last one as an SO(8) space time vector boson.

2.3 The massless spectrum of the heterotic string

The massless left and right-moving states are tensored together to give the $\mathcal{N} = 1$ super gravity multiplet

$$|q_v\rangle \otimes \alpha_{-1,\mu}|0\rangle \begin{cases} g_{\mu\nu} & \text{graviton} \\ B_{\mu\nu} & \text{two form field} \\ \phi & \text{dilaton} \end{cases} , \; |q_s\rangle \otimes \alpha_{-1,\mu}|0\rangle \begin{cases} \Psi_\mu & \text{gravitino} \\ & \\ \psi & \text{dilatino} \end{cases}$$

and the super Yang-Mills multiplet

$$\left.\begin{array}{l} |q_v\rangle \otimes \alpha^I_{-1}|0\rangle \\ |q_v\rangle \otimes |P\rangle \end{array}\right\} A_\mu \quad \text{gauge bosons} \qquad , \qquad \left.\begin{array}{l} |q_s\rangle \otimes \alpha^I_{-1}|0\rangle \\ |q_s\rangle \otimes |P\rangle \end{array}\right\} \lambda \quad \text{gauginos}$$

The internal $2{\cdot}8$ oscillators form the Cartan elements of the gauge group. The quantized internal momenta P form the $2 \cdot 240$ roots of the two E_8s (see Appendix A). Together they form the 496 states of the adjoint representation of $E_8 \times E_8$.

2.4 Orbifold compactifications

The fact that string theory fixes the space time dimensionality is very extraordinary but with $d = 10$ the dimensionality does not match our observed 4 space time dimensions. To solve this problem one does the same as in the case of the 16 residual dimensions of the bosonic left-movers: Compactification on a six torus T^6 assuming that its volume is sufficiently small to lead to our observed Newtonian gravity law[4].

$$M_{9,1} \xrightarrow{\text{Compactification}} M_{3,1} \otimes \frac{\mathbb{R}^6}{\Lambda_6} = M_4 \otimes T^6. \tag{2.4.1}$$

This simple compactification has certain problems when one looks at the splitting of the representations of $SO(8)$ into $SO(2) \times SO(6)$. From the splitting of the Dynkin Diagram in figure 2.1. $SO(2)$ is isomorph to U(1) which is the helicity of the particles in the 4 dimensional non compact space. Consequently the spinorial and vectorial weights of

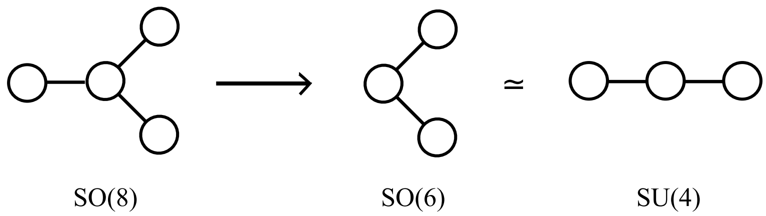

Figure 2.1: The group theoretical breaking of $SO(8)$ to $SO(6)$ which is equivalent to $SU(4)$

[4]The compactified dimensions has to be in the sub millimeter regime to meet the experimental values.

SO(8) of equation (2.2.6) and equation (2.2.7) decompose as

$$8_s = \left(\pm\frac{1}{2}, \pm\frac{1}{2}, \pm\frac{1}{2}, \pm\frac{1}{2}\right) \;\rightarrow\; \pm\left(+\frac{1}{2}, \underline{\pm(\frac{1}{2}, \frac{1}{2}), \frac{1}{2}}\right),$$
$$8_v = \underline{(\pm 1, 0, 0, 0)} \;\rightarrow\; (\pm 1, 0, 0, 0) \;+\; (0, \underline{\pm 1, 0, 0}).$$

The 4d gravitino is identified as the sum of the decomposed weight that has a helicity of 3/2 ,

$$\pm\left(\frac{3}{2}, \underline{\pm(\frac{1}{2}, \frac{1}{2}), \frac{1}{2}}\right),$$

which has from the 4d point of view a degeneracy of 4 since this is a 4 and a $\bar{4}$ of the internal SU(4).
So instead of 1 super partner for the graviton there are 4 gravitini and instead of $\mathcal{N} = 1$ there is $\mathcal{N} = 4$ SUSY. Four super symmetries have a lot of nice theoretical but not phenomenological properties like vanishing of the β-function[5] and non chirality. A phenomenologically more appealing super symmetry is $\mathcal{N} = 1$ since it is the only super symmetry in 4 dimensions that provides a chiral spectrum [23].
The reason why one gets the 4 super symmetries is that the internal SO(6) symmetry of the T^6 is the one of a flat space in particular the torus has trivial holonomy. To achieve $\mathcal{N} = 1$ one has to demand an SU(3) holonomy since then not all 4 spinors are covariantly constant but only one. Manifolds with such a holonomy group are called Calaby-Yau manifolds and were excessively studied in the literature [24]. However these spaces are still very complicated since in most cases the metric is not known and string theory is very hard to handle on non flat spaces. The other possibility to compactify the space are orbifolds that are flat everywhere with exception of some finite points and posses a discrete subgroup of SU(3) holonomy.

2.4.1 Definition of an orbifold and its properties

Orbifolding means to mod out a discrete finite symmetry of a given manifold. This can be an Abelian or a non-Abelian symmetry like $\mathbb{Z}_N$ or S_N. Here we will deal with Abelian symmetries only and focus later especially on $\mathbb{Z}_2 \times \mathbb{Z}_4$. Thus an $\mathbb{Z}_N$ or $\mathbb{Z}_N \times \mathbb{Z}_M$ symmetry of the six dimensional compact space is further modded out. Concrete this means to mod out a point group $P_{\mathbb{Z}_N \times \mathbb{Z}_M}$ of the compactification lattice of the torus.

$$\mathrm{T}^6 \xrightarrow{\text{Orbifolding}} \frac{\mathrm{T}^6}{\mathbb{Z}_N \times \mathbb{Z}_M} = \frac{\mathbb{R}^6}{P_{\mathbb{Z}_N \times \mathbb{Z}_M} \ltimes \Lambda_6} = \frac{\mathbb{R}^6}{\mathbb{S}_6} \tag{2.4.2}$$

The group action of the lattice identification and the Abelian point group can be naturally combined in a semi-direct product $\ltimes$ to the space group $\mathbb{S}_6 = P_{\mathbb{Z}_N \times \mathbb{Z}_M} \ltimes \Lambda_6$, a discritised

[5] Vanishing of the regularization group functions implies that this is a conformal field theory again.

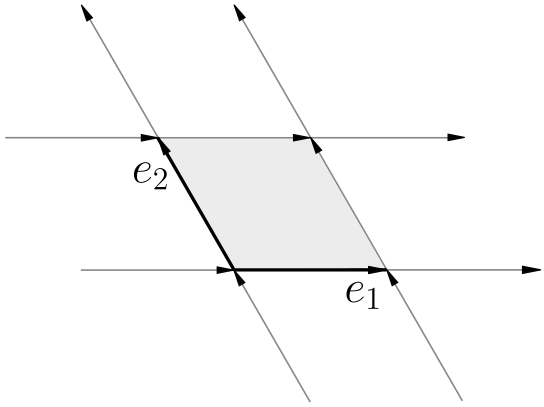

Figure 2.2: The geometry of a T^2 torus on an SU(3) Lie lattice. Due to the identification of points that differ by lattice vectors, the fundamental domain lies within they gray region.

version of the Euclidean group.
However there is only a finite amount of different six dimensional base lattices that allow for modding out a point group. It was shown that for six dimensional lattices with $\mathbb{Z}_N$ point groups, N has to be 3,4,6,7,8 or 12 [25].
For $\mathbb{Z}_N \times \mathbb{Z}_M$ point groups with N=2,3,4,6 and M being an integer multiple of N smaller than 8 are allowed (except for $\mathbb{Z}_2 \times \mathbb{Z}_3$). The basis of the torus lattices is expressed via the simple roots of some Lie algebra.
For example a two dimensional torus with SU(3) Lie lattice has the simple roots

$$\begin{aligned} e_1 &= \left(\sqrt{2}, 0\right) , \\ e_2 &= \left(-\frac{1}{\sqrt{2}}, \frac{\sqrt{3}}{\sqrt{2}}\right) \end{aligned}$$

and is graphically depicted in figure 2.2. This lattice has clearly a $\mathbb{Z}_3$ rotation symmetry about 120^o. Turning to T^6 one has to distinguish the choice of the lattice structures underlying the T^6 between a factorisable and a non-factorisable lattice.
If a lattice is factorisable, it is possible to continuously deform it such that T^6 factorises into $T^2\times$ $T^2\times$ T^2 while still preserving its point group. If this is not possible then it is a non-factorisable lattice. From this it follows that a T^6 is only factorisable if the geometry is a direct product of Lie lattices with rank 2 at most. For $\mathbb{Z}_2 \times \mathbb{Z}_4$ and all possible $\mathbb{Z}_N$ point groups the lattices are given in table 2.1 taken from [32] [11]. For simplicity we want T^6 to be factorisable so we have to choose the right Lie lattice for $\mathbb{Z}_2 \times \mathbb{Z}_4$ when we introduce the geometry in the fourth chapter.
As already mentioned in the $\mathbb{Z}_3$ example, the orbifold action is embedded as a discrete rotation, so it is generated by the three Cartan elements of SU(4). If we complexify the internal coordinates $X^i \in \mathbb{R}^6$ to

$$Z^i = X^{2i-1} + iX^{2i}$$

the orbifold action can be written as a diagonal complex 3×3 matrix

$$\theta = \mathrm{diag}(e^{2\pi v_N^1}, e^{2\pi v_N^2}, e^{2\pi v_N^3}) \tag{2.4.3}$$

Point Group Order	Lie Lattice	factorisable
$\mathbb{Z}_3$	$\mathrm{SU}(3)^3$	Yes
$\mathbb{Z}_4$	$SU(4)^2$	No
	$SO(5) \times SU(4) \times SU(2)$	No
	$SO(5)^2 \times SU(2)^2$	Yes
$\mathbb{Z}_{6-I}$	$G_2^2 \times SU(2)^2$	Yes
$\mathbb{Z}_{6-II}$	$G_2 \times SU(3) \times SU(2)^2$	Yes
	$SU(6) \times SU(2)$	No
	$SU(3) \times SO(8)$	No
	$SU(3) \times SO(7) \times SU(2)$	No
$\mathbb{Z}_7$	$SU(7)$	No
$\mathbb{Z}_{8-I}$	$SO(9) \times SO(5)$	No
$\mathbb{Z}_{8-II}$	$S0(10) \times SU(2)$	No
	$SO(9) \times SU(2)^2$	No
$\mathbb{Z}_{12-I}$	E_6	No
	$\mathrm{F}_4 \times SU(3)$	No
$\mathbb{Z}_{12-II}$	$\mathrm{F}_4 \times SU(2)^2$	No
$\mathbb{Z}_2 \times \mathbb{Z}_4$	$\mathrm{SU}(2)^2 \times \mathrm{SO}(4)^2$	Yes
	$\mathrm{SO}(6)^2$	No
	$\mathrm{SO}(6) \times \mathrm{SO}(4) \times \mathrm{SU}(2)$	No
	$\mathrm{SO}(8) \times \mathrm{SO}(4)$	No
	$\mathrm{SO}(10) \times \mathrm{SU}(2)$	No
	$\mathrm{SO}(12)$	No

Table 2.1: All possible Z_N orbifolds and their possible T^6 Lie lattice structures. The last column specifies whether the lattices are factorisable upon an appropriate choice of torus coordinates.

acting on the 3 complex coordinates with the shift vector

$$v_N = \left(0, v_N^1, v_N^2, v_N^3\right) .$$

This vector will completely specify the action of the orbifold on the internal lattice. The zeroth component has been chosen to clarify that the orbifold does not act on the non compact direction and to define a proper scalar product between v_N and the SO(8) weights q which will be needed in the next chapter. For θ to be of order N, it follows for v_N that

$$\theta^N = \mathbb{1} \quad \Rightarrow \quad N v_N^i \in \mathbb{Z} \quad \forall i \tag{2.4.4}$$

and for θ to be an element of SU(3) it follows that

$$\mathrm{Det}(\theta) = 1 \quad \Rightarrow \quad v_N^1 + v_N^2 + v_N^3 \in \mathbb{Z}. \tag{2.4.5}$$

If the second condition is chosen to be exactly zero, there are only two independent shift vector components. The rotations are then generated by only two independent Cartan elements making it an element of SU(3) which is just the Calabi-Yau condition for $\mathcal{N} = 1$ super symmetry. This will become clearer in the next chapter when we describt how the shifts act on the gravitino weights. For every component of v_N that is chosen to be zero, the amount of super symmetry is increased by a factor of 2 again.
Since there are two Cartan generators at our disposal it is also possible to add a second independent rotational matrix ω generated by a second shift vector w

$$\omega = \mathrm{diag}(e^{2\pi v_M^1}, e^{2\pi v_M^2}, e^{2\pi v_M^3}) \tag{2.4.6}$$

of order M. This is just the enlargement to a $\mathbb{Z}_N \times \mathbb{Z}_M$ orbifold. Since there are only two Cartan elements of SU(3) it is not possible to enlarge this further to three point groups. Also v_M has to satisfy

$$M v_M^i = \mathbb{Z} \quad \forall i\,, \tag{2.4.7a}$$
$$v_M^1 + v_M^2 + v_M^3 = \mathbb{Z}. \tag{2.4.7b}$$

In that way it is possible to let θ and ω act trivial in one of the three tori as long as it is not the same. A convenient choice for the two shifts is thus

$$v_N = \frac{1}{N}(0, 1, -1, 0)\,,$$
$$v_M = \frac{1}{M}(0, 0, 1, -1).$$

A $\mathbb{Z}_N \times \mathbb{Z}_M$ orbifold twist is then given by

$$\theta^l \cdot \omega^k = \mathrm{diag}(e^{2\pi(lv^1+kw^1)}, e^{2\pi(lv^2+kw^2)}, e^{2\pi(lv^3+kw^3)})\,,$$

with $l, k \in \mathbb{N}_0$ and $l < N, k < M$.
Since we discuss $\mathbb{Z}_2 \times \mathbb{Z}_4$ later, our choice of the shift vectors is

$$v_2 = \frac{1}{2}(0, 1, -1, 0)\,, \tag{2.4.8}$$
$$v_4 = \frac{1}{4}(0, 0, 1, -1). \tag{2.4.9}$$

2.4.2 Twisted sectors and fixed points

A very important property of orbifolds is the appearance of fixed points or planes:
These are points or planes which are identified with respect to lattice shifts and rotations. In figure 2.3 it becomes clear that there are fixed points that stay invariant under the orbifold action. Therefore, the orbifold does not act freely on the lattice. Depending how often the rotation acts on the tori, there are N or $N \times M$ twisted sectors (including the trivial sector). But not all of these sectors are inequivalent since the k^{th} sector is the inverse

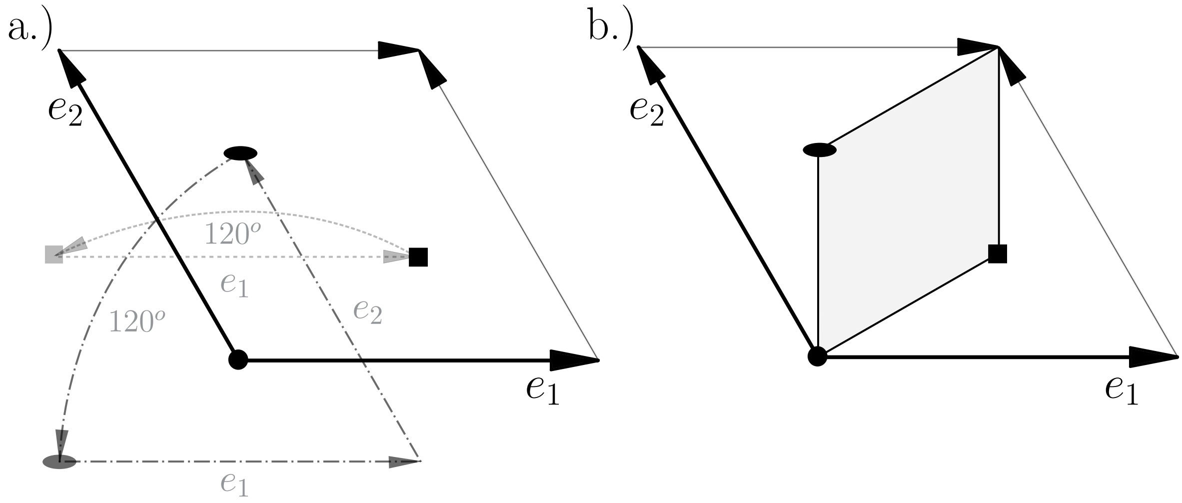

Figure 2.3: The three fixed points of one T^2 torus in a $\mathbb{Z}_3$ orbifold. Picture a.) shows the fixed points. The zero point is a trivial fixed point. The other two have to be shifted with lattice vectors after the rotation to return to their old position. Picture b.) shows the new fundamental domain which is 1/3 of the original one.

of the $(N-k)^{\text{th}}$ and therefore it also has the same fixed point structure. It turns out that strings are attached to the fixed points and that representations are only completed by their CPT conjugates that are provided by the strings living in the inverse twisted sectors. This is why the $\mathbb{Z}_3$ example is exceptionally simple since there is only one independent twisted sector.

Every fixed point $z_f \in \mathbb{C}^3$ is related to an element of the space group[6] $g(\theta^k \cdot \omega^l, n_\alpha e_\alpha) \in \mathbb{S}$

$$\begin{aligned} z_f &= g(\theta^k \cdot \omega^l, n_\alpha e_\alpha) z_f \\ &= (\theta^k \cdot \omega^l) z_f + n_\alpha e_\alpha \\ \Leftrightarrow z_f &= (\mathbb{1} - \theta^k \cdot \omega^l)^{-1} n_\alpha e_\alpha \end{aligned} \tag{2.4.10}$$

so that we talk about constructing elements g instead of the fixed points themselves.

Two space group elements are multiplied via

$$g(\theta, e_\alpha)\tilde{g}(\omega, e_\beta) = \hat{g}(\theta \cdot \omega, e_\alpha + \theta e_\beta)\,. \tag{2.4.11}$$

Therefore the inverse of an element is given as

$$(g(\theta, e_1))^{-1} = g(\theta^{-1}, -\theta^{-1} e_1)\,, \tag{2.4.12}$$

so that we get the formula for conjugation

$$(h(\omega, e_2))^{-1}\, g(\theta, e_1) h(\omega, e_2) = \tilde{g}\left(\theta, \omega^{-1}\left[e_1 + (\theta - \mathbb{1}) e_2\right]\right)\,, \tag{2.4.13a}$$

which will be usefully later.

The appearance of fixed points is an essential property of orbifolds. They also imply that there is a non vanishing curvature on the manifold. This is depicted in figure 2.4. Here we

[6]For the $\mathbb{Z}_N$ case put $l = 0$.

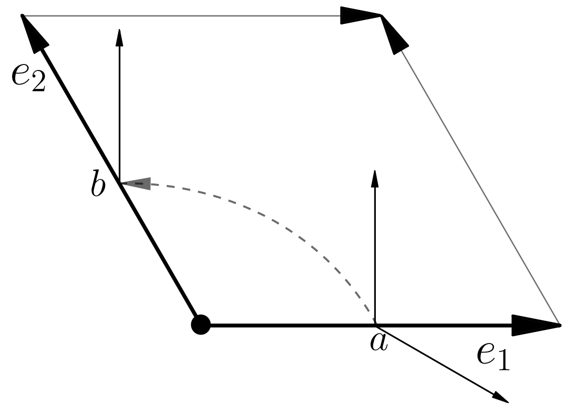

Figure 2.4: Example of a parallel transport of a vector around a closed path under the orbifold action encircling the fixed point at the origin. This signals the non trivial curvature of the orbifold that is concentrated at the fixed point.

start with an arbitrary vector starting on point a. Since the space is coming from the flat torus, one can parallel transport the vector with the flat metric to position b.The vector is then taken back to the original position a but with a 120° twist due to the orbifold identification. From the orbifold point of view this was a closed path encircling the fixed point at the origin. In that way it was possible to rotate the vector under a closed path so that there is a non trivial curvature on the space.
This states that the manifold is flat everywhere except for the fixed points. Fixed points thus concentrate, such that they are curvature singularities. So an orbifold is not a regular manifold.
A quantum field theory that describes point like particles would not be well defined on an orbifold, though strings are extended objects and they can enclose the singularities, so that the theory is still well defined. Due to the fact that the space is basically flat, the heterotic string theory stays solvable on that space.
On the other hand there is the problem of moduli stabilisation that is not addressed in this work: The moduli describe e.g. geometric properties of the internal six dimensional space like the volume. These properties can vary freely and look like scalar fields from the four dimensional perspective. To solve string theory the internal geometry must be fixed by giving vevs to them. This in turn will blow up the singularities and changes the orbifold geometry to a smooth Calabi-Yau manifold [26] [27].

2.5 Strings on orbifolds

The orbifold geometry allows that an internal string coordinate $Z \in \mathbb{C}^3$ can now close under a space group element $g \in \mathbb{S}$

$$Z^i(\tau, \sigma + \pi) = gZ(\tau, \sigma). \tag{2.5.1}$$

If g involves a trivial twist, e.g. $g(\mathbb{1}, n_\alpha e_\alpha)$ then the string lives in the untwisted sector and is free to move there and can move on the whole orbifold. Matter in this sector is called bulk matter. To satisfy equation (2.5.1) for an arbitrary $g(\theta^k, n_\alpha e_\alpha)$, the mode expansion of the internal coordinates has to satisfy

$$\begin{aligned} Z^i(\tau, \sigma+\pi) &= \quad z^i \quad + \quad p^i\tau \quad + \text{oscillators} \\ &= (\theta^k z)^i + n_\alpha e^i_\alpha + (\theta^k p)^i \tau \quad + \text{oscillators}^* . \end{aligned}$$

From comparing the two equations it becomes clear that the center of mass position z^i has to be a fixed point/plane and that either the twist or the momentum p^i has to be trivial in the given torus. Thus the twisted string is attached to a fixed point/plane and cannot move away from it.
Also the oscillators α^i_m change to $\alpha^i_{m+\eta^i}$ with $kv^i = 0$ mod 1 such that[7] $0 < \eta^i < 1$. Note that also the oscillators have been complexified and were split up into holomorphic $\alpha^i_{m+\eta^i}$ and anti-holomorphic ones $\alpha^{\bar{i}}_{m+\bar{\eta}^i}$ with $\bar{\eta}^i = 1 - \eta^i$. Due to this the right-moving momenta q and their mass equation is shifted for a non trivial constructing element $g(\theta^k, n_\alpha e_\alpha)$ to

$$q_{\text{sh}} = q + kv \tag{2.5.3}$$

$$\frac{M_-^2}{8} = \frac{q_{\text{sh}}^2}{2} - \frac{1}{2} + \delta_c \, . \tag{2.5.4}$$

With $\delta_c = \frac{1}{2}\sum i = 1^3 \eta^i(\bar{\eta}^i)$ is the change in the ground energy of the k^{th} twisted sector.

2.5.1 Modular invariance and shift embedding

To preserve modular invariance it is also necessary to embed the orbifold space group $\mathbb{S}$ into the gauge degrees of freedom $\mathbb{S} \hookrightarrow \mathbb{G}$ with the gauge twisting group $\mathbb{G}$. The gauge twisting group $\mathbb{G}$ is embedded as an inner automorphism of the $E_8 \times E_8$ lattice. Since an automorphism acts freely there are no fixed points in the gauge part and the embedding can be realized as a shift acting on the $E_8 \times E_8$ lattice. An element of $\mathbb{S}$ is associated to an element of $\mathbb{G}$ as

$$g(\theta^k \cdot \omega^l, n_\alpha e_\alpha) \hookrightarrow (kV_N + lV_M, n_\alpha A_\alpha)$$

that acts on the 16 internal left-moving coordinates as a shift

$$X^I(\sigma^+\pi) = gX^I(\sigma^+) = X^I(\sigma^+) + kV^I_N + lV^I_M + n_\alpha A^I_\alpha.$$

Twists with $g(\theta^k \cdot \omega^l, 0)$ therefore induce the shifts $kV_N + lV_M$ and lattice translations $g(\mathbb{1}, n_\alpha e_\alpha)$ are accompanied by the shifts $n_\alpha A_\alpha$.
The associated lattice translations A_α are called discrete **Wilson lines** [10] since they are inherited from non contractible cycles on the underlying torus which can support non vanishing gauge background.

[7] The same line of argumentation is also true for the fermionic coordinates changing their oscillators as well.

The embedding must be a homomorphism such that the properties of the space group transfer to the gauge embedding. Hence

$$
\begin{aligned}
g(\theta,0)^N &= g(\mathbb{1},0) && \hookrightarrow \quad NV_N \in \Lambda_{E_8\times E_8}\,, && \text{(2.5.5a)}\\
g(\theta,0)^M &= g(\mathbb{1},0) && \hookrightarrow \quad MV_M \in \Lambda_{E_8\times E_8}\,, && \text{(2.5.5b)}\\
g(\theta,0)\cdot(\mathbb{1},e_\beta) &= g(\theta,e_\alpha) && \hookrightarrow \quad A_\alpha = A_\beta\,, && \text{(2.5.5c)}\\
g(\theta,e_\alpha)^{K_\alpha} &= g\left(\theta^{K_\alpha},\sum_{i=0}^{K_\alpha}\theta^i e_\alpha\right) = g(\theta^{K_\alpha},0) && \hookrightarrow \quad K_\alpha A_\alpha \in \Lambda_{E_8\times E_8}\,. && \text{(2.5.5d)}
\end{aligned}
$$

The first two equations constrain the order of the shift embeddings. The last two fix the maximal amount of independent Wilson lines one can assign as well as their order. The amount of Wilson lines is thus maximally six in $\mathbb{Z}_2\times\mathbb{Z}_2$ and minimally zero in $\mathbb{Z}_6\times\mathbb{Z}_6$. Additionally modular invariance of the partition function requires the conditions [3]

$$
\begin{aligned}
N(V_N^2 - v^2) &= 0 \bmod 2\,, && \text{(2.5.6a)}\\
M(V_M^2 - w^2) &= 0 \bmod 2\,, && \text{(2.5.6b)}\\
M(V_N V_M - v\cdot w) &= 0 \bmod 2\,, && \text{(2.5.6c)}\\
T_\alpha(A_\alpha\cdot V_{N/M}) &= 0 \bmod 2\,, && \text{(2.5.6d)}\\
T_\alpha A_\alpha^2 &= 0 \bmod 2\,, && \text{(2.5.6e)}\\
\gcd(T_\alpha,T_\beta)(A_\alpha\cdot A_\beta) &= 0 \bmod 2 \text{ for } \alpha\neq\beta\,. && \text{(2.5.6f)}
\end{aligned}
$$

For the classification of inequivalent shift embeddings in chapter 3 only the first three conditions are important. Note that one can relax condition three, four and six by adding lattice vectors to the shifts and Wilson lines.

2.5.2 The left-mover

The embedding of the shifts into the gauge degrees of freedom also changes the left-moving momenta P and its mass equation for a given fixed point, similar to the change of right-movers that were shifted by v, to

$$
\begin{aligned}
P_{\text{sh}} &= P + kV_N + lV_M + n_\alpha A_\alpha\,,\\
\frac{M_-^2}{8} &= \frac{P_{\text{sh}}^2}{2} + \tilde{N} - 1 + \delta_c\,.
\end{aligned}
$$

The oscillator number $\tilde{N}$ is fractional and the vacuum energy δ_c is the same as in the right-moving case.

2.5.3 Forming orbifold invariant states

The last chapter emphasized that the mass equations of left and right-movers depend on the fixed point and the twisted sector. Therefore the Hilbert space splits up into Hilbert spaces of fixed points $\mathcal{H}_g$ with states that fulfill the boundary condition

$$Z(\tau, \sigma + \pi) = gZ(\tau, \sigma). \tag{2.5.7}$$

Multiplying by another arbitrary element h yields

$$\begin{aligned}(hZ)(\tau, \sigma + \pi) =& hgZ(\tau, \sigma)\\ =& hgh^{-1}(hZ)(\tau, \sigma).\end{aligned}$$

If $[g, h] = 0$ then Z and hZ close under the same constructing element g and therefore belong to the same Hilbert space $\mathcal{H}_g$. Each constructing element has a centraliser

$$\mathcal{Z}_g = \{h \,|\, [g, h] = 0\} \ , \tag{2.5.8}$$

which is the set of elements h that map the Hilbert space $\mathcal{H}_g$ to itself.
However, an element h induces a phase when applied on a string state,

$$|q_{sh,g}\rangle \otimes \tilde{\alpha}|p_{sh,g}\rangle \xrightarrow{h} \phi|q_{sh,g}\rangle \otimes \tilde{\alpha}|p_{sh,g}\rangle \stackrel{!}{=} |q_{sh,g}\rangle \otimes \tilde{\alpha}|p_{sh,g}\rangle. \tag{2.5.9}$$

The factor ϕ is the orbifold phase which has to be trivial such that a state can appear in the spectrum. Together with the mass equation that is given by the constructing element, a string state has to respect all projection conditions that are induced by the elements of its centraliser.

2.5.4 The orbifold phase

The orbifold phase results from the non trivial behavior of the left and right-movers under space group elements $h(\theta^m \cdot \omega^n, n_\alpha e_\alpha) \in \mathbb{S}$ of the centraliser.
Since a right-mover $|q_{\mathrm{sh}}\rangle$ corresponds to a vertex operator $e^{-2iq_{\mathrm{sh}}H}$ with the bosonised H-momentum H^i [30] and transforms as

$$\begin{aligned}H^i \xrightarrow{h}& H^i + \pi(mv^i + nw^i) = H^i + \pi v_h^i \,,\\ |q_{\mathrm{sh}}\rangle \xrightarrow{h}& e^{-2iq_{\mathrm{sh}}\cdot v_h}\,|q_{\mathrm{sh}}\rangle.\end{aligned}$$

A left-mover $|P_{\mathrm{sh}}\rangle$ corresponds similarly to a vertex operator $e^{2\pi i P_{\mathrm{sh}}\cdot X}$ and transforms as

$$\begin{aligned}X \xrightarrow{h}& X + mV_N + nV_M + n_\alpha A_\alpha = X + V_h \,,\\ |P_{\mathrm{sh}}\rangle \xrightarrow{h}& e^{2iP_{\mathrm{sh}}\cdot V_h}\,|P_{\mathrm{sh}}\rangle.\end{aligned}$$

The holomorphic and anti holomorphic oscillators $\alpha^i_{n-\eta^i}$ and $\alpha^{\bar{i}}_{n+\eta^i}$ exhibit the transformation behavior [28]

$$\begin{aligned}\alpha^i_{n-\eta^i} \xrightarrow{h}& e^{2\pi i v^i}\alpha^i_{n-\eta^i} \,,\\ \alpha^{\bar{i}}_{n+\eta^i} \xrightarrow{h}& e^{-2\pi i v^i}\alpha^i_{n-\eta^i} \,.\end{aligned}$$

Putting all these terms together yields the phase ϕ

$$
\begin{aligned}
\phi &= e^{2\pi i\left(P_{\mathrm{sh}}V_h-(q_{\mathrm{sh}}-N+\bar{N})\cdot v_h\right)}\phi_{\mathrm{vac}} \, , \\
&= e^{2\pi i\left(P_{\mathrm{sh}}\cdot V_h-(q_{\mathrm{sh}}-N+\bar{N})\cdot v_h\right)}e^{-\pi i(V_g\cdot V_h-v_g\cdot v_h)} \, ,
\end{aligned}
\tag{2.5.10}
$$

where the contribution of the vacuum phase ϕ_{vac} is explained in the appendix A of [3] and N^i and $\bar{N}^i$ are the holomorphic and anti-holomorphic oscillator numbers.
A physical string state has to have a trivial orbifold phase for all elements h of the centraliser of its constructing element.

2.5.5 Summary and untwisted spectrum

Now all steps to build up an orbifold model and calculate its spectrum are in principal known. The model itself is completely specified by

1. the choice of the lattice,
2. the choice of the shifts v_N & v_M,
3. the shift embeddings V_N & V_M,
4. the choice of the Wilson lines A_α.

Getting the particle spectrum is then straight forward although it involves a big amount of calculations. This amount increases by the increased number of Wilson switched on. Without any Wilson line the matter spectrum of all fixed points of a given sector coincides. After switching on Wilson lines the degeneracy breaks into classes of fixed points that are accompanied by the same Wilson line and with the same matter content. Also the gauge group for every fixed point can vary, hence the notion of local GUTs, which means that the certain fixed points can have a gauge enhancement to a GUT group like SO(10) and matter representations are complete under them.
The gauge group of the untwisted sector is the 4 dimensional one and it is also a subgroup of all local gauge groups. Also the super gravity multiplet is found in the untwisted sector, so we have a closer look at it.
The constructing element of the untwisted sector is the trivial element $g(\mathbb{1}, 0)$. All elements commute with g so that one has to project with every shift and every Wilson line. Let us first look at the SUGRA multiplet. It is given by

$$
|q\rangle \otimes \alpha^{\mu}_{-1}|0\rangle \xrightarrow{h} e^{-2\pi i q\cdot v_h}|q\rangle \otimes \alpha^{\mu}_{-1}|0\rangle
$$

The SUGRA multiplet can only be invariant for weights q that are orthogonal (mod 1) to the shift vectors v_N and v_M. This is only true for the 4d weight vector $q_v = \pm(1, 0, 0, 0)$ which gives the 4d graviton and only for one choice of the spinorial roots q_s that give the gravitino. For simplicity one can choose the weights $q_s = \pm\left(\frac{1}{2}, \frac{1}{2}, \frac{1}{2}, \frac{1}{2}\right)$. v_N and v_M in turn have to satisfy

$$\sum_i v_N^i = 0\,,$$
$$\sum_i v_M^i = 0\,,$$

which is just the Calabi-Yau condition from chapter 2.4 to guarantee $\mathcal{N} = 1$ SUSY.
The untwisted gauge group is given by the states that give the Cartan elements and the roots of the gauge groups that transform as

$$\begin{array}{rcl} |q\rangle \otimes \alpha_{-1}^I|0\rangle & \stackrel{h}{\rightarrow} & e^{-2\pi i q\cdot v_h} \quad |q\rangle \otimes \alpha_{-1}^I|0\rangle \\ |q\rangle \otimes |P\rangle & \stackrel{h}{\rightarrow} & e^{-2\pi i(q\cdot v_h + P\cdot V_h)}|q\rangle \otimes \alpha_{-1}^\mu|0\rangle . \end{array}$$

The Cartan elements have to have the same q's as the SUGRA multiplet to be orthogonal to the shifts. Therefore the 16 Cartan vector multiplets survive the projection, showing that the rank of the gauge group cannot be reduced by orbifolding. The Cartans and the charged gauge bosons and gauginos have to have the same 4d weights q_s and q_v, to properly identify them to the same gauge multiplet. The unbroken roots of the gauge multiplet therefore have to satisfy

$$\begin{aligned} P \cdot V_N &= 0 \bmod 1\,, \\ P \cdot V_M &= 0 \bmod 1\,, \\ P \cdot A_\alpha &= 0 \bmod 1 \quad \forall \alpha\,. \end{aligned}$$

Shift embeddings and Wilson lines project out some of the 480 roots of $E_8 \times E_8$ and break the group down to a subgroup with the same rank. If q_s and q_v are not orthogonal to the twists then we have charged matter[8].
Since the weights of E_8 have norm square 2 and consequently also the weights of the broken gauge group as well and the untwisted spectrum of the E_8's splits up and simplifies the analysis.

[8]An exception are singlets that can be interpreted as geometric moduli but this will not be discussed in this work.

Chapter 3

Classification of the $\mathbb{Z}_2 \times \mathbb{Z}_4$ orbifold

The discussions in the last chapter were very general and served as an introduction to the heterotic string and orbifold compactifications. In this chapter we will focus on the $\mathbb{Z}_2 \times \mathbb{Z}_4$ orbifold. In the spirit of the Mini Landscape searches [5], [6] we try to discuss the $\mathbb{Z}_2 \times \mathbb{Z}_4$ as completly as possible in order to set a good starting point for the discussion of models with MSSM like properties.
In the last chapter it became clear by what determines the field spectrum and the gauge group of a given orbifold geometry:

$$\boxed{\begin{array}{l}\text{Shift embedding } V_2 \text{ and } V_4\\ \text{Wilson Lines } A_\alpha\end{array}} \xrightarrow{\text{Enters in}} \boxed{\begin{array}{l}\text{Mass equation}\\ \text{Orbifold phase}\end{array}}$$

Here we will focus mainly on the classification of the shift embeddings V_2 and V_4 and deliver some spectra with additional Wilson lines in chapter 4.
If one wants to embed the shifts v_2 and v_4, the simplest choice is the standard embedding that automatically satisfies the modularity conditions:

$$V_2 = (v_2^i, 0^{13}) \,,$$
$$V_4 = (v_4^i, 0^{13}) \,.$$

Since the modular invariance conditions are the only restrictions, more embeddings are possible. The shifts will enter in the mass equation and the orbifold phase determining the spectrum and the question arises whether there is a symmetry transformation between shifts leading to the same spectrum. So the question this chapter addresses is, how many inequivalent embeddings of V_2 and V_4 there are.

3.1 Symmetries of the spectrum

In order to investigate when spectra are equivalent, one should look at the symmetries of the equations that determines them. To begin with, the modularity conditions on the shifts are given by

$$V_2 = \frac{\Lambda_{E_8\times E_8}}{2}\,, \tag{3.1.1a}$$
$$V_4 = \frac{\Lambda_{E_8\times E_8}}{4}\,, \tag{3.1.1b}$$
$$2\left(V_2^2 - v_2^2\right) = 0 \bmod 2\,, \tag{3.1.1c}$$
$$4\left(V_4^2 - v_4^2\right) = 0 \bmod 2\,, \tag{3.1.1d}$$
$$2(V_2\cdot V_4 - v_2\cdot v_4) = 0 \bmod 2\,. \tag{3.1.1e}$$

They enter the mass equation and the orbifold phase in the $T(k,l)$ twisted sector:

$$\begin{aligned} P_{\mathrm{sh}} &= P + kV_2 + lV_4\,,\\ \frac{M_-^2}{8} &= \frac{P_{\mathrm{sh}}^2}{2} - 1 + \tilde{N} + \delta_c = 0\,,\\ \phi &= e^{2\pi i\left(P_{\mathrm{sh}}\cdot V_h - (q_{\mathrm{sh}} - N + \bar{N})\cdot v_h\right)} e^{-2\pi i\frac{1}{2}(V_g\cdot V_h - v_g\cdot v_h)}\,. \end{aligned}$$

Clearly the isometries of the scalar product that enters the mass equation and the orbifold phase and are also symmetries of the spectrum. These isometries are the automorphisms of the Lie lattice from which the vectors originate. This will be analyzed in the next section. One can also add a lattice vector to V_2 and V_4. Even though this does not change the untwisted sector, it does affect the third modularity condition in equation (3.1.1a) and the twisted spectrum. This will be analyzed in the next chapter.

3.2 Automorphism of $E_8 \times E_8$

We are looking for the group of automorphisms of the $E_8 \times E_8$ root lattice, i.e. the transformations that leaves the group structure invariant. Basically there are two kinds of automorphisms: The lattice automorphism $Aut(\Gamma)$ and the inner automorphism $IAut(\mathbb{G})$ of the group $\mathbb{G}$.
The lattice automorphisms $Aut(\Gamma)$ are those automorphisms that permute simple roots α_i of the Dynkin diagram. In terms of the Cartan matrix

$$A_{i,j} = 2\frac{\alpha_i\cdot\alpha_j}{\alpha_i\cdot\alpha_i}\,,$$

these are permutations π of entries that leave the structure of the matrix invariant, i.e.

$$Aut(\Gamma) = \left\{\pi \in S_{\mathrm{rank}(\mathbb{G})} | A_{\pi(i),\pi(j)} = A_{i,j}\right\}\,. \tag{3.2.1}$$

The Dynkin diagram of E_8 given in figure A.1 in appendix A shows that there are no lattice automorphisms[1].

[1] Interchanging the two E_8 is considered when we reconstruct all embeddings from tensoring the E_8 embeddings with itself.

An inner group automorphism $h \in IAut(\mathbb{G})$ acts on a group element $x \in \mathbb{G}$ as a conjugation

$$x \xrightarrow{h} b \circ x \circ b^{-1} . \tag{3.2.2}$$

with $\circ$ being the group operation and $b \in \mathbb{G}$. The automorphisms that are no inner ones are called *outer automorphism* .
The automorphism group is then given as the semi-direct product of lattice and inner automorphisms

$$Aut(\mathbb{G}) = Aut(\Gamma) \ltimes IAut(\mathbb{G}). \tag{3.2.3}$$

Since E_8 has no lattice automorphisms its automorphism group is given only by the inner automorphisms.
Still we are interested in the automorphism group of a direct product of two E_8s that can be bigger then the direct product of two automorphism groups. However, elements of the direct product $\mathbb{G} \times \tilde{\mathbb{G}}$ transform as

$$\begin{aligned}(a, b) &\rightarrow (x, y) \cdot (a, b) \cdot (x^{-1}, y^{-1}) \\ &= (x \circ a \circ x^{-1}, y \circ b \circ y^{-1})\end{aligned} \tag{3.2.4}$$

respecting the law of composition of elements of direct product groups. Thus we see that the inner automorphism group of a direct product is indeed the direct product of the inner automorphisms. Further information can be found in [7] and in [4].
Keeping this in mind we only need to care about the inner automorphisms of one E_8 and its eight dimensional shift embedding V.
Once we found all inequivalent shifts in one E_8, we can combine them with themselves to give a complete 16 dimensional $E_8 \times E_8$ vector in way that also the modularity conditions of equation (3.1.1a) are fulfilled.

3.3 The Weyl Group

We are only interested in the inner automorphisms of the E_8 root lattice. They are given by the Weyl group [28]. The Weyl group itself is generated by Weyl reflections. These are reflections on a hyperplane perpendicular to a simple root of the Lie lattice. In that way every Weyl reflection σ_α is characterised by a root α and acts on a vector $V \in E_8$ as

$$\begin{aligned}\tilde{V}^i = (\sigma V)^i &= V^i - 2\frac{\alpha \cdot V}{\alpha \cdot \alpha}\alpha^i \\ &= (\mathbb{1}^{i,j} - \alpha^i \alpha^j) V_j.\end{aligned} \tag{3.3.1}$$

since $\alpha^2 = 2$. In the last equation it becomes clear that $\sigma_\alpha = \sigma_{-\alpha}$ and due to

$$\begin{aligned}\sigma_\alpha^T \sigma_\alpha &= \sigma_\alpha \sigma_\alpha \\ &= (\mathbb{1} - \alpha\alpha^T)(\mathbb{1} - \alpha\alpha^T) \\ &= \mathbb{1} - 2\alpha\alpha^T + \alpha(\alpha^2)\alpha^T \\ &= \mathbb{1}\end{aligned}$$

it is also an orthogonal transformation as one would expect from intuitive notion of a reflection.
Some examples of Weyl group elements are given by the simple roots $\alpha = (-1, 1, 0^6)$ and $\tilde{\alpha} = (1, 1, 0^6)$ that generate the Weyl reflections

$$\sigma_\alpha = \left(\begin{array}{cc|c} 0 & 1 & \\ 1 & 0 & 0 \\ \hline \multicolumn{2}{c}{0} & \mathbb{1}_{6\times 6} \end{array}\right), \quad \sigma_{\tilde{\alpha}} = \left(\begin{array}{cc|c} 0 & -1 & \\ -1 & 0 & 0 \\ \hline \multicolumn{2}{c}{0} & \mathbb{1}_{6\times 6} \end{array}\right)$$

$$\Rightarrow \sigma_\alpha \sigma_{\tilde{\alpha}} = \left(\begin{array}{cc|c} -1 & 0 & \\ 0 & -1 & 0 \\ \hline \multicolumn{2}{c}{0} & \mathbb{1}_{6\times 6} \end{array}\right)$$

Clearly σ_α is a permutation and $\sigma_\alpha \sigma_{\tilde{\alpha}}$ gives a reflection of two components[2].
Figure 3.1 shows a simple example of the three dimensional Lie lattice of SU(4). The root lattice of SU(4) has rank three and therefore three simple roots that build up the lattice. In figure 3.1 they are given by the vectors

$$\alpha_1 = (0, 1, 1)^T, \quad \alpha_2 = (1, 0, -1)^T, \quad \alpha_3 = (0, -1, 1)^T \tag{3.3.2}$$

representing the SU(4) Dynkin diagram:

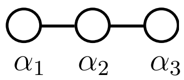

Since all 12 roots of SU(4) have the same length, they fit into a three dimensional cube shown in part a.). In part b.) we illustrate a Weyl reflection σ_{α_2} which can be seen as a reflection on a plane perpendicular to α_2. This reflection in fact is the same as permuting coordinates to $(x, y, z) \to (z, y, x)$. As one can see from the Dynkin diagram of SU(4) there is also a permutation symmetry when we exchange α_1 and α_3. This is a lattice automorphism that maps one complex representation to the conjugate one. Together with the Weyl reflections this generates the outer automorphisms of SU(4). Let us now turn to the actual problem of finding all inequivalent pairs of V_2 and V_4 shifts. To do so let us suppose we already found all inequivalent shifts of V_4. Then take a fixed candidate $V_{4,f}$ and pair it up with all inequivalent V_2 shifts that cannot be connected via Weyl reflections σ_α. Since these transformations have to be seen as transformations of the whole lattice, all E_8 lattice vectors will transform under the Weyl reflection as

$$(V_2, V_{4,f}) \xrightarrow{\text{Weyl reflection}} (\sigma_\alpha V_2, \sigma_\alpha V_{4,f}). \tag{3.3.3}$$

[2]This can of course be extended to all components.

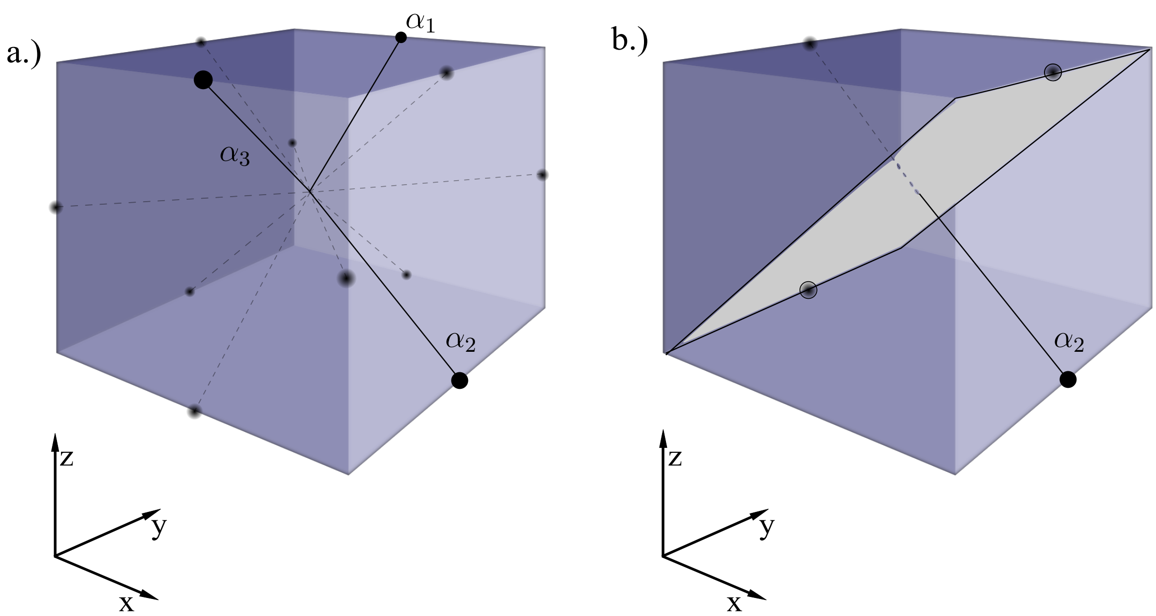

Figure 3.1: Picture a.) shows the SU(4) cube and all its 12 roots lying on the edges. The positive and simple ones are black while the others are grey. Picture b.) shows a Weyl reflection on the plane perpendicular to a simple root α_2 which corresponds to an change of the x and z coordinate.

To guarantee invariance of the spectrum we have to demand that the Weyl reflections leave $V_{4,f}$ invariant.

$$\begin{aligned} \sigma_\alpha V_{4,f} = (\mathbb{1} - \alpha\alpha^T)V_{4,f} &\stackrel{!}{=} V_{4,f} \\ \Leftrightarrow \alpha \cdot V_{4,f} &\stackrel{!}{=} 0\,. \end{aligned} \tag{3.3.4}$$

So we have to demand that $V_{4,f}$ is orthogonal to the reflection root or equivalently that it is parallel to the hyperplane of the reflection.

3.4 The strategy

In the further discussion we investige under which circumstances two shifts are connected via a Weyl group element. A Weyl group element can then be a consecutive execution of multiple Weyl reflections. For this we focus only on the symmetries of the lattice, in particular of only one E_8 factor taking modular invariance into account later. However, due to the high symmetry of the E_8 root lattice its Weyl group has 696.729.600 elements [29] so even with latest computers, it is extremely time and memory consuming to generate all these elements and then check whether the shifts V_2 are related.
To do the calculations in a reasonable amount of time we check only for equivalence up to

Number	$4V_4$
0	(0,0,0,0,0,0,0,0)
1	(2,2,0,0,0,0,0,0)
2	(1,1,0,0,0,0,0,0)
3	(2,1,1,0,0,0,0,0)
4	(4,0,0,0,0,0,0,0)
5	(2,0,0,0,0,0,0,0)
6	(3,1,0,0,0,0,0,0)
7	(2,2,2,0,0,0,0,0)
8	(3,1,1,1,1,1,0,0)
9	(1,1,1,1,1,1,1,-1)

Table 3.1: Table of all inequivalent shift embeddings of $\mathbb{Z}_4$ taken from [12]. Notice the shift number 3 which is the standard embedding for a $\mathbb{Z}_4$ orbifold.

Weyl reflections. Further equivalences can be checked at the level of the spectrum later. For the analysis we used the 10 inequivalent $\mathbb{Z}_4$ shift vectors from [12] that are given in table 3.1. We take these 10 V_4 shifts and construct all possible V_2 shifts for each one of them. After this we relate the shifts V_2 that give an equivalent spectrum.

3.5 Computer aided construction of inequivalent $\mathbb{Z}_2$ shifts

This section describes the most important parts of the Mathematica algorithm we wrote to calculate all inequivalent V_2 shifts[3]. Note that in the further discussions the shift

$$V_2 = \sum_{i=1}^{8} \frac{n_i \alpha_i}{2}$$

with α_i being the simple roots of E_8. To be of order 2, we illustrate the shifts as $2V_2$ for convenience. Our choice of simple roots of E_8 is given in table D.1 in appendix D.
Clearly all components n_i can be zero or one, since we consider half lattice vectors. The Dynkin diagram of E_8 shows that there is a maximal norm square of the shifts, such that V_2 is free of lattice vectors, which is 8! This becomes clear by looking at the only two simple root combinations that can achieve that:

Since the scalar product of two adjacent roots is $\alpha_i \alpha_j = -1$, every additional root would not change or even reduce the norm of the two $V_{2,\mathrm{max}}$ combinations.

[3]We are highly grateful for the help of Matthias Schmitz.

$$
\begin{aligned}
V_{2,\mathrm{max1}} &= \alpha_1 + \alpha_3 + \alpha_5 + \alpha_7 \\
V_{2,\mathrm{max2}} &= \alpha_2 + \alpha_4 + \alpha_6 + \alpha_8
\end{aligned}
$$

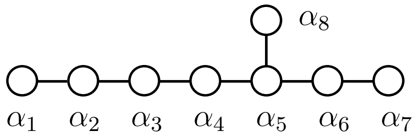

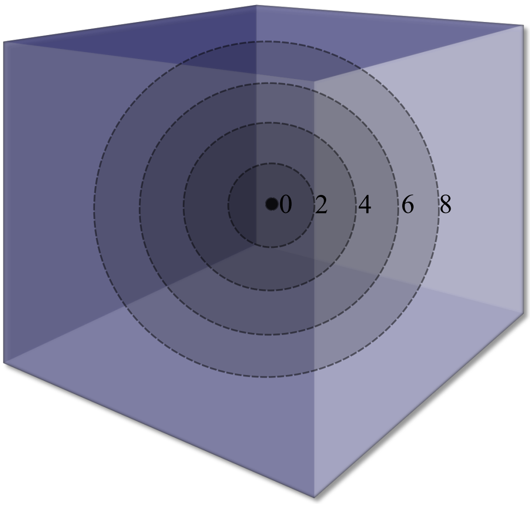

$\xrightarrow{\text{Cutting out}}$

S^7	Norm	#Elements
	0	1
	2	240
	4	2160
	6	6720
	8	17520

Figure 3.2: A schematical picture how the sets illustrated as spheres of norm 0,2,4,6 and 8 are cut out of the cube. On the right, the number of vectors that are contained in each sphere are given. Notice that the norm square 2 sphere is the set of the 240 roots of the adjoint representation of E_8.

3.5.1 Generating all vectors

Since the maximal norm square of V_2 is 8 and V_2 can also be a spinorial root so, we know that a component has to fulfill[4] $2V_2^i \in \mathbb{Z}$ so that the maximal component is

$$
V^i_{2,max} = \left\lfloor (\sqrt{8} \cdot 2) \right\rfloor = 5\,.
$$

Using this, we generate all vectors $V_{2,cube} = \sum_i^8 \frac{a_i}{2}$ such that $a_i \in [-5,5]$ with $V^2_{2,cube} \leq 8$ which is an 8 dimensional cube of side length 10.
When constructing systematically all vectors in the cube, we look for the ones that have a norm square divisible by two and are given by integer linear combinations of the positive simple roots.
With this procedure we cut out the vectors given by the intersection of spheres of norm square 0,2,4,6 and 8 and the E_8 lattice, schematically depicted in figure 3.2.

[4]Note our convention that V_2 has already been multiplied by a factor of two!

3.5.2 Generating the Weyl reflections

Now that we have all vectors we have to merge them into equivalence classes. To relate shifts by Weyl reflections we go step by step:

1. Fix one of the 10 $V_{4,f}$'s.

2. Take all roots that satisfy $\alpha_i \cdot V_{4,f} = 0$ and get the set of possible reflections.

3. All vectors in one class get a label '*class*' thats value shows their equivalence class.

Vector	*class*
V_1	1
V_2	2
V_3	3
.	.
.	.

4. Go through the complete list and fix one of the vectors to V_{original} with equivalence class $'class'_{\text{original}}$. Then calculate all possible Weyl reflected vectors $V_{\text{Weyl},i}$.

	Vector	*class*
V_{original} :	V_1	1
$\downarrow$	V_2	2
$V_{\text{Weyl},3}$:	V_3	3
	.	.
	.	.

5. $V_{\text{Weyl},i}$ has to be in the same sphere since Weyl reflections are orthogonal transformations so that we can compare the equivalence class '$class_{\text{original}}$' with the one of $V_{\text{Weyl},i}$ which is denoted as $class_{\text{Weyl}}$.

6. If the classes are different then two equivalence classes have to be merged together. The list of equivalence classes of the vectors is run through and the value of $class_{\text{Weyl}}$ is replaced by $class_{\text{original}}$.

	Vector	*class*
V_{original} :	V_1	1
$\downarrow$	V_2	2
$V_{\text{Weyl},3}$:	V_3	1
	.	.
	.	.

A schematical picture is given in figure 3.3. In this way sets of inequivalent vectors are formed, such that the amount of vectors is hugely reduced. The number of equivalence classes for $V_{4,f} = (3,1,1,1,1,1,0,0)$ for example is 151. Table 3.2 shows the reduction of all shift embeddings.

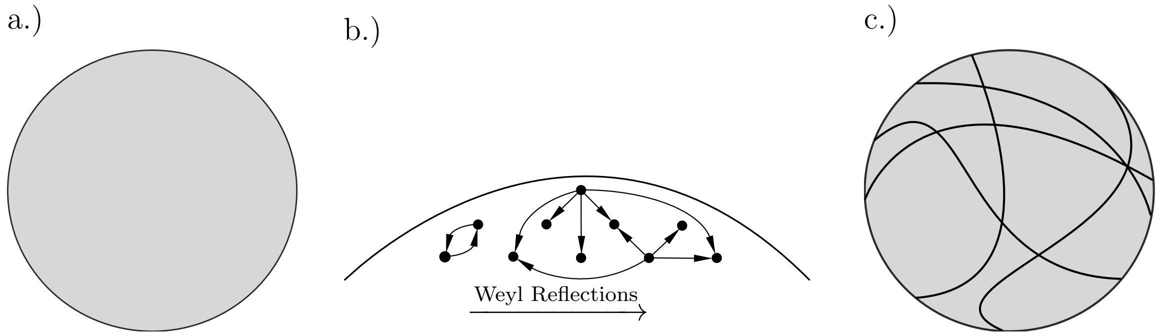

Figure 3.3: Schematical picture how the set of all vectors a.) is split up into sectors of different equivalence classes c.). This happens in picture b.): There a part of the sphere is taken and points/vectors on the sphere are identified by Weyl reflections drawn as arrows.

3.5.3 Merging classes of different norms

Since for every $V_{4,f}$ we have a number of order 100 equivalence classes. We want to reduce this amount further. To do so we first investigate whether there are combinations of Weyl reflections that are invalid by themselves, i.e

$$\sigma_\alpha V_{4,f} \neq V_{4,f}\ ,$$

but could identify the vector in higher combinations. We checked this for Weyl group elements up to order three but we could never find any valid combination! This is the step where we miss higher elements that leave $V_{4,f}$ invariant and under which we relate V_2 elements because we could not test for all Weyl group elements. However to identify such equivalent embeddings we test them later at the level of the complete spectrum.
To decrease the amount of vectors further we give up the inequivalence by Weyl reflections and allow two embeddings to be equivalent up to lattice translations. As mentioned earlier adding lattice vectors λ to $V_{2/4}$ changes only the twisted matter spectrum while the untwisted spectrum and especially the gauge group stays the same. Therefore these models are called *brother models* [3].
To compensate the loss of inequivalence we will construct all lattice translations that lead to inequivalent models in section 3.5.6.
When we allow identification up to lattice translations we can merge whole sets of equivalent classes: Assume that one finds V_2 and $\tilde{V}_2$ from two distinct equivalence classes which differ by a lattice translation

$$\begin{aligned} V_2 &= \tilde{V}_2 + \lambda \qquad |\sigma\cdot\ , \\ \Leftrightarrow \sigma V_2 &= \sigma\tilde{V}_2 + \sigma\lambda\ , \\ V_2' &= \tilde{V}_2' + \lambda'\ . \end{aligned} \tag{3.5.1}$$

In the second line we multiplied with **any** allowed Weyl reflection such that also all other elements in the two sets differ by a lattice shift. This simplifies the computation because

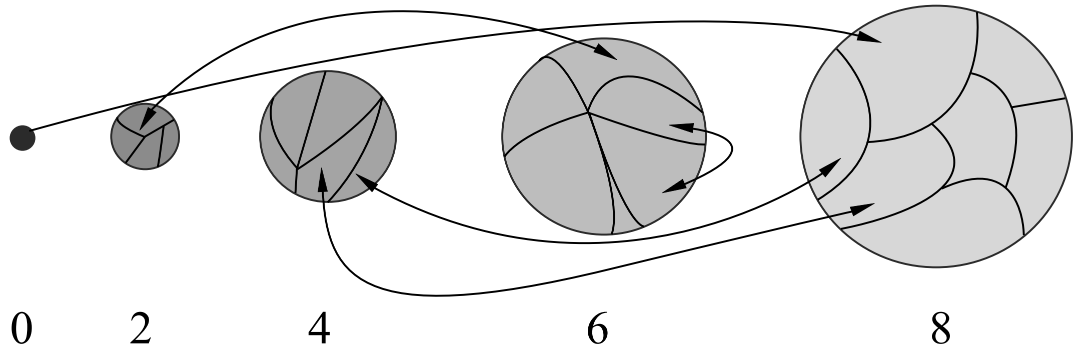

Figure 3.4: Schematic view of how equivalent classes of different norms are merged when elements differ by a lattice vector.

one instance fulfilling equation (3.5.1) is enough to completely render two sets equivalent. This is graphically depicted in figure 3.4. According to the identification in equation (3.5.1) the difference in the norm square of two equivalent vectors

$$\begin{aligned} \tilde{V_2}^2 - V_2^2 &= 2\sigma V_2 \cdot \lambda + \lambda^2 \,, \\ &\in \mathbb{Z} + 2\mathbb{Z} = \mathbb{Z} \,, \end{aligned} \tag{3.5.2}$$

has to be by an integer or in our convention of writing $2V_2$

$$\tilde{V_2}^2 - V_2 \in 4\mathbb{Z} \,, \tag{3.5.3}$$

four times an integer. This is depicted in figure 3.4 because there are no arrows relating two neighboured spheres[5]. Table 3.2 shows how many equivalent classes exist for each of the 10 V_4 shifts. The table in the appendix D shows also one V_2 as representative.
From the table it becomes clear that we could reduce the amount of shifts from 781 to **84** which is almost a factor of 10. The last column of table 3.2 shows also how the amount gets further reduced to **75** by identifying embeddings that lead to the same spectrum and are maybe related by higher equivalence relations. See section 3.5.7 for the discussion.
By this we got all inequivalent embeddings that are possible. Still these are only embeddings in one E_8, so we have to join them together in a way that the modularity conditions are fulfilled.

3.5.4 Determining the gauge group

Although the shifts have not yet been recombined to full 16 dimensional lattice vectors, the 8 dimensional ones are sufficent to get the untwisted matter spectrum as well as the gauge group since here both E_8's stay decoupled! So in this section it is described how we get the gauge group associated to each of the gauge embeddings in six steps:

[5]The only exception is the zero norm set that can only be related to the norm 8 sphere.

$4V_{4,f}$	V_2 Eq. Classes	Lattice identification	Further reduction
(0,0,0,0,0,0,0,0)	6	3	3
(2,2,0,0,0,0,0,0)	31	6	6
(1,1,0,0,0,0,0,0)	31	6	6
(2,1,1,0,0,0,0,0)	78	9	9
(4,0,0,0,0,0,0,0)	48	7	6
(2,0,0,0,0,0,0,0)	48	7	6
(3,1,0,0,0,0,0,0)	153	13	12
(2,2,2,0,0,0,0,0)	146	12	9
(3,1,1,1,1,1,0,0)	152	12	10
(1,1,1,1,1,1,1,-1)	88	9	9
Sum of Shifts:	781	84	75

Table 3.2: Table of equivalent classes before and after merging classes whose elements differed by a lattice vector. Notice that $(2,0^7)$ and $(4,0^7)$ are the same on the level of equivalence classes as well as $(1,1,0^6)$ and $(2,2,0^6)$. In the last column we further reduce the shifts that give the same spectrum.

1. We take only the positive roots P of E_8 that fulfill
$$P \cdot V_2 = 0 \text{ mod } 1\,,$$
$$P \cdot V_4 = 0 \text{ mod } 1\,.$$

2. To identify the groups, we need the positive and simple roots. Since non-simple roots can be decomposed into integer linear combinations of simple ones we are looking for the roots for which this is not possible:
$$P_i \neq P_j + P_k \quad \forall \text{ j , k} \quad .$$

3. We divide the simple roots into sets that only contain roots that are not orthogonal to at least one other root in the set.
The number of simple roots in a set (j) gives the rank of the gauge group $Rank(j)$ and the number of sets gives the amount of semi-simple non-Abelian Lie groups N_{Groups}. Since the orbifold projection does not act on the 8 Cartan elements α^I_{-1} of E_8 the rank is preserved. Consequently the number of U(1)s is given
$$\#_{U(1)} = 8 - \sum_i^{N_{Groups}} \text{Rank}(i)$$

4. To identify a semi simple gauge group we calculate its Cartan matrix
$$A_{ij} = 2\frac{P_i \cdot P_j}{P_i^2}\,.$$

$4V_{\mathbb{Z}_4}$	$2V_{\mathbb{Z}_4}$	Group Decomposition	
(3,1,1,1,1,1,0,0)	$(0,0,0,0,0,0,0,0)$	SU(8)×SU(2)	♣
	$(-1,-1,0,0,0,0,0,0)$	SU(6)×SU(2)^2×U(1)	♠
	$(-1,0,0,0,0,0,1,0)$	SU(6)×SU(2)×U(1)^2	♢
	$(-1,0,0,0,0,1,0,0)$	SU(4)^2×SU(2)×U(1)	
	$(0,-1,0,0,0,0,1,0)$	SU(6)×SU(2)×U(1)^2	♢
	$(0,-1,0,0,0,1,0,0)$	SU(6)×SU(2)^2×U(1)	♠
	$(0,0,0,0,0,0,-1,1)$	SU(8)×SU(2)	♣
	$(-1,0,0,1,-1,1,0,0)$	SU(6)×SU(2)^2×U(1)	♡
	$(-\frac{1}{2},-\frac{3}{2},\frac{1}{2},\frac{1}{2},\frac{1}{2},\frac{1}{2},-\frac{1}{2},\frac{1}{2})$	SU(8)×U(1)	
	$(-1,-1,-1,0,0,0,0,1)$	SU(4)^2×U(1)^2	
	$(0,-1,-1,0,0,0,-1,1)$	SU(4)^2×SU(2)×U(1)	
	$(0,0,1,-1,-1,-1,0,0)$	SU(6)×SU(2)^2×U(1)	♡

Table 3.3: The 13 equivalence classes of $\mathbb{Z}_2$ shift embeddings for $V_{4,f} = (3,1,1,1,1,0,0)$ with a given representative and their corresponding gauge group. Same symbols in the last column signal that these embeddings could be equivalent.

Since all roots of E_8 have the same length, the Cartan matrix is symmetric and hence only simply laced Lie groups can appear.

5. The Cartan matrix gets the canonical form by reordering the simple roots such that also the Dynkin labels of the matter representations are in the canonical form.

As an example the $V_{4,f}$ shift $(3,1,1,1,1,1,0,0)$ and all its compatible V_2 shifts as well as their gauge groups are given in table 3.3. The whole table of the shift vectors and their corresponding gauge groups for all 10 $V_{4,f}$ is given in table D.2 in appendix D. Table 3.3 already shows that there are still some embeddings that give the same gauge group as others and thus may be equivalent to them. This could mean that there are equivalences that can relate these embeddings we have not found. But we check them on the level of their spectra in section 3.5.7. Before calculating the spectra however, we first have to pair the shifts to form modular invariant $E_8 \times E_8$ vectors.

3.5.5 Pairing the shifts

Now we pair the shifts to form 16 dimensional $E_8 \times E_8$ vectors. At this point we have to make sure that the three modularity conditions are fulfilled

$$4(V_4^2 - v_4^2) = 0 \bmod 2 \tag{3.5.4}$$
$$2(V_2^2 - v_2^2) = 0 \bmod 2 \tag{3.5.5}$$
$$2(V_2 \cdot V_4 - v_2 \cdot v_4) = 0 \bmod 2. \tag{3.5.6}$$

To do so we first go through the 10 $\mathbb{Z}_4$ vectors, fix a $V_{4,1}$ vector and pair it with another shift vector $V_{4,2}$ such that the first modularity condition is fulfilled. Then we fix a $V_{2,1}$ shift vector that is compatible with $V_{4,1}$ and pair it with $V_{2,2}$ that is compatible with $V_{4,2}$ such that they fulfill the second modularity condition. Since both E_8's can be interchanged, we also have to guarantee that we do not over-count.
The combined set $V_4 = (V_{4,1}, V_{4,2})$ and $V_2 = (V_{2,1}, V_{2,2})$ has then to be checked to fulfill the third modularity condition as well.
Since we allowed to add lattice vectors to the shifts when we did the classification we can use this to weaken the third modularity condition by shifting

$$\begin{aligned} V_2 &\to V_2 + \alpha \quad \text{with } \alpha \in \Gamma_{E_8 \times E_8} \\ V_4 &\to V_4 + \beta \quad \text{with } \beta \in \Gamma_{E_8 \times E_8} \end{aligned}$$

The first two conditions are not changed by this action since the lattice is integral and even:

$$\begin{aligned} 4(V_4^2 - v_4^2) \to & 4(V_4^2 - v_4^2) + 4\beta^2 + 2(4V_4 \cdot \beta) \\ = & 4(V_4^2 - v_4^2) + 4\mathbb{Z} + 2\mathbb{Z} \equiv 0 \text{ mod } 2 \end{aligned}$$

and similarly for the second condition. The third condition changes under the shifts to

$$\begin{aligned} 2(V_2 \cdot V_4 - v_2 \cdot v_4) \to & \; 2(V_2 \cdot V_4 - v_2 \cdot v_4) + 2V_2 \cdot \beta + 2V_4 \cdot \alpha + \alpha \cdot \beta \\ = & \; 2(V_2 \cdot V_4 - v_2 \cdot v_4) + \quad \mathbb{Z} \quad + \quad \frac{\mathbb{Z}}{2} \quad + \; 2\mathbb{Z} \equiv 0 \text{ mod } \frac{1}{2} \, . \end{aligned}$$

Essentially the $V_4 \cdot \alpha$ scalar product weakens the third modularity condition from mod 2 down to mod $\frac{1}{2}$ such that $2(V_2 \cdot V_4 - v_2 \cdot v_4) = M$ can still be half integer valued, which by adding lattice shifts later.
Using this method we obtain **187** models that get reduced in the following to **144** given in table D.3 in appendix D.

3.5.6 Adding lattice vectors

As one can see in table D many of the 144 models still do not satisfy the third modularity condition. We will now cure this by adding lattice vectors and also try to recapture the loss of inequality we introduced when we classified the different shift embeddings. When we add lattice vectors α and β to V_2 and V_4 we can ask how many choices there are that lead to different models.
To answer this we have to check how the mass equation and orbifold phase transforms:
First we start by considering $P_{\text{sh}} = P + kV_2 + lV_4$ and P that solves the mass equation

$$\frac{(P + kV_2 + lV_4)^2}{2} - 1 + \tilde{N} + \delta_c = 0 \, .$$

When we add lattice vectors this changes to

$$\frac{\left(\tilde{P} + k(V_2 + \alpha) + l(V_4 + \beta)\right)^2}{2} - 1 + \tilde{N} + \delta_c = 0\,.$$

Clearly $\tilde{P} = P - k\alpha - l\beta$ solves the mass equation as well, so the mass equation is not changed and neither is P_{sh}, which enters the orbifold phase.
The orbifold phase under the projection element $h(\theta^m \cdot \omega^n, n_\alpha e_\alpha)$ with $V_h = mV_2 + nV_4$ and $v_h = mv_2 + nv_4$

$$\phi_o = e^{2\pi i\left(P_{\mathrm{sh}}\cdot V_h - (q_{\mathrm{sh}} - N + \bar{N})\cdot v_h\right)} e^{-2\pi i \frac{1}{2}(V_g \cdot V_h - v_g \cdot v_h)} \tag{3.5.7}$$

changes under the addition of lattice vectors to

$$\phi = \phi_o e^{2\pi i \frac{1}{2}(kn - ml)\left[2V_2 \cdot - \mathbb{Z} - \frac{M}{2}\right]}\,. \tag{3.5.8}$$

where $M = 2(V_2 \cdot V_4 - v_2 \cdot v_4)$ is the mismatch in the third modularity condition. A detailed derivation of the formula is found in appendix C. In the literature this phase is called the *brother phase* [3].
A short look at the phase reveals that the untwisted matter spectrum and the gauge group does not change as expected for brother models.
Another observation is that $2V_2 \cdot \beta \in \mathbb{Z}$, so there can be at most two different brother phases leading to different models. This means that we get at most **two different brother models** by adding lattice vectors to the shifts and that the orbifold phase difference between these two models can only be $e^{\pi i}$!

3.5.7 Further reduction

Now we have the complete shift embeddings and their gauge groups as well as the possibility to construct both brother models. As mentioned before, there still exists the possibility that we have equivalent embeddings that are related by higher equivalences. To filter out these as well, we have to compare the complete matter spectra. The program we used get the spectrum is described in section 4.4. The strategy for the last filter is thus:

1. Take two models with the same $(V_{4,1}) \oplus (V_{4,2})$.
2. Look for models with the same gauge group.
3. Take two models with the same $V_{2,1}$ but different $V_{2,2}$[6].
4. $V_{2,2}^2$ -$\tilde{V}_{2,2}^2$ has to be zero mod 4 according to equation (3.5.2).
5. Compare the matter spectra of both brother models.

If their spectra coincide then the embeddings $V_{2,2}$ and $\tilde{V}_{2,2}$ are equivalent. When this is the case, we highlighted embeddings with the same letter right next to the shift vector as in the example of $(3, 1, 1, 1, 1, 0, 0)$ in table 3.4 as well as in the full table D.2 in appendix D. From the 187 we started with, we thus eliminated **43** that were equivalent to other ones,

[6]We do the same also by fixing $V_{2,2}$ and comparing $V_{2,1}$.

$4V_{\mathbb{Z}_4}$	$2V_{\mathbb{Z}_2}$	Group Decomposition	
(3,1,1,1,1,1,0,0)	$(0,0,0,0,0,0,0,0)$	SU(8)×SU(2)	
	$(-1,-1,0,0,0,0,0,0)$	SU(6)×SU(2)^2×U(1)	**A**
	$(-1,0,0,0,0,0,1,0)$	SU(6)×SU(2)×U(1)^2	**B**
	$(-1,0,0,0,0,1,0,0)$	SU(4)^2×SU(2)×U(1)	
	$(0,-1,0,0,0,0,1,0)$	SU(6)×SU(2)×U(1)^2	**B**
	$(0,-1,0,0,0,1,0,0)$	SU(6)×SU(2)^2×U(1)	**A**
	$(0,0,0,0,0,0,-1,1)$	SU(8)×SU(2)	
	$(-1,0,0,1,-1,1,0,0)$	SU(6)×SU(2)^2 ×U(1)	**C**
	$(-\frac{1}{2},-\frac{3}{2},\frac{1}{2},\frac{1}{2},\frac{1}{2},\frac{1}{2},-\frac{1}{2},\frac{1}{2})$	SU(8)×U(1)	
	$(-1,-1,-1,0,0,0,0,1)$	SU(4)^2×U(1)^2	
	$(0,-1,-1,0,0,0,-1,1)$	SU(4)^2×SU(2)×U(1)	
	$(0,0,1,-1,-1,-1,0,0)$	SU(6)×SU(2)^2×U(1)	**C**

Table 3.4: The reduced list of $V_{4,f} = (3,1,1,1,1,1,0,0)$. The same letter in the las column indicates an equivalent spectrum.

GUT Gauge Group	Number of Models
SO(10)	35
E_6	26
$SU(5)$	25

Table 3.5: Summary of GUT candidates in the 144 inequivalent models.

such that we end up with **144** inequivalent ones given in table D.3.

3.6 Comment on the models

To incorporate our standard model in a unified theory we are looking for E_6, SO(10) and SU(5) models. Table 3.5 shows how many different instances of the 3 most common GUT models we could find. The most promising models are the SO(10) and E_6 models since one complete SM model family can be incorporated in one representation, the **16** of SO(10) or the **27** of E_6 as pointed out in appendix B. We also have smaller GUT groups like SU(5) and SU(4)×$SU(2)^2$ but they have the additional problem that one SM family comes from multiple representations. In section 4.5.3 we will point out that it is much harder to control the amount of net families in that groups. Besides that it turns out that small representations are also very likely to be charged under hidden gauge groups as well.

Chapter 4

A Benchmark Model

In this section we present a benchmark model with an SO(10) gauge group in our $\mathbb{Z}_2 \times \mathbb{Z}_4$ classification that gets broken down to the SM gauge group and results in three net families. To do so we first discuss the geometry we used in our orbifold models. After that we present a general scheme in our models how the Wilson lines have to be introduced and briefly describe the computer program we wrote to get the spectrum. We then describe some good candidates without Wilson lines. Finally we pick out one of them as our benchmark model and calculate the complete spectrum.

4.1 The geometry of the orbifold models

Up to now we could hold the discussion about the $\mathbb{Z}_2 \times \mathbb{Z}_4$ gauge embedding very general and did not need the actual geometry beyond the two shift vectors v_2 and v_4 that enter the modularity conditions. Now we need to discuss the geometry in order to calculate the spectrum.
For our models we take the factorisable $\mathrm{SU}(2)^2 \times \mathrm{SO}(4)^2$ Lie lattice with the two common shift vectors

$$\begin{aligned} v_2 =& \frac{1}{2}(0, 1, -1, 0)\,, \\ v_4 =& \frac{1}{4}(0, 0, 1, -1)\,. \end{aligned}$$

Including the untwisted sector there are 8 sectors but two of them share the same fixed point structure. All five twisted sectors a given in table 4.1.

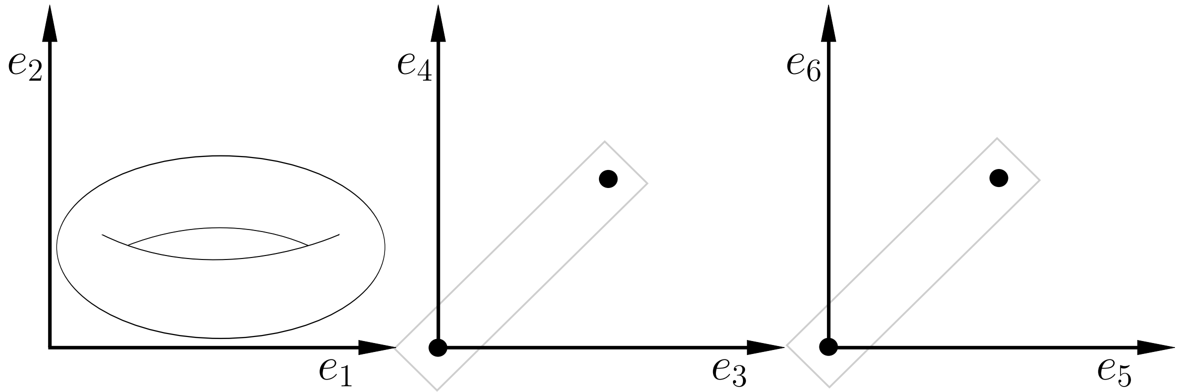

Sector: $T(0,1)/T(0,3)$	Fixed Tori: 4	Fixed Tori$_s$: 0

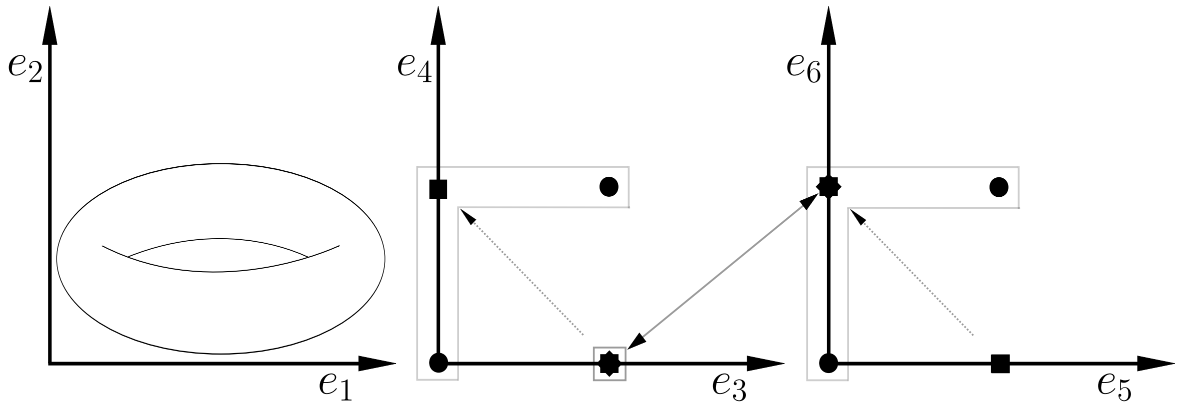

Sector: $T(0,2)$	Fixed tori: 4	Fixed tori$_s$: 6

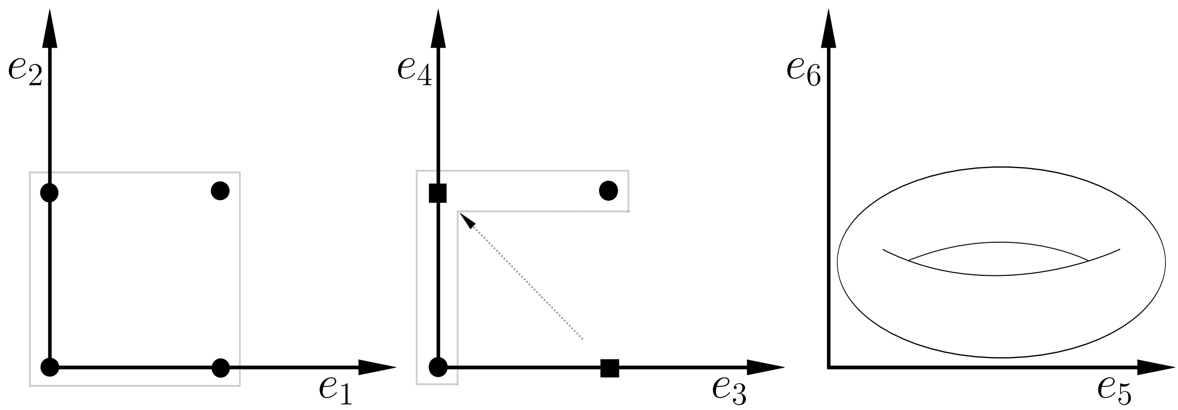

Sector: $T(1,0)$	Fixed tori: 8	Fixed tori$_s$: 4

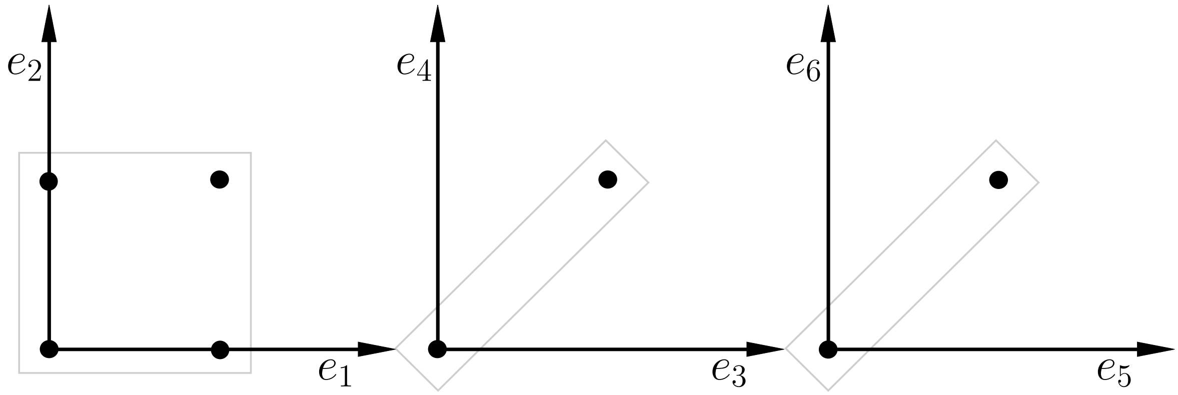

Sector: $T(1,1)/T(1,3)$	Fixed Points: 16	Fixed Points$_s$: 0

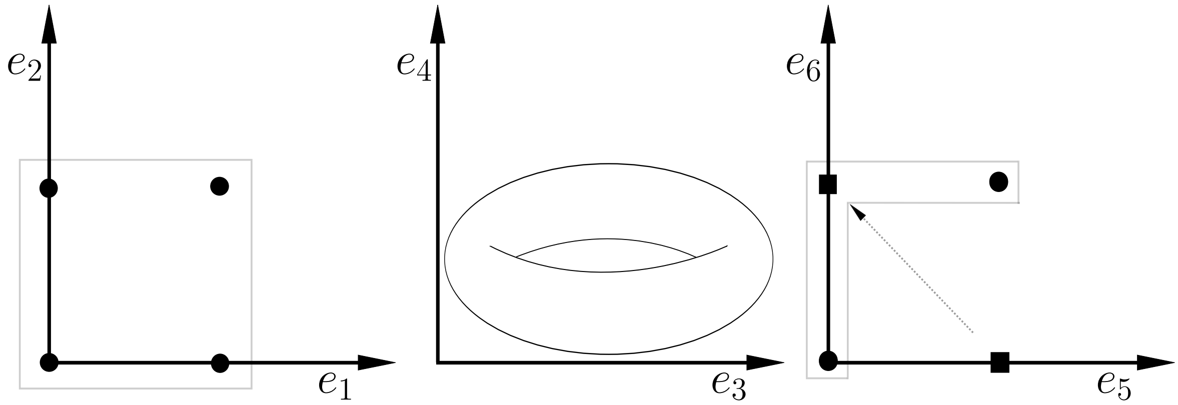

Sector: $T(1,2)$	Fixed tori: 8	Fixed tori$_s$: 4

Figure 4.1: The fixed point structures of the five independent twisted sectors. Note that the amount of special fixed points is highlighted with a subscript.

The geometry has some features making it more complicated than the simple $\mathbb{Z}_3$ example from section 2.4.1, so it requires futher explanation.
Let us start with the $T(0,1)/T(0,3)$ sector. This is a pure $\mathbb{Z}_4$ sector that has 2 fixed points in the second and third torus. The inequivalent fixed points are framed by a grey box and pair to 4 fixed tori. The $T(1,1)/T(1,3)$ is the mixed $\mathbb{Z}_2 \times \mathbb{Z}_4$ sector that has $4 \times 2 \times 2$ fixed points, in contrast to all other sectors which have only fixed tori. However, for our choice of a left chiral super field[1], one cannot solve the mass equation in the $T(1,1)$ sector and this sector will always be empty.

[1]Our concention is that a left chiral super field has **positive** first component.

Let us now turn to the $T(1,0)$ sector. This one has 4 fixed points in the first and second torus. Two of them are also $\mathbb{Z}_4$ fixed points, depicted as black dots but two of them are purely $\mathbb{Z}_2$ fixed points shown as black squares. The Hilbert spaces of these two elements are mapped onto each other by a suitable $\mathbb{Z}_4$ orbifold element. This can be seen by looking at these fixed points:

$$g_{s,1}(\theta, e_3) \quad \text{and} \quad g_{s,2}(\theta, e_4)\,.$$

Conjugation with a $\mathbb{Z}_4$ element $h(\omega, 0)$ on $g_{s,1}$ using equation (2.4.13a) yields

$$\begin{aligned} h^{-1} g_{s,1} h &= g(\theta, \omega^{-1} e_3)\,, \\ &= g_{s,2}(\theta, -e_4)\,. \end{aligned}$$

The fixed points corresponding to the conjugacy classes of $g_{s,1}$ are mapped to the ones[2] of $g_{s,2}$. In the figures this is depicted by the dashed arrow that identifies two fixed points. The same behaviour is found in the $T(0,2)$ sector because here we encounter the $\mathbb{Z}_2$ subgroup of $\mathbb{Z}_4$. It is easiest to see this by simply taking all 16 fixed points and conjugate with $h(\omega, 0)$:

1. The four $\mathbb{Z}_4$ fixed points are mapped to themselves:

$$\begin{aligned} g_1(\omega^2, 0) &\simeq g_1(\omega^2, 0) \\ g_2(\omega^2, e_3 + e_4) &\simeq g_2(\omega, -e_4 + e_3) \\ g_3(\omega^2, e_5 + e_6) &\simeq g_3(\omega, e_6 - e_5) \\ g_4(\omega^2, e_3 + e_4 + e_5 + e_6) &\simeq g_4(\omega, -e_4 + e_3 + e_6 - e_5). \end{aligned}$$

2. The 12 $\mathbb{Z}_2$ fixed points on the other hand are identified pairwise:

$$\begin{aligned} g_5(\omega^2, e_6) &\simeq g_{11}(\omega, -e_5) \\ g_6(\omega^2, e_4) &\simeq g_{12}(\omega, e_3) \\ g_7(\omega^2, e_4 + e_6) &\simeq g_{13}(\omega, e_3 - e_5) \\ g_8(\omega^2, e_3 + e_6) &\simeq g_{14}(\omega, -e_4 - e_5) \\ g_9(\omega^2, e_4 + e_5 + e_6) &\simeq g_{15}(\omega, e_3 + e_6 - e_5) \\ g_{10}(\omega^2, e_3 + e_4 + e_5) &\simeq g_{16}(\omega, -e_4 + e_3 + e_6). \end{aligned}$$

These fixed points are the ones drawn in the picture. Note that there are 3×3 fixed points from pairing up the fixed points in the grey boxes but also a unique tenth combination highlighted with a black arrow.

The considerations above show that some fixed points are identified under the orbifold. These fixed points are exactly those that do not trivially commute with any $h(\omega, n_\alpha e_\alpha)$ and therefore have a different centraliser. They are replaced by $h(\omega^2, n_\alpha e_\alpha)$ because they

[2]The negative coefficient of e_4 shows that the fixed point lies outside the fundamental domain but coincides with $g_{s,2}$ inside it.

	1	2	3	4	5	6	7	8
Sector	$T(0,0)$	$T(0,1)$	$T(0,2)$	$T(0,3)$	$T(1,0)$	$T(1,1)$	$T(1,2)$	$T(1,3)$
Fixed points$_n$	0	4	4	4	8	16	8	16
Fixed points$_s$	-	-	6	-	4	-	4	-

Table 4.1: The number of normal and special fixed points highlighted with a subscript.

lie in the $\mathbb{Z}_2$ subgroup of $\mathbb{Z}_4$ and do commute.
As a consequence, at these *special* points the projection with respect to ω/v_4 i.e under V_4 gets multiplied by a factor of two and therefore equal to one for more states.
The amount of fixed points is given below every sector and *special* fixed tori are denoted with a subscript s. The rule is that every fixed point that is not a pure Z_4 fixed point must be a special one and enjoys relaxed projection conditions.
Table 4.1 summarizes the amount of fixed points and special fixed points in all sectors.

4.2 The brother phase and special fixed points

The relaxed projection conditions make special fixed points particularly interesting. A state that appears at a fixed point will also appear at the special fixed point in the same sector.
We can now use the knowledge we gained about the *brother phase* and see how the sectors are affected by it: Let us assume the two brother models fulfill all modularity conditions already. Matter originating at a fixed point of the constructing element $g(\theta^k \cdot \omega^l, n_\alpha e_\alpha)$ in one model will get the phase shift ϕ_Δ in the orbifold phase when one projects with an centraliser element $h(\theta^m \cdot \omega^n, n_\beta e_\beta)$ given by

$$\phi_\Delta = e^{\pi i(kn - lm)} \,. \tag{4.2.1}$$

From this we can see that all special fixed points, that are projected with $n = 2$ at a sector with an even l, are not affected by ϕ_Δ while the normal fixed points usually are. Especially in the fifth twisted sector $T(1,0)$ the special fixed points are invariant while the normal ones gets a phase such that the local spectrum is altered. Also the third twisted sector $T(0,2)$ is unique in the sense that it is not affected at all. The detailed argumentation and the effect on all twisted sectors is given in appendix C.1.
As a rule one can see that the untwisted and the $T(0,2)$ sectors as well as the matter at the special fixed points are not affected by the brother phase.
These rules give some control over the spectrum by switching to the brother model and give an intuition what to expect.

Gut Gauge Group	Needed Wilson lines
E_6	3
SO(10)	2
SU(5)	1

Table 4.2: Table of the number of Wilson lines needed to break the GUT gauge group down to the SM gauge group.

4.3 Fixed point degeneracy and the need for Wilson lines

In chapter 3 we found many promising GUT gauge groups that are summarised in table 4.2. If we want to break the gauge group further down at this stage we have to assign Wilson lines.

The geometry we chose allows for four Wilson lines: Two in the first torus since this is the pure $\mathbb{Z}_2$ torus, and one in the second and the third torus each, since there the two basis vectors are identified under a $\mathbb{Z}_4$ rotation. The order of the Wilson lines is obviously in the first torus. But also the other Wilson lines have order 2, since $\mathbb{Z}_4$ has a $\mathbb{Z}_2$ subgroup such that there are space group elements

$$(\omega^2, e_\beta) \cdot (\omega^2, e_\beta) = (\mathbb{1}, \omega^2 e_\beta + e_\beta) = (\mathbb{1}, 0) \quad \text{for } \beta = 3, 4, 5, 6 \tag{4.3.1}$$

forcing the Wilson lines in the second and third torus to be of order two as well.

In the end we have four Wilson lines of order two at disposal. A rough rule of thumb is, that one can break N/2 simple roots of a gauge group with one Wilson line of order N. This means that we need at least one, or up to three Wilson lines to break our GUT models down to SU(3)× SU(2)× U(1). The minimal amount of needed Wilson lines to break to the SM gauge group is also depicted in table 4.2. For the standard model it is also crucial to have three generations of standard model families.

Anyhow, if a family and its conjugate appear in the spectrum i.e. a **16** and a $\overline{\mathbf{16}}$ of SO(10) then one can decouple them from the spectrum of the low energy effective action by assigning a vev to a singlet S or a product of them in the super potential $\mathcal{W}$ of the form

$$\mathcal{W} \supset \mathbf{S}\mathbf{16}\overline{\mathbf{16}} \tag{4.3.2}$$

and give them a mass at the GUT scale. Of course this term has to satisfy all string selection rules found in [30]. But at this point we worry only about the net number of families and the problem of decoupling is not addressed here. In this way one would move away from the *orbifold point* where no field has a vev.

In our calculated spectra, however, it turns out that there is always an even net number of families in the untwisted sector. A look at the degeneracy of the fixed points in table 4.1 reveals that this is always an even number as well. Thus we also have to consider in which tori we should switch on Wilson lines to break the degeneracy down to an odd number. The

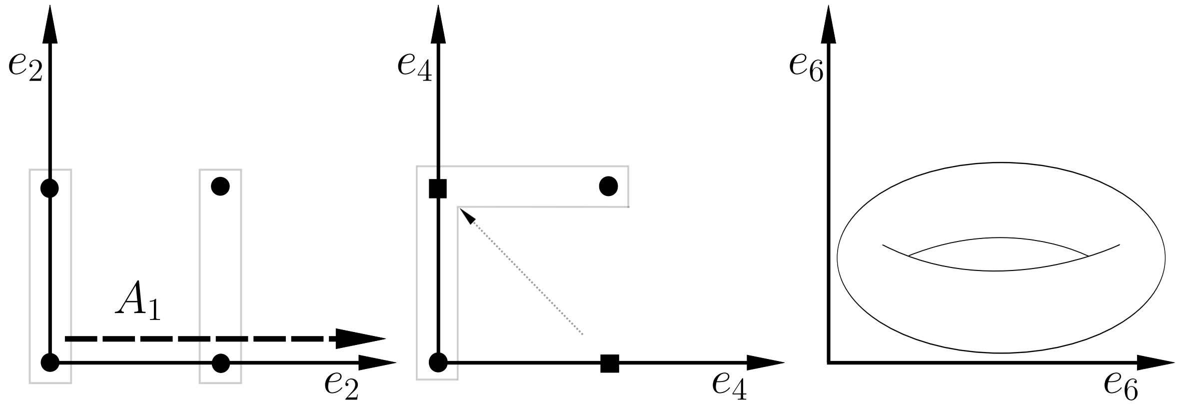

Figure 4.2: The $T(1,0)$ twisted sector with one Wilson line in the e_1 direction. Note that the previous equivalent class of fixed points is now broken into two.

Wilson lines can project out different representations at the various fixed points depending on the local gauge group. Knowing how the degeneracy breaks is extremely useful in the process of selecting models that can in principal lead to three net families without making a brute force search.
To get a good model with three net families and SM model gauge group we used the following strategy:

1. Get schemes how degeneracies break by switching on Wilson lines in various tori.

2. Get matter spectra without Wilson lines.

3. Find models that can have three net families by breaking the fixed point degeneracy via a possible scheme.

4. Get the full spectrum including Wilson lines.

4.3.1 Breaking the fixed point degeneracy with Wilson lines

The introduction of Wilson lines will change all projection conditions and local shits of the fixed points, but we can still collect classes of fixed points that have the same local shifts and the same projection conditions, as we already did when dividing in normal and special fixed points.
An easy example of how the classes of fixed points split by one Wilson line is shown in figure 4.2. The fixed points on the left of the first torus are in one class. The constructing elements of them have no shifts in the direction of the Wilson line A_1. Consequently the local shift of the strings attached to them is not changed. Also all centraliser elements have no element associated with the Wilson line. So let us take the constructing element

$g(\theta, e_2)$. The six generating elements of the centraliser are

1. $h(\theta, e_2)$	2. $h(\omega, 0)$
3. $h(\theta, e_2 + e_5)$	4. $h(\omega, e_5)$
5. $h(\theta, e_2 + e_6)$	6. $h(\omega, e_5 + e_6)$

As one can see there is no element in the e_1 direction, so this fixed point does not feel the Wilson line at all. This is in contrast to the two other fixed points of the first torus. Let us take the constructing element $g(\theta, e_1)$. Its centraliser is

1. $h(\theta, e_1)$	2. $h(\omega, 0)$
3. $h(\theta, e_1 + e_5)$	4. $h(\omega, e_5)$
5. $h(\theta, e_1 + e_6)$	6. $h(\omega, e_5 + e_6)$

This time there are three elements that include the translation in the e_1 direction. For a twisted string at this fixed point, not only the local shifts is changed due to the constructing element but also the twist θ comes always together with a Wilson line, such that the matter and the local gauge group are different to the ones of the first example. In this case the $8 + 4_s$ fixed points in this sector get broken down to $4 + 2_s$ that do not feel the Wilson line at all: Their mass equation is still

$$\frac{M_-^2}{8} = \frac{(P + kV_2 + lV_4)^2}{2} + \tilde{N} - 1 + \delta_c \,,$$

and in this particular case all centralisers do not even include e_1. It has the same matter content as found without the Wilson line. The left-mover mass equation of the other fixed points changes to

$$\frac{M_-^2}{8} = \frac{(P + kV_2 + lV_4 + n_\alpha A_\alpha)^2}{2} + \tilde{N} - 1 + \delta_c \,.$$

Additionally, the centraliser introduces the Wilson lines into the projection, leading to locally different gauge groups. The task is to find a set of Wilson lines that breaks to the SM gauge group, fulfills the modularity conditions and projects out the right amount of families. The analysis of the conditions of states have been done for all 16 combinations and is summarised table 4.3. A deeper analysis can be found in [13]. Table 4.3 shows the 16 combinations of how the four Wilson lines can be switched on. In addition, we give the degeneracy of fixed points where mass equation and projection conditions are the same and unaffected by the Wilson lines.
Since there is the problem that we always have an even number of families we need a Wilson line configuration that breaks the multiplicities to an odd number. To achieve this we need at least two Wilson lines , i.e. schemes 6 and 11. All other configurations with more than two Wilson lines are viable as well.
It should be noticed that these rules are restricted. It is too complicated to see whether there appear some new representations in sectors that are affected by Wilson lines. When

Scheme	W1	W2	W3	W4	$T(0,1\text{or}3)$	$T(0,2)$	$T(1,0)$	$T(1,1\text{or}3)$	$T(1,2)$
1	-	-	-	-	4	4 6	8 4	16	8 4
2	1	-	-	-	4	4 6	4 2	8	4 2
3	-	1	-	-	4	4 6	4 2	8	4 2
4	-	-	1	-	2	2 2 2	4 4	8	8 4
5	-	-	-	1	2	2 2 2	8 4	8	4 4 0
6	1	1	-	-	4	4 6	2 1	4	2 1
7	1	-	-	1	2	2 2 2	2 2	4	4 2
8	1	-	-	1	2	2 2 2	4 2	4	2 2
9	-	1	1	-	2	2 2 2	2 2	4	4 2
10	-	1	-	1	2	2 2 2	4 2	4	2 2
11	-	-	1	1	1	1 3 0	4 4	4	4 4
12	1	1	1	-	2	2 2 2	1 1	2	2 1
13	1	1	-	1	2	2 2 2	2 1	2	1 1
14	1	-	1	1	1	1 3 0	2 2	2	2 2
15	-	1	1	1	1	1 3 0	2 2	2	2 2
16	1	1	1	1	1	1 3 0	1 1	1	1 1

Table 4.3: List of the 16 combinations of Wilson lines and the degeneracies of each fixed point. A 1 signals if the Wilson line is switched on. The numbers in the count how many states do not feel the local shift in the mass equation and have the same projection conditions.

we consider also sectors that are affected by Wilson line projections it is hard to say which representations are projected out, like in the untwisted sector. The values in the table especially the unaffected matter fixed points that posses the full unbroken gauge group. In this way table 4.3 gives an intuition how to assign the Wilson lines. One should also keep in mind that one has to check which representations survive the projection of the Wilson lines. As said, this is very hard to predict and in the end only the complete spectrum gives clarity.

4.4 Program for determining the spectrum

This section briefly discusses a program that calculates the spectrum of our $\mathbb{Z}_2 \times \mathbb{Z}_4$ orbifold model. The detailed description can be found in [13].
A schematic outline is given in figure 4.3. We will get the spectrum in seven steps. Steps 1 and 2 will deal with the right-moving side, determine all the fixed points and solve the mass equations. Steps 3 and 4 specify the left-movers shift embedding and Wilson lines. In the last three steps we join left and right-movers to get the spectrum.

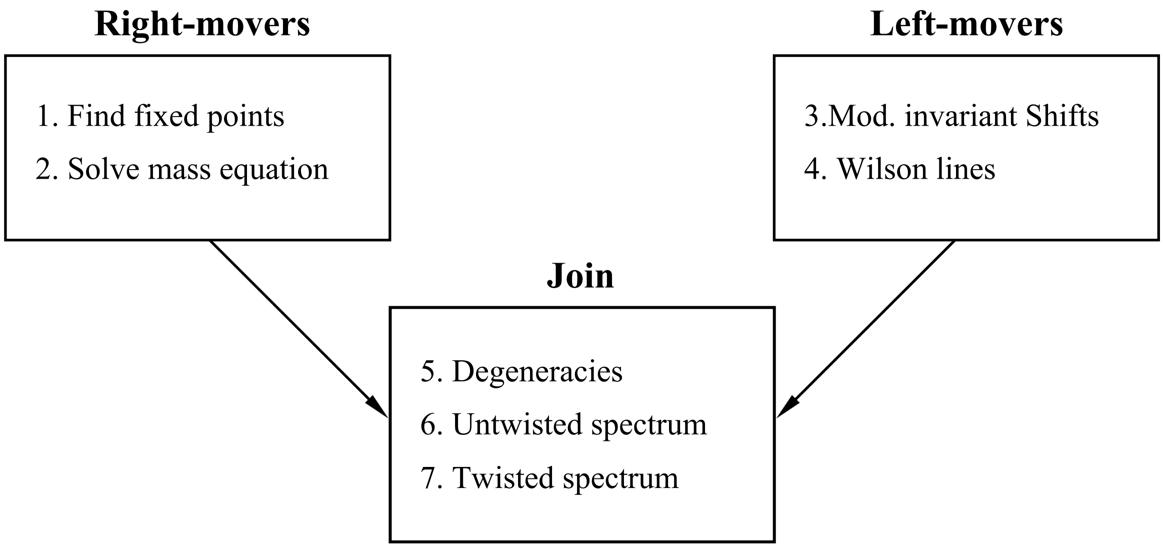

Figure 4.3: The schematic seven steps we followed to get the spectrum.

4.4.1 Right-movers

1. Fixed points
In the first part the twist matrices θ and ω in the lattice basis are specified. Then we assign names to the twisted sectors. After that the fixed points in the fundamental domain and their sets of commuting elements $\mathcal{Z}_g$ is found.

2. Mass equation and phase
The left-mover is a 4 dimensional vector such that the mass equation can easily be solved. This is done for all sectors with all possible oscillator configurations. Finally their scalar products with v_2 and v_4 are calculated which gives a tuple that will be used to compensate the orbifold phase from the right-movers and are of the form $(R \cdot v_2, R \cdot v_4)$ with $R^i = q_s h^i - N^i + \tilde{N}^i$.

4.4.2 Left-movers

3. Choose modular invariant pair and brother model
The information of the 144 inequivalent models is provided as well as the additional phase to cure the third modularity condition and decide a brother model.

4. Fix Wilson lines
Wilson lines which fulfill the modularity conditions (2.5.6a) are introduced and specified in which torus they act.

4.4.3 Join left-and right-movers

5. Wilson lines and degeneracy
Equivalence classes of fixed points that have the same constraints with respect to the mass equation and the projections are identified in order to keep the calculation simple.

6. Calculate untwisted spectrum
The root P of $E_8 \times E_8$ that are orthogonal (mod 1) to the Wilson lines, and satisfy the two conditions

$$(P \cdot V_2, P \cdot V_4) = (R \cdot v_2, R \cdot v_4) = 0 \text{ mod } 1 \tag{4.4.1}$$

for all right-movers R, are found. If the projection conditions are fulfilled, the highest Dynkin label is calculated to identify the representation.

7. Calculate twisted spectrum
The left-movers mass equation is solved according to the algorithm proposed in [31] for every twisted sector and fixed point class. The projection conditions imposed by the centraliser are computed and tried to be solved by an appropriate right-mover. If the state is invariant, the highest Dynkin label with respect to the 4d gauge group is given such that the representation can be identified.

4.5 Models without Wilson lines

In the previous chapter it was made clear how to get the matter spectrum. Following our strategy we first look at the matter spectrum of our models without Wilson lines and then try to apply Wilson lines in one of our schemes from table 4.3 to break down to three families. Some interesting candidates are now presented as well as the the Wilson line configuration needed to break the degeneracy down in the right fashion. However, one should note that it is not trivial to find Wilson lines that fulfill all modularity conditions and break the gauge group as well as the representations in a desired way.

4.5.1 E_6 models

One standard model family can be accommodated in a **27** or a $\overline{\mathbf{27}}$ of E_6. For a general discussion of the GUT groups see appendix B. To keep the discussion simple, only matter that is charged under E_6 is given since all the other matter is charged under the hidden gauge group and will not interact with the standard model matter.
The first example is given in table 4.4 that shows a matter spectrum and how we can control its spectrum. Note that the breaking of the gauge group is not given in the table since we are only interested the right amount of net families. First we switch to the other brother model that adds additional matter content at the normal fixed points of the fifth sector. The three Wilson lines will then break E_6 to SU(3)×SU(2)× U(1)^3 and reduce the

Model: 62, Gauge Group: $\mathbf{E_6}\times$U(1)^2|SO(10)$\times$SU(4)

(a) Matter content at the 8 sectors of model 62.

Twisted Sector	1	2	3	4	5	6	7	8
27 of E_6	1·(**27**)1·($\overline{\mathbf{27}}$)	0	0	0	0	0	0	0
FP. Degeneracy	1	4	4	4	8	16	8	16
27 of E_6	-	-	0	-	1·(**27**)	-	0	-
FP degeneracy$_s$	-	-	6	-	4	-	4	-
Total Amount of **27**'s	1·(**27**)1·($\overline{\mathbf{27}}$)	0	0	0	4·(**27**)	0	0	0

(b) Matter content at the 8 sectors of the brother model and 3 Wilson lines.

Twisted Sector	1	2	3	4	5	6	7	8
27 of E_6	1·(**27**)1·($\overline{\mathbf{27}}$)	0	0	0	1·(**27**)	0	0	0
FP Degeneracy	1	2	2 2	2	2	2	1	2
27 of E_6	-	-	0	0	1·(**27**)	-	0	-
FP Degeneracy$_s$	-	-	2	-	1	-	1	-
Total Amount of **27**'s	1·(**27**)1·($\overline{\mathbf{27}}$)	0	0	0	3·(**27**)	0	0	0

Table 4.4: The effect on the model 62 when switched to the brother model and turned on three Wilson lines. The matter content can be manipulated by switching to the brother model, whereas the degeneracy can be reduced by the three Wilson lines in the first and third torus (scheme 13).

degeneracy of the fixed points. Thus we can have three complete families of E_6 coming from the fifth sector.
Another interesting model is given in table 4.5. This model posses exceptionally many **27**'s. We can also observe the rules we obtained when we switch to the other brother model: While the matter in the second and fourth sector is changed from a **27** to a $\overline{\mathbf{27}}$, the third sector is invariant. This model could be a realistic model, since we have many possible **27** that can source the three families, but it is not clear which scheme we should apply.

4.5.2 SO(10) model

Now let us turn to a promising SO(10) model. This model will also be our benchmark model. Since SO(10) models need only two Wilson lines to break the gauge group down to the SM gauge group they are easier to handle than E_6 models and one has more freedom in them. One SM family can be accommodated in the **16** of SO(10)(see appendix B). Once again we get a **16** in the fifth twisted sector by adding different lattice vectors and obtain the correct fixed point degeneracy by introducing two Wilson lines. Note that the degeneracy of the fifth sector is not affected by assigning a third Wilson line in the fourth

Model: 3, Gauge Group: SO(16)| $\mathbf{E_6}\times$U$(1)^2$

(a) Matter content at the 8 sectors of model 3.

Twisted Sector	1	2	3	4	5	6	7	8
27 of E_6	3·(**27**)1·($\overline{\mathbf{27}}$)	1·($\overline{\mathbf{27}}$)	1·(**27**)	1·($\overline{\mathbf{27}}$)	0	0	0	0
FP. Degeneracy	1	4	4	4	8	16	8	16
27 of E_6 of E_6	-	-	1·(**27**)	-	0	-	0	-
FP. Degeneracy$_s$	-	-	6	-	4	-	4	-
Total Amount of **27**'s	3·(**27**)1·($\overline{\mathbf{27}}$)	4·($\overline{\mathbf{27}}$)	10·($\overline{\mathbf{27}}$)	4·($\overline{\mathbf{27}}$)	0	0	0	0

(b) Matter content at the 8 sectors of the brother model.

Twisted Sector	1	2	3	4	5	6	7	8
27 of E_6	3·(**27**),1·($\overline{\mathbf{27}}$)	1·(**27**)	1·(**27**)	1·(**27**)	0	0	0	0
FP Degeneracy	1	4	4	4	8	16	8	16
27 of E_6	-	-	1·(**27**)	-	0	-	0	-
FP Degeneracy$_s$	-	-	6	-	4	-	4	-
Total Amount of **27**'s	3 ·(**27**)1·($\overline{\mathbf{27}}$)	4·(**27**)	10·($\overline{\mathbf{27}}$)	4·(**27**)	0	0	0	0

Table 4.5: A Model with a big amount of representations and its brother model.

Model 67, Gauge Group: **SO(10)** $\times$U$(1)^3$|SO(10)$\times$SU(4)

(a) Matter content at the 8 sectors of model 67

Sector	1	2	3	4	5	6	7	8
16 of SO(10)	2·(**16**)2·(**16**)	0	0	0	0	0	0	0
FP. Degeneracy	1	4	4	4	8	16	8	16
16 of SO(10)	-	-	0	-	1·(**16**)	-	0	-
FP. Degeneracy$_s$	-	-	6	-	4	-	4	-
Total Amount of **16**'s	2·(**16**)2·(**16**)	0	0	0	4·(**16**)	0	0	0

(b) Matter content at the 8 sectors of the brother model and 2 Wilson lines.

Sector	1	2	3	4	5	6	7	8
16 of SO(10)	2·(**16**)2·($\overline{\mathbf{16}}$)	0	0	0	1·(**16**)	0	0	0
FP. Degeneracy	1	4	4	4	2	4	2	4
16 of SO(10)	-	-	0	-	1·(**16**)	-	0	-
FP. Degeneracy$_s$	-	-	6	-	1	-	1	-
Total Amount of **16**'s	2·(**16**)2·(**16**)	0	0	0	3(·**16**)	0	0	0

Table 4.6: The two brother models of model number 67. Adding a different lattice vector results in getting a **16** in the fifth twisted sector. Introduction of two Wilson lines gives then the right degeneracy to yield three net **16**s in the fifth twisted sector.

Model 104, Gauge Group: SO(12)×SU(2)×U(1)|**SU(5)**×SU(3)×U(1)^2

Twisted Sector	1	2	3	4	5	6	7	8
5 of SU(5)	$1(\mathbf{5},\overline{\mathbf{3}})1(\overline{\mathbf{5}})2(\overline{\mathbf{5}},\mathbf{3})$	$1(\mathbf{2},\mathbf{5})$	$1(\mathbf{5})$	0	$1(\overline{\mathbf{5}},\mathbf{3})$	0	$1(\mathbf{5})$	0
10 of of SU(5)	$1(\mathbf{10})1(\mathbf{10},\mathbf{3})$	0	0	0	0	0	0	0
FP. Degeneracy	1	4	4	4	8	16	8	16
5 of SU(5)	-	-	$2(\mathbf{5})$	-	$1(\overline{\mathbf{5}},\mathbf{3})$	-	$2(\mathbf{5})$	-
10 of SU(5)	-	-	0	-	$1(\overline{\mathbf{10}})$	-	0	-
FP. Degeneracy$_s$	-	-	6	-	4	-	4	-
Total Amount of **5**'s	$1(\mathbf{5},\overline{\mathbf{3}})1(\overline{\mathbf{5}})2(\overline{\mathbf{5}},\mathbf{3})$	$4(\mathbf{2},\mathbf{5})$	$16(\mathbf{5})$	0	$16(\overline{\mathbf{5}},\mathbf{3})$	0	$16(\mathbf{5})$	0
Total Amount of **10**'s	$1(\mathbf{10})1(\mathbf{10},\mathbf{3})$	0	0	0	$4(\overline{\mathbf{10}})$	0	0	0

Table 4.7: An example spectrum of an SU(5) model. The high amount **5**s and **10**s is hard to control with Wilson lines. Additionally it is very likely the matter is charged under the SU(3) or the SU(2) as well, as shown in sector one, two and five.

torus, such that we have many possibilities to further tune the spectrum, while keeping the three **16**s save. We take this as our benchmark model and in section 4.6 we will assign two modular invariant Wilson lines which break the gauge groups to the one of the standard model.

4.5.3 A note on Pati-Salam and SU(5) Models

We also have many SU(5) and SU(4)× SU(2)× SU(2) models in our classification. They are actually closer to the SM than for example E_6, so we should consider them as well.
Looking at these models reveals that all SU(5) groups come with an SU(3) in the same E_8. In all cases there are **5**s in the bulk that are charged under the SU(3) as an example in table 4.7 shows. It turns out that there are always **5**s charged under SU(3) so that one has to break the SU(3) as well[3]. If we want to break the SU(3) with Wilson lines we lose freedom to use them to manipulate other parts of the spectrum. Another disadvantage is that we have to control two types of representations namely the **5**s and the **10**s of SU(5) and it is very difficult to fix the right amount for both of them especially when Wilson lines break the hidden SU(3) which introduces additional matter multiplicities. However this does not mean that these models are hopeless, they are only harder to handle but it is still worthy to do a systematic search in them. The same argumentation holds for Pati-Salam models.
In the end it is the structure of SO(10) and E_6 that makes them exceptionally good GUT candidates. First only one amount of representations has to be controlled and second, the groups are large enough such that there are (mainly) no additional low rank gauge groups in the same E_8 such that it could happen that matter is charged under these groups as well. The SU(5) models could be still interesting for a systematical analysis later, but we

[3]One is not forced to break them with Wilson lines with vevs.

have such a big selection of models that can be broken down to the SM gauge group, that E_6 and SO(10) models are favoured.

4.6 The benchmark model

As a benchmark model we take model 67 and introduce two Wilson lines in the first torus. They are given by

$$A_1 = (\frac{17}{4}, -\frac{17}{4}, -\frac{15}{4}, -\frac{19}{4}, -\frac{15}{4}, -\frac{15}{4}, \frac{5}{4}, \frac{7}{4})(\frac{1}{4}, \frac{1}{4}, -\frac{3}{4}, \frac{1}{4}, -\frac{1}{4}, -\frac{3}{4}, -\frac{1}{4}, \frac{1}{4})$$
$$A_2 = (1, -1, -1, -1, -1, -\frac{1}{2}, 0, \frac{1}{2})(0, \frac{1}{2}, -\frac{1}{2}, \frac{1}{2}, 0, -\frac{1}{2}, \frac{1}{2}, \frac{1}{2})$$

They fulfill all 7 modularity conditions, namely

$$A_1 \cdot A_1 = A_2 \cdot A_2 = A_1 \cdot A_2 = A_1 \cdot V_2 = A_2 \cdot V_2 = A_1 \cdot V_4 = A_2 \cdot V_4 = A_1 \cdot A_2 = 0 \bmod 1$$

The Wilson lines break the gauge group to

$$SO(10)|\underbrace{SO(10) \times SU(4)}_{\text{Hidden}} \xrightarrow{A_1} SU(5)|\underbrace{SU(3) \times SU(5)}_{\text{Hidden}}$$
$$SU(5)|\underbrace{SU(3) \times SU(5)}_{\text{Hidden}} \xrightarrow{A_2} SU(3) \times SU(2)|\underbrace{SU(2) \times SU(4)}_{\text{Hidden}}.$$

Note that the U(1) factors were omitted. The spectrum for this model is given in table 4.8. It shows the 8 sectors and their matter representations with respect to the bulk gauge group. Note that there are 3 complete families in the fifth twisted sector as predicted from the Wilson line scheme. There appears also a lot of other matter in the twisted sectors but this originates mostly from complete **10**s of SO(10) and can be decoupled. From these **10**s we can take the $(\mathbf{1}, \mathbf{2})$ as our Higgses. Also the adjoint matter, e.g. the gauge multiplet, is not shown.

Note that this model has no non-Abelian anomalies. In principal all residual $(\mathbf{3}, \mathbf{1})$ and $(\overline{\mathbf{3}}, \mathbf{1})$ in the spectrum should decouple but for this one needs the U(1) charges which will be subject of further study.

In the end the benchmark model could be a very promising candidate to achieve an MSSM like spectrum. It is very interesting that all SM matter originates from twisted sectors with an SO(10) GUT group which is not the case in the $\mathbb{Z}_2 \times \mathbb{Z}_2$ orbifold in [15].

#	Sector	SM Matter $SU(3) \times SU(2)$	Hidden Matter$SU(2) \times SU(4)$
1	T(0,0)	$4{\cdot}(\overline{\mathbf{3}},\mathbf{1})$ $2{\cdot}(\mathbf{3},\mathbf{1})$ $8{\cdot}(\mathbf{1},\mathbf{1})$	$1{\cdot}(\mathbf{1},\overline{\mathbf{4}})$ $1{\cdot}(\mathbf{1},\mathbf{6})$
2	T(0,1)	$16{\cdot}(\mathbf{1},\mathbf{1})$	
3	T(0,2)	$16{\cdot}(\mathbf{1},\mathbf{1})$	
4	T(0,3)	$8{\cdot}(\mathbf{1},\mathbf{1})$	
6	T(1,1)		
5	T(1,0)	$4{\cdot}(\mathbf{3},\mathbf{1})$ $2{\cdot}(\overline{\mathbf{3}},\mathbf{2})$ $8{\cdot}(\mathbf{1},\mathbf{2})$ $40{\cdot}(\mathbf{1},\mathbf{1})$ $\left.\begin{array}{l} 3\cdot(\overline{\mathbf{3}},\mathbf{2}) \\ 6\cdot(\mathbf{3},\mathbf{1}) \\ 3\cdot(\mathbf{1},\mathbf{2}) \\ 3\cdot(\mathbf{1},\mathbf{1}) \end{array}\right\} \quad 3\cdot(\mathbf{16})_{SO(10)}$	$4{\cdot}(\mathbf{2},\mathbf{1})$ $4{\cdot}(\mathbf{1},\mathbf{4})$
6	T(1,1)		
7	T(1,2)	$1{\cdot}(\mathbf{3},\mathbf{1})$ $1{\cdot}(\overline{\mathbf{3},\mathbf{1}})$ $2{\cdot}(\mathbf{1},\mathbf{2})$ $33{\cdot}(\mathbf{1},\mathbf{1})$	$7{\cdot}(\mathbf{1},\overline{\mathbf{4}})$ $5{\cdot}(\mathbf{1},\mathbf{4})$ $4{\cdot}(\mathbf{2},\mathbf{1})$
8	T(1,3)	$8{\cdot}(\mathbf{1},\mathbf{1})$	$4{\cdot}(\mathbf{2},\mathbf{1})$

Table 4.8: The spectrum of the Benchmark model with two Wilson lines. The twisted sectors are given in the first two columns and matter charged under the SM or hidden gauge group in the third and fourth. Note the three complete families in the fifth twisted sector come from 3 **16**s of local SO(10) GUT points.

Chapter 5

Conclusion

In this work we considered the $E_8 \times E_8$ heterotic string compactified on a $\mathbb{Z}_2 \times \mathbb{Z}_4$ orbifold and asked whether there are models with realistic properties. Modularity of the 1-loop partition function forced us to embed the shifts into the gauge degrees of freedom and thus $E_8 \times E_8$ gets broken. To find realistic models we wanted first to find all embeddings that are inequivalent with respect to the automorphisms of $E_8 \times E_8$. Since E_8 has only inner automorphisms, the whole automorphism group is given by the direct product of the two E_8s, which makes it sufficient to focus on one E_8 and care about modular invariance later. To do so we took the 10 inequivalent $\mathbb{Z}_4$ shifts from [12] and constructed all sets of $\mathbb{Z}_2$ shifts that could not be related by Weyl reflections, that leave the corresponding $\mathbb{Z}_4$ shift invariant, and that could not be related by a lattice shift. Because the whole Weyl group of E_8 is very big we could not check for higher combinations of Weyl reflections. By allowing lattice shifts we broke the strict inequivalence because lattice shifts affect the twisted matter spectrum. In that way we constructed **84** $\mathbb{Z}_2 \times \mathbb{Z}_4$ shifts in one E_8. To eliminate higher equivalent embeddings we removed shifts that led to the same spectra as other ones and gained **75** embeddings in one E_8. When we paired the shifts to $E_8 \times E_8$ vectors in a modular invariant way we got **144** models. We allowed lattice shifts in our classification but this lead to inequivalent spectra in the twisted sectors. Models that differ by lattice vectors in such a way are called *brother models*. The structure of our orbifold allowed only for **two different brother models** .
When we computed the gauge group we found **35 SO(10)** , **26** E_6 and **25 SU(5)** models. In the fourth chapter we introduced the geometry of our factorized SU(2)^2×SO(4)^2 Lie lattice we chose and analyzed its fixed point structure and properties. The analysis showed that the geometry possessed *special* fixed points whose matter enjoyed relaxed projection conditions, in contrast to normal fixed points, and are also invariant under the brother phase.
To achieve a realistic model with three net families and the SM gauge group it was inevitable to introduce Wilson lines. Depending on the way Wilson lines were switched on, we developed a strategy how to find promising candidates. In the following we presented 3 interesting candidates and the way how we could manipulate the matter content. One of them is taken as a benchmark model. We assigned two modular invariant Wilson lines

that break to the SM gauge group in the bulk and got three net families coming from local SO(10) GUT points.
All this shows that $\mathbb{Z}_2 \times \mathbb{Z}_4$ is a very promising orbifold scheme that even has multiple very promising GUT candidates to achieve an MSSM like model.

Outlook

There are still many questions in the benchmark model, that have to be addressed when we want to come closer to MSSM like models. One of them is to get a good global model where we can decouple all unwanted matter. For this we have to check if we can give them a mass term at the level of the effective SUGRA action so we have to know their U(1) charges as well. One of the U(1)s we have is anomalous, which will introduce an *Fayet-Iliopoulos* [33] term in the effective action and introduce vevs for the fields. Of course we have to make sure that the Hypercharge is not anomalous.
Also F-and D-term flatness have to be addressed such that we get a SUSY vacuum configuration. This in turn will affect the geometry and blow up the singularities to a smooth CY manifold what should also be analysed further. A big topic will also be the computation of Yukawa couplings and the search for a $\mathbb{Z}_4^R$-symmetry to forbid unwanted couplings.

Appendix A

Facts about E_8

The group E_8 is the biggest exceptional Lie group. The group is uniquely defined by the geometrical properties of its positive and simple roots which can be graphically expressed through the Dynkin diagram. The smallest non trivial representation of E_8 is the adjoint

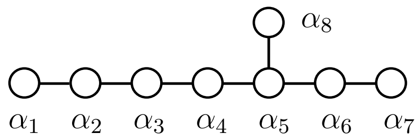

Figure A.1: The Dynkin diagram of E_8

representation which coincides with the fundamental. It is given by all roots of norm squared 2 which are the vectorial roots

$$\underline{(\pm 1, \pm 1, 0, 0, 0, 0, 0, 0)}\,, \tag{A.0.1}$$

giving $4\binom{8}{2} = 112$ combinations and the spinorial roots

$$(\pm\frac{1}{2}, \pm\frac{1}{2}, \pm\frac{1}{2}, \pm\frac{1}{2}, \pm\frac{1}{2}, \pm\frac{1}{2}, \pm\frac{1}{2}, \pm\frac{1}{2},)\,, \tag{A.0.2}$$

with an even number of minus signs such that there are $2\binom{8}{0}+2\binom{8}{2}+\binom{8}{4} = 128$ combinations. Adding the 8 Cartan elements there are 248 elements in the adjoint representation.

Appendix B

Group theoretical GUT breaking

This section is a short summary of the group theoretical breaking of E_6 and its representations down to the standard model. We focus on breaking schemes of GUT groups i.e. E_6, SO(10) and SU(5).
The representations can be systematically labelled by the Dynkin labels. These are the weight vectors μ_j of the given representation multiplied by the positive simple roots α_i of the group G i.e.

$$\Lambda_j^i = 2\frac{\mu_j \cdot \alpha_i}{\alpha_i \cdot \alpha_i},$$

with i=1,..,Rank(G), j=1,..,Dim(Representation).
The highest Dynkin label is then the one with only positive integers. To get the dimensionality of the representation one has to subtract for a positive entry n in the μ^{th} component of the Dynkin label, n times the μ^{th} row of the Cartan-matrix until there are only non-positive entries left. The amount of different Dynkin labels gives the dimensionality of the representation.
The Dynkin label also reflects the symmetry of the Dynkin diagram. E.g. complex conjugation means reflecting the Dynkin diagram along its symmetry axis. A Dynkin label of a given representation gets then transformed into the highest root of the conjugate representation. In this way it is especially easy to see which representations are self adjoint i.e. invariant under relabeling of the components and which ones are conjugate to each other and share the same dimensionality. The reflection of the the roots of the Dynkin diagram is an outer automorphism of the group, such that complex representations are only possible for groups that posses that symmetry. E.g. not the case for E_8.

B.1 E_6

We begin with the discussion of E_6. The Dynkin diagram is given in figure B.1. As one can see from the Dynkin diagram, the lattice has a reflection symmetry and therefore it

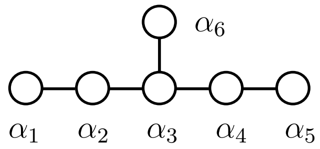

Figure B.1: The Dynkin diagram of E_6

can have complex representations. The most important representations of E_6 are given by

$$
\begin{array}{lll}
(0,0,0,0,0,1) & \mathbf{78} & \text{adjoint}\,, \\
(1,0,0,0,0,0) & \mathbf{27} & \text{fundamental}\,, \\
(0,0,0,0,1,0) & \overline{\mathbf{27}} & \text{anti-fundamental}\,.
\end{array}
$$

B.2 SO(10)

E_6 can be broken down to SO(10) by removing the root[1] $\alpha_5(/\alpha_1)$. The breaking of the Dynkin diagram is graphically depicted in figure B.2. The splitting of the E_6 representa-

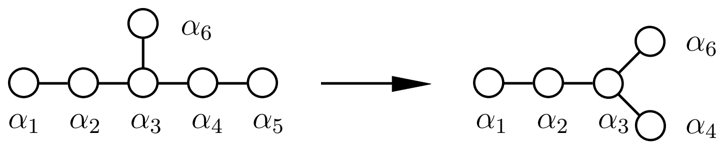

Figure B.2: Splitting of the E_6 Dynkin diagram into the one of SO(10) by deleting one of the exterior roots.

tions into SO(10) representations is then.

$$
\begin{aligned}
&\mathbf{78} \to \mathbf{45} \oplus \mathbf{16} \oplus \overline{\mathbf{16}} \oplus \mathbf{1}\,, \\
&\mathbf{27} \to \mathbf{16} \oplus \mathbf{10} \oplus \mathbf{1}\,.
\end{aligned}
$$

B.3 SU(5)

SO(10) can be further broken down to SU(5) by deleting one of the spinorial roots α_4 or α_5 in the Dynkin diagram. This is depicted in figure B.3. According to the splitting the

[1]For simplicity we do not consider the extended Dynkin diagrams.

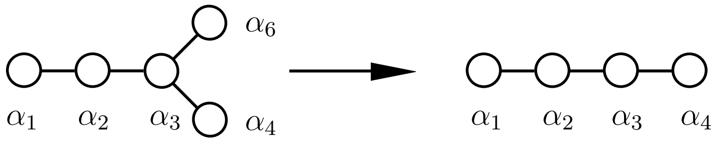

Figure B.3: Splitting of the $SO(10)$ Dynkin diagram into the one of SU(5) by deleting one of the spinorial roots.

representations branch like

$$\begin{aligned}
&\mathbf{45} \to \mathbf{24} \oplus \mathbf{10} \oplus \overline{\mathbf{10}} \oplus \mathbf{1} \\
&\mathbf{16} \to \mathbf{10} \oplus \overline{\mathbf{5}} \oplus \mathbf{1} \\
&\mathbf{10} \to \mathbf{5} \oplus \overline{\mathbf{5}}
\end{aligned}$$

B.4 Standard Model

SU(5) is finally a good candidate to break down to the standard model gauge group SU(3)$\times$ SU(2)$\times$ U(1) by projecting out one of the middle roots α_2 or α_3 shown in figure B.4. The

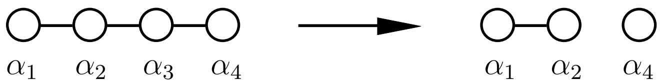

Figure B.4: Splitting of the SU(5) Dynkin diagram to the SM Dynkin diagram with SU(3)$\times$SU(2)$\times$U(1).

representations of SU(5) split according to

$$\begin{aligned}
\mathbf{24} &\to (\mathbf{8},\mathbf{1})_0 \oplus (\mathbf{1},\mathbf{3})_0 \oplus (\mathbf{3},\mathbf{2})_{-\frac{5}{6}} \oplus (\overline{\mathbf{3}},\mathbf{2})_{\frac{5}{6}}\,, \\
\mathbf{5} &\to (\mathbf{3},\mathbf{1})_{-\frac{1}{3}} \oplus (\mathbf{1},\mathbf{2})_{\frac{1}{2}}\,, \\
\overline{\mathbf{10}} &\to (\overline{\mathbf{3}},\mathbf{2})_{-\frac{1}{6}} \oplus (\mathbf{3},\mathbf{1})_{-\frac{2}{3}} \oplus (\mathbf{1},\mathbf{1})_1\,,
\end{aligned}$$

where the subscript denotes the $U(1)$ hypercharge. So from the SU(5) point of view we need one **5** and one $\overline{\mathbf{10}}$. SO(10) unifies the matter further since the **5** and the $\overline{\mathbf{10}}$ of SU(5) are both in a **16** as well as a singlet that can be the right handed neutrino. This SM family as well as a **10** of SO(10) that includes the Higgs, can be accommodated in a **27** of E_6

Appendix C

Change of the orbifold phase under lattice shifts

We define $P_{\text{sh}} = P + V_g$, where the shift vector $V_g = kV_2 + lV_4$ corresponds to constructing element of a fixed point. The shifts according to an element of the centraliser $V_h = mV_2 + nV_4$ gives then the orbifold phase:

$$\phi_o = e^{2\pi i\left(P_{\text{sh}}\cdot V_h - (q_{\text{sh}} - N + \bar{N})\cdot v_h\right) - \frac{1}{2}(V_g\cdot V_h - v_g\cdot v_h)} .$$

When we add lattice vectors α and β to V_2 and V_4 P_{sh} still solves the mass equation. The orbifold phase thus shifts to

$$\begin{aligned}
\phi &= e^{2\pi i\left[P_{\text{sh}}\cdot\tilde{V}_h - R\cdot v_h - \frac{1}{2}(\tilde{V}_g\cdot\tilde{V}_h - v_g\cdot v_h)\right]} ,\\
&= e^{2\pi i\left[P_{\text{sh}}\cdot(V_h + k\alpha + n\beta) - R\cdot v_h - \frac{1}{2}(V_g + k\alpha + l\beta)\cdot(V_h + m\alpha + n\beta) + \frac{1}{2}(v_g\cdot v_h)\right]} ,\\
&= \phi_o e^{2\pi i\left[P_{\text{sh}}\cdot(m\alpha + n\beta) - \frac{1}{2}(V_g\cdot(m\alpha + n\beta) + (k\alpha + l\beta)\cdot V_h + (k\alpha + l\beta)\cdot(m\alpha + n\beta))\right]} ,
\end{aligned}$$

simplifying the expression and using that $P \cdot \alpha \in \mathbb{Z}$ this yields

$$\begin{aligned}
\phi &= \phi_o e^{2\pi i\frac{1}{2}[(kV_2 + lV_4)\cdot(m\alpha + n\beta) - (k\alpha + l\beta)\cdot(mV_2 + nV_4) - kn\alpha\cdot\beta + ml\alpha\cdot\beta]} \\
&= \phi_o e^{2\pi i\frac{1}{2}(kn - lm)[V_2\cdot\beta - V_4\cdot\alpha + \alpha\cdot\beta]} ,
\end{aligned} \tag{C.0.1}$$

where we used that $\alpha \cdot \beta \in \mathbb{Z}$ and therefore that

$$e^{\pi i\alpha\cdot\beta} = e^{-\pi i\alpha\cdot\beta} .$$

When we take the third modularity condition

$$2\left(\tilde{V}_2 \cdot \tilde{V}_4 - v_2 \cdot v_4\right) = M = 0 \bmod 2 ,$$

it changes by the additional lattice vectors to

$$M + 2V_2 \cdot \beta + 2V_4 \cdot \beta + \alpha \cdot \beta = 2\mathbb{Z} ,$$

	1	2	3	4	5	6	7	8
Sector	T(0,0)	T(0,1)	T(0,2)	T(0,3)	T(1,0)	T(1,1)	T(1,2)	T(1,3)
Phase normal fp	$(0,0)$	$(\frac{1}{2},0)$	$(0,0)$	$(\frac{1}{2},0)$	$(0,\frac{1}{2})$	$(\frac{1}{2},\frac{1}{2})$	$(0,\frac{1}{2})$	$(\frac{1}{2},\frac{1}{2})$
Phase special fp	-	-	$(0,0)$	-	$(0,0)$	-	$(0,0)$	-

Table C.1: Brother phase in tuple form for each sector.

such that we can substitute this condition into equation (C.0.1), yielding

$$\tilde{\phi} = \phi_0 e^{2\pi i \frac{1}{2}(kn-lm)\left[2V_2\beta - \mathbb{Z} + \frac{M}{2}\right]} \,. \tag{C.0.2}$$

C.1 Lattice shifts and $\mathbb{Z}_2 \times \mathbb{Z}_4$ sectors

Demanding a trivial orbifold phase (without Wilson lines) translates in the conditions[1]

$$\begin{aligned} m\left(P + \frac{1}{2}kV_2 + \frac{1}{2}lV_4\right) \cdot V_2 =& m(q^i + kv_2^i + lv_4^i - N^i + \bar{N}^i) \cdot v_2^i \mod 1 = mx\,, \\ n\left(P + \frac{1}{2}kV_2 + \frac{1}{2}lV_4\right) \cdot V_4 =& n(q^i + kv_2^i + lv_4^i - N^i + \bar{N}^i) \cdot v_4^i \mod 1 = ny\,. \end{aligned}$$

The left-mover's phase has to be compensated by the right-mover's phase modulo 1. Let us label a right-mover by the two numbers (x,y) that can compensate the phase of a left-mover and give a representation.

If we add a lattice vector to V_2 and V_4, we get the additional phase $e^{\pi i(kn-ml)(2V_2\beta-\mathbb{Z})}$ such that (x,y) is shifted according to table C.1. This table makes clear that the matter at the special fixed points and in the untwisted and T(0,2) sector is always protected.

It turns out that each twisted sector has only one right-mover configuration that solves the mass equation. This means that two brother models will always differ in the matter content in all these points. If the sector has additional special fixed points, then only matter can appear which is always included in that sector. In this way one can use the brother phase to project out matter and let matter from special fixed points also appear/vanish at the normal ones.

[1] The vacuum phase was included.

Appendix D

Tables

Root Number	simple roots
1	$(-\frac{1}{2},+\frac{1}{2},+\frac{1}{2},+\frac{1}{2},+\frac{1}{2},+\frac{1}{2},+\frac{1}{2},-\frac{1}{2})$
2	$(1,-1,0,0,0,0,0,0)$
3	$(0,1,-1,0,0,0,0,0)$
4	$(0,0,1,-1,0,0,0,0)$
5	$(0,0,0,1,-1,0,0,0)$
6	$(0,0,0,0,1,-1,0,0)$
7	$(0,0,0,0,0,1,-1,0)$
8	$(-\frac{1}{2},-\frac{1}{2},-\frac{1}{2},-\frac{1}{2},+\frac{1}{2},+\frac{1}{2},+\frac{1}{2},+\frac{1}{2})$

Table D.1: Our choice of the simple roots of E_8.

$4V_{\mathbb{Z}_4}$	$2V_{\mathbb{Z}_2}$	Group Decomposition	
$(0,0,0,0,0,0,0,0)$	$(0,0,0,0,0,0,0,0)$	E_8	
	$(-1,0,0,0,0,0,1,0)$	$E_7\times$SU(2)	
	$(-1,-1,-1,0,0,0,0,1)$	SO(16)	
(2,2,0,0,0,0,0,0)	$(0,0,0,0,0,0,0,0)$	$E_7\times$SU(2)	
	$(-1,1,0,0,0,0,0,0)$	$E_7\times$SU(2)	
	$(-1,0,0,0,0,0,1,0)$	$E_6\times$U(1)^2	
	$(-1,1,0,0,0,0,0,0)$	SO(12)$\times$SU(2)^2	
	$(-1,-1,-1,0,0,0,0,1)$	SO(12)$\times$SU(2)^2	
	$(-1,0,-1,-1,0,0,0,1)$	SU(8)$\times$U(1)	

$4V_{\mathbb{Z}_4}$	$2V_{\mathbb{Z}_2}$	Group Decomposition	
(1, 1, 0, 0, 0, 0, 0, 0)	$(0,0,0,0,0,0,0,0)$	$E_7\times$U(1)	
	$(-1,1,0,0,0,0,0,0)$	$E_7\times$U(1)	
	$(-1,0,0,0,0,0,1,0)$	$E_6\times$U(1)^2	
	$(-1,1,0,0,0,0,0,0)$	SO(12)$\times$SU(2)$\times$U(1)	
	$(-1,-1,-1,0,0,0,0,1)$	SO(12)$\times$SU(2)$\times$U(1)	
	$(-1,0,-1,-1,0,0,0,1)$	SU(8)$\times$U(1)	
(2,1,1,0,0,0,0,0)	$(0,0,0,0,0,0,0,0)$	$E_6\times$SU(2)$\times$U(1)	
	$(-1,0,1,0,0,0,0,0)$	$E_6\times$U(1)^2	
	$(-1,0,0,0,0,0,1,0)$	SO(10)$\times$SU(2)$\times$U(1)^2	
	$(-1,0,1,0,0,0,0,0)$	SO(10)$\times$U(1)^3	
	$(0,0,0,-1,0,0,1,0)$	SU(6)$\times$SU(2)$^2\times$U(1)	
	$(0,-1,1,0,0,0,0,0)$	$E_6\times$SU(2)$\times$U(1)	
	$(-1,-1,-1,0,0,0,0,1)$	SO(10)$\times$SU(2)$\times$U(1)^2	
	$(-1,-1,0,-1,0,0,0,1)$	SU(6)$\times$SU(2)$\times$U(1)^2	
	$(-1,0,0,-1,-1,0,0,1)$	SU(6)$\times$SU(2)$^2\times$U(1)	
(4,0,0,0,0,0,0,0)	$(0,0,0,0,0,0,0,0)$	SO(16)	
	$(-1,0,0,0,0,0,1,0)$	SO(12)$\times$SU(2)^2	**A**
	$(-\frac{1}{2},-\frac{1}{2},-\frac{1}{2},-\frac{1}{2},-\frac{1}{2},-\frac{1}{2},\frac{1}{2},\frac{1}{2})$	SU(8)$\times$U(1)	
	$(0,-1,0,0,0,0,1,0)$	SO(12)$\times$SU(2)^2	**A**
	$(0,0,0,0,0,-2,0,0)$	SO(16)	
	$(-\frac{3}{2},-\frac{1}{2},-\frac{1}{2},\frac{1}{2},\frac{1}{2},\frac{1}{2},\frac{1}{2},\frac{1}{2})$	SU(8)$\times$U(1)	
	$(-1,-1,-1,0,0,0,0,1)$	SO(8)^2	
(2,0,0,0,0,0,0,0)	$(0,0,0,0,0,0,0,0)$	SO(14)$\times$U(1)	
	$(-1,0,0,0,0,0,1,0)$	SO(12)$\times$U(1)^2	
	$(-\frac{1}{2},-\frac{1}{2},-\frac{1}{2},-\frac{1}{2},-\frac{1}{2},-\frac{1}{2},\frac{1}{2},\frac{1}{2})$	SU(7)$\times$U(1)^2	
	$(0,-1,0,0,0,0,1,0)$	SO(10)$\times$SU(2)$^2\times$U(1)	
	$(0,0,0,0,0,-2,0,0)$	SO(14)$\times$U(1)	
	$(-\frac{3}{2},-\frac{1}{2},-\frac{1}{2},\frac{1}{2},\frac{1}{2},\frac{1}{2},\frac{1}{2},\frac{1}{2})$	SU(7)$\times$U(1)^2	
	$(-1,-1,-1,0,0,0,0,1)$	SU(4)$\times$SO(8)$\times$U(1)	
(3,1,0,0,0,0,0,0)	$(0,0,0,0,0,0,0,0)$	SO(12)$\times$SU(2)$\times$U(1)	
	$(-1,1,0,0,0,0,0,0)$	SO(12)$\times$SU(2)$\times$U(1)	
	$(-1,0,0,0,0,0,1,0)$	SO(10)$\times$U(1)^3	**A**
	$(-1,1,0,0,0,0,0,0)$	SO(12)$\times$SU(2)$\times$U(1)	
	$(-\frac{1}{2},-\frac{1}{2},-\frac{1}{2},-\frac{1}{2},-\frac{1}{2},-\frac{1}{2},\frac{1}{2},\frac{1}{2})$	SU(6)$\times$U(1)^3	
	$(-\frac{1}{2},\frac{1}{2},-\frac{1}{2},-\frac{1}{2},-\frac{1}{2},-\frac{1}{2},-\frac{1}{2},\frac{1}{2})$	SU(6)$\times$SU(2)$\times$U(1)^2	
	$(0,-1,0,0,0,0,1,0)$	SO(10)$\times$U(1)^3	**A**
	$(0,0,-1,0,0,0,1,0)$	SO(8)$\times$SU(2)$^3\times$U(1)	
	$(0,0,0,0,0,-2,0,0)$	SO(12)$\times$SU(2)$\times$U(1)	
	$(-\frac{3}{2},-\frac{1}{2},-\frac{1}{2},\frac{1}{2},\frac{1}{2},\frac{1}{2},\frac{1}{2},\frac{1}{2})$	SU(6)$\times$SU(2)$\times$U(1)^2	
	$(-\frac{3}{2},\frac{1}{2},-\frac{1}{2},-\frac{1}{2},\frac{1}{2},\frac{1}{2},\frac{1}{2},\frac{1}{2})$	SU(6)$\times$U(1)^3	
	$(-1,-1,-1,0,0,0,0,1)$	SO(8)$\times$SU(2)^3 $\times$U(1)	
	$(-1,0,-1,-1,0,0,0,1)$	SU(4)$^2\times$U(1)^2	

$4V_{\mathbb{Z}_4}$	$2V_{\mathbb{Z}_4}$	Group Decomposition	
(2,2,2,0,0,0,0,0)	$(0,0,0,0,0,0,0,0)$	SO(10)×SU(4)	
	$(-1,-1,0,0,0,0,0,0)$	SO(10)×SU(2)^2×U(1)	**A**
	$(-1,0,0,0,0,0,1,0)$	SO(8)×SU(2)^2×U(1)^2	
	$(-1,0,1,0,0,0,0,0)$	SO(10)×SU(2)^2×U(1)	**A**
	$(-\frac{1}{2},-\frac{1}{2},-\frac{1}{2},-\frac{1}{2},-\frac{1}{2},-\frac{1}{2},\frac{1}{2},\frac{1}{2})$	SU(5)×SU(3)×U(1)^2	**B**
	$(-\frac{1}{2},-\frac{1}{2},\frac{1}{2},-\frac{1}{2},-\frac{1}{2},-\frac{1}{2},-\frac{1}{2},\frac{1}{2})$	SU(5)×SU(3)×U(1)^2	**B**
	$(0,0,0,-1,0,0,1,0)$	SU(4)^2×SU(2)^2	
	$(0,0,0,0,0,-2,0,0)$	SO(10)×SU(4)	
	$(-\frac{3}{2},-\frac{1}{2},-\frac{1}{2},\frac{1}{2},\frac{1}{2},\frac{1}{2},\frac{1}{2},\frac{1}{2})$	SU(5)×SU(3)×U(1)^2	**C**
	$(-\frac{3}{2},\frac{1}{2},\frac{1}{2},-\frac{1}{2},-\frac{1}{2},\frac{1}{2},\frac{1}{2},\frac{1}{2})$	SU(5)×SU(3)×U(1)^2	**C**
	$(-1,-1,-1,0,0,0,0,1)$	SO(8)×SU(4)×U(1)	
	$(-1,-1,0,-1,0,0,0,1)$	SU(4)×SU(2)^4×U(1)	
(3,1,1,1,1,1,0,0)	$(0,0,0,0,0,0,0,0)$	SU(8)×SU(2)	
	$(-1,-1,0,0,0,0,0,0)$	SU(6)×SU(2)^2×U(1)	**A**
	$(-1,0,0,0,0,0,1,0)$	SU(6)×SU(2)×U(1)^2	**B**
	$(-1,0,0,0,0,1,0,0)$	SU(4)^2×SU(2)×U(1)	
	$(0,-1,0,0,0,0,1,0)$	SU(6)×SU(2)×U(1)^2	**B**
	$(0,-1,0,0,0,1,0,0)$	SU(6)×SU(2)^2×U(1)	**A**
	$(0,0,0,0,0,0,-1,1)$	SU(8)×SU(2)	
	$(-1,0,0,1,-1,1,0,0)$	SU(6)×SU(2)^2×U(1)	**C**
	$(-\frac{1}{2},-\frac{3}{2},\frac{1}{2},\frac{1}{2},\frac{1}{2},\frac{1}{2},-\frac{1}{2},\frac{1}{2})$	SU(8)×U(1)	
	$(-1,-1,-1,0,0,0,0,1)$	SU(4)^2×U(1)^2	
	$(0,-1,-1,0,0,0,-1,1)$	SU(4)^2×SU(2)×U(1)	
	$(0,0,1,-1,-1,-1,0,0)$	SU(6)×SU(2)^2×U(1)	**C**
(1,1,1,1,1,1,1,-1)	$(0,0,0,0,0,0,0,0)$	SU(8)×U(1)	
	$(0,0,0,0,-1,-1,0,0)$	SU(6)×SU(2)×U(1)^2	
	$(-1,0,0,0,0,0,1,0)$	SU(6)×SU(2)×U(1)^2	
	$(-\frac{1}{2},-\frac{1}{2},-\frac{1}{2},-\frac{1}{2},-\frac{1}{2},-\frac{1}{2},\frac{1}{2},\frac{1}{2})$	SU(7)×U(1)^2	
	$(-\frac{1}{2},-\frac{1}{2},-\frac{1}{2},-\frac{1}{2},\frac{1}{2},\frac{1}{2},\frac{1}{2},\frac{1}{2})$	SU(5)×SU(3)×U(1)^2	
	$(0,0,0,0,0,-2,0,0)$	SU(8)×U(1)	
	$(-\frac{1}{2},\frac{1}{2},\frac{1}{2},\frac{1}{2},\frac{1}{2},-\frac{3}{2},\frac{1}{2},-\frac{1}{2})$	SU(7)×U(1)^2	
	$(-\frac{1}{2},-\frac{1}{2},-\frac{1}{2},-\frac{1}{2},\frac{1}{2},-\frac{3}{2},\frac{1}{2},\frac{1}{2})$	SU(5)×SU(3)×U(1)^2	
	$(-1,-1,-1,0,0,0,0,1)$	SU(4)^2×U(1)^2	

Table D.2: Possible shift vectors and their gauge groups in one E_8. The same letter in the last column shows shifts leading to an equivalent spectrum.

M #	$V_{4,f}$:$(0,0,0,0,0,0,0,0)(1,1,0,0,0,0,0,0)$	M	Gauge Group
1	$(0,0,0,0,0,0,0,0)(-1,0,0,0,0,0,1,0)$	0	$E_8 \vert E_6 \times \mathrm{U}(1)^2$
2	$(-1,0,0,0,0,0,1,0)(-1,0,-1,-1,0,0,0,1)$	0	$E_7 \times \mathrm{SU}(2) \vert \mathrm{SU}(8) \times \mathrm{U}(1)$
3	$(-1,-1,-1,0,0,0,0,1)(-1,0,0,0,0,0,1,0)$	0	$\mathrm{SO}(16) \vert\ E_6 \times \mathrm{U}(1)^2$
	$V_{4,f}$: $(0,0,0,0,0,0,0,0)(3,1,0,0,0,0,0,0)$		
4	$(0,0,0,0,0,0,0,0)(-1,0,0,0,0,0,1,0)$	$-\frac{1}{2}$	$E_8 \vert \mathrm{SO}(10) \times \mathrm{U}(1)^3$
5	$(0,0,0,0,0,0,0,0)(-\frac{1}{2},\frac{1}{2},-\frac{1}{2},-\frac{1}{2},-\frac{1}{2},-\frac{1}{2},-\frac{1}{2},\frac{1}{2})$	0	$E_8 \vert \mathrm{SU}(6) \times \mathrm{SU}(2) \times \mathrm{U}(1)^2$
6	$(-1,0,0,0,0,0,1,0)(-\frac{3}{2},-\frac{1}{2},-\frac{1}{2},\frac{1}{2},\frac{1}{2},\frac{1}{2},\frac{1}{2},\frac{1}{2})$	-1	$E_7 \times \mathrm{SU}(2) \vert \mathrm{SU}(6) \times \mathrm{SU}(2) \times \mathrm{U}(1)^2$
7	$(-1,0,0,0,0,0,1,0)(-1,0,-1,-1,0,0,0,1)$	$-\frac{1}{2}$	$E_7 \times \mathrm{SU}(2) \vert \mathrm{SU}(4)^2 \times \mathrm{U}(1)^2$
8	$(-1,-1,-1,0,0,0,0,1)(-1,0,0,0,0,0,1,0)$	$-\frac{1}{2}$	$\mathrm{SO}(16) \vert \mathrm{SO}(10) \times \mathrm{U}(1)^3$
9	$(-1,-1,-1,0,0,0,0,1)(-\frac{1}{2},\frac{1}{2},-\frac{1}{2},-\frac{1}{2},-\frac{1}{2},-\frac{1}{2},-\frac{1}{2},\frac{1}{2})$	0	$\mathrm{SO}(16) \vert \mathrm{SU}(6) \times \mathrm{SU}(2) \times \mathrm{U}(1)^2$
	$V_{4,f}$: $(2,2,0,0,0,0,0,0)(1,1,0,0,0,0,0,0)$		
10	$(0,0,0,0,0,0,0,0)(-1,0,0,0,0,0,1,0)$	0	$E_7 \times \mathrm{SU}(2) \vert E_6 \times \mathrm{U}(1)^2$
11	$(-1,-1,0,0,0,0,0,0)(-1,0,-1,-1,0,0,0,1)$	-1	$E_7 \times \mathrm{SU}(2) \vert \mathrm{SU}(8) \times \mathrm{U}(1)$
12	$(-1,0,0,0,0,0,1,0)(-1,0,-1,-1,0,0,0,1)$	$-\frac{1}{2}$	$E_6 \times \mathrm{U}(1)^2 \vert \mathrm{SU}(8) \times \mathrm{U}(1)$
13	$(-1,1,0,0,0,0,0,0)(-1,0,-1,-1,0,0,0,1)$	0	$\mathrm{SO}(12) \times \mathrm{SU}(2)^2 \vert \mathrm{SU}(8) \times \mathrm{U}(1)$
14	$(-1,-1,-1,0,0,0,0,1)(-1,0,0,0,0,0,1,0)$	-1	$\mathrm{SO}(12) \times \mathrm{SU}(2)^2 \vert\ E_6 \times \mathrm{U}(1)^2$
15	$(-1,0,-1,-1,0,0,0,1)(-1,0,0,0,0,0,1,0)$	$-\frac{1}{2}$	$\mathrm{SU}(8) \times \mathrm{U}(1) \vert E_6 \times \mathrm{U}(1)^2$
	$V_{4,f}$: $(2,2,0,0,0,0,0,0)(3,1,0,0,0,0,0,0)$		
16	$(0,0,0,0,0,0,0,0)(-1,0,0,0,0,0,1,0)$	$-\frac{1}{2}$	$E_7 \times \mathrm{SU}(2) \vert \mathrm{SO}(10) \times \mathrm{U}(1)^3$
17	$(0,0,0,0,0,0,0,0)(-\frac{1}{2},\frac{1}{2},-\frac{1}{2},-\frac{1}{2},-\frac{1}{2},-\frac{1}{2},-\frac{1}{2},\frac{1}{2})$	0	$E_7 \times \mathrm{SU}(2) \vert \mathrm{SU}(6) \times \mathrm{SU}(2) \times \mathrm{U}(1)^2$
18	$(-1,-1,0,0,0,0,0,0)(-\frac{3}{2},-\frac{1}{2},-\frac{1}{2},\frac{1}{2},\frac{1}{2},\frac{1}{2},\frac{1}{2},\frac{1}{2})$	-2	$E_7 \times \mathrm{SU}(2) \vert \mathrm{SU}(6) \times \mathrm{SU}(2) \times \mathrm{U}(1)^2$
19	$(-1,-1,0,0,0,0,0,0)(-1,0,-1,-1,0,0,0,1)$	$-\frac{3}{2}$	$E_7 \times \mathrm{SU}(2) \vert \mathrm{SU}(4)^2 \times \mathrm{U}(1)^2$
20	$(-1,0,0,0,0,0,1,0)(-\frac{3}{2},-\frac{1}{2},-\frac{1}{2},\frac{1}{2},\frac{1}{2},\frac{1}{2},\frac{1}{2},\frac{1}{2})$	$-\frac{3}{2}$	$E_6 \times \mathrm{U}(1)^2 \vert \mathrm{SU}(6) \times \mathrm{SU}(2) \times \mathrm{U}(1)^2$
21	$(-1,0,0,0,0,0,1,0)(-1,0,-1,-1,0,0,0,1)$	-1	$E_6 \times \mathrm{U}(1)^2 \vert \mathrm{SU}(4)^2 \times \mathrm{U}(1)^2$
22	$(-1,1,0,0,0,0,0,0)(-\frac{3}{2},-\frac{1}{2},-\frac{1}{2},\frac{1}{2},\frac{1}{2},\frac{1}{2},\frac{1}{2},\frac{1}{2})$	-1	$\mathrm{SO}(12) \times \mathrm{SU}(2)^2 \vert \mathrm{SU}(6) \times \mathrm{SU}(2) \times \mathrm{U}(1)^2$
23	$(-1,1,0,0,0,0,0,0)(-1,0,-1,-1,0,0,0,1)$	$-\frac{1}{2}$	$\mathrm{SO}(12) \times \mathrm{SU}(2)^2 \vert \mathrm{SU}(4)^2 \times \mathrm{U}(1)^2$
24	$(-1,-1,-1,0,0,0,0,1)(-1,0,0,0,0,0,1,0)$	$-\frac{3}{2}$	$\mathrm{SO}(12) \times \mathrm{SU}(2)^2 \vert \mathrm{SO}(10) \times \mathrm{U}(1)^3$
25	$(-1,-1,-1,0,0,0,0,1)(-\frac{1}{2},\frac{1}{2},-\frac{1}{2},-\frac{1}{2},-\frac{1}{2},-\frac{1}{2},-\frac{1}{2},\frac{1}{2})$	-1	$\mathrm{SO}(12) \times \mathrm{SU}(2)^2 \vert \mathrm{SU}(6) \times \mathrm{SU}(2) \times \mathrm{U}(1)^2$
26	$(-1,0,-1,-1,0,0,0,1)(-1,0,0,0,0,0,1,0)$	-1	$\mathrm{SU}(8) \times \mathrm{U}(1) \vert \mathrm{SO}(10) \times \mathrm{U}(1)^3$
27	$(-1,0,-1,-1,0,0,0,1)(-\frac{1}{2},\frac{1}{2},-\frac{1}{2},-\frac{1}{2},-\frac{1}{2},-\frac{1}{2},-\frac{1}{2},\frac{1}{2})$	$-\frac{1}{2}$	$\mathrm{SU}(8) \times \mathrm{U}(1) \vert \mathrm{SU}(6) \times \mathrm{SU}(2) \times \mathrm{U}(1)^2$
	$V_{4,f}$: $(1,1,0,0,0,0,0,0)(4,0,0,0,0,0,0,0)$		
28	$(-1,0,0,0,0,0,1,0)(0,0,0,0,0,0,0,0)$	0	$E_6 \times \mathrm{U}(1)^2 \vert \mathrm{SO}(16)$
29	$(-1,0,0,0,0,0,1,0)(0,0,0,0,0,-2,0,0)$	0	$E_6 \times \mathrm{U}(1)^2 \vert \mathrm{SO}(16)$
30	$(-1,0,0,0,0,0,1,0)(-\frac{3}{2},-\frac{1}{2},-\frac{1}{2},\frac{1}{2},\frac{1}{2},\frac{1}{2},\frac{1}{2},\frac{1}{2})$	$-\frac{3}{2}$	$E_6 \times \mathrm{U}(1)^2 \vert \mathrm{SU}(8) \times \mathrm{U}(1)$
31	$(-1,0,0,0,0,0,1,0)(-1,-1,-1,0,0,0,0,1)$	-1	$E_6 \times \mathrm{U}(1)^2 \vert \mathrm{SO}(8) \times \mathrm{SO}(8)$
32	$(-1,0,-1,-1,0,0,0,1)(-1,0,0,0,0,0,1,0)$	-1	$\mathrm{SU}(8) \times \mathrm{U}(1) \vert \mathrm{SO}(12) \times \mathrm{SU}(2)2$
33	$(-1,0,-1,-1,0,0,0,1)(-\frac{1}{2},-\frac{1}{2},-\frac{1}{2},-\frac{1}{2},-\frac{1}{2},-\frac{1}{2},\frac{1}{2},\frac{1}{2})$	$-\frac{1}{2}$	$\mathrm{SU}(8) \times \mathrm{U}(1) \vert \mathrm{SU}(8) \times \mathrm{U}(1)$

M #	$V_{4,f}$:$(1,1,0,0,0,0,0,0)(1,1,1,1,1,1,1,-1)$	M	Gauge Group
34	$(0,0,0,0,0,0,0,0)(-\frac{1}{2},-\frac{1}{2},-\frac{1}{2},-\frac{1}{2},-\frac{1}{2},-\frac{1}{2},\frac{1}{2},\frac{1}{2})$	$-\frac{1}{2}$	$E_7\times\mathrm{U}(1)\|SU(5)$
35	$(0,0,0,0,0,0,0,0)(-\frac{1}{2},-\frac{1}{2},-\frac{1}{2},-\frac{1}{2},\frac{1}{2},\frac{1}{2},\frac{1}{2},\frac{1}{2})$	0	$E_7\times\mathrm{U}(1)\|\mathrm{SU}(5)\times\mathrm{SU}(3)\times\mathrm{U}(1)^2$
36	$(-1,-1,0,0,0,0,0,0)(-\frac{1}{2},\frac{1}{2},\frac{1}{2},\frac{1}{2},\frac{1}{2},-\frac{3}{2},\frac{1}{2},-\frac{1}{2})$	0	$E_7\times\mathrm{U}(1)\|\mathrm{SU}(7)\times\mathrm{U}(1)^2$
37	$(-1,-1,0,0,0,0,0,0)(-\frac{1}{2},-\frac{1}{2},-\frac{1}{2},-\frac{1}{2},\frac{1}{2},-\frac{3}{2},\frac{1}{2},\frac{1}{2})$	-1	$E_7\times\mathrm{U}(1)\|\mathrm{SU}(5)\times\mathrm{SU}(3)\times\mathrm{U}(1)^2$
38	$(-1,0,0,0,0,0,1,0)(0,0,0,0,0,0,0,0)$	0	$E_6\times\mathrm{U}(1)^2\|\mathrm{SU}(8)\times\mathrm{U}(1)$
39	$(-1,0,0,0,0,0,1,0)(0,0,0,0,0,-2,0,0)$	$-\frac{1}{2}$	$E_6\times\mathrm{U}(1)^2\|\mathrm{SU}(8)\times\mathrm{U}(1)$
40	$(-1,0,0,0,0,0,1,0)(-1,-1,-1,0,0,0,0,1)$	-1	$E_6\times\mathrm{U}(1)\|\mathrm{SU}(4)^2\times\mathrm{U}(1)^2$
41	$(-1,1,0,0,0,0,0,0)(-\frac{1}{2},\frac{1}{2},\frac{1}{2},\frac{1}{2},\frac{1}{2},-\frac{3}{2},\frac{1}{2},-\frac{1}{2})$	$\frac{1}{2}$	$\mathrm{SO}(12)\times\mathrm{SU}(2)\times\mathrm{U}(1)\|\mathrm{SU}(7)\times\mathrm{U}(1)^2$
42	$(-1,1,0,0,0,0,0,0)(-\frac{1}{2},-\frac{1}{2},-\frac{1}{2},-\frac{1}{2},\frac{1}{2},-\frac{3}{2},\frac{1}{2},\frac{1}{2})$	$-\frac{1}{2}$	$\mathrm{SO}(12)\times\mathrm{SU}(2)\times\mathrm{U}(1)\|\mathrm{SU}(5)\times\mathrm{SU}(3)\times\mathrm{U}(1)^2$
43	$(-1,-1,-1,0,0,0,0,1)(-\frac{1}{2},-\frac{1}{2},-\frac{1}{2},-\frac{1}{2},-\frac{1}{2},-\frac{1}{2},\frac{1}{2},\frac{1}{2})$	-1	$\mathrm{SO}(12)\times\mathrm{SU}(2)\times\mathrm{U}(1)\|\mathrm{SU}(7)\times\mathrm{U}(1)^2$
44	$(-1,-1,-1,0,0,0,0,1)(-\frac{1}{2},-\frac{1}{2},-\frac{1}{2},-\frac{1}{2},\frac{1}{2},\frac{1}{2},\frac{1}{2},\frac{1}{2})$	$-\frac{1}{2}$	$\mathrm{SO}(12)\times\mathrm{SU}(2)\times\mathrm{U}(1)\|\mathrm{SU}(5)\times\mathrm{SU}(3)\times\mathrm{U}(1)^2$
45	$(-1,0,-1,-1,0,0,0,1)(0,0,0,0,-1,-1,0,0)$	$-\frac{1}{2}$	$\mathrm{SU}(8)\times\mathrm{U}(1)\|\mathrm{SU}(6)\times\mathrm{SU}(2)\times\mathrm{U}(1)^2$
46	$(-1,0,-1,-1,0,0,0,1)(-1,0,0,0,0,0,1,0)$	0	$\mathrm{SU}(8)\times\mathrm{U}(1)\|\mathrm{SU}(6)\times\mathrm{SU}(2)\times\mathrm{U}(1)^2$
	$V_{4,f}$: $(2,1,1,0,0,0,0,0)(2,0,0,0,0,0,0,0)$		
47	$(0,0,0,0,0,0,0,0)(-\frac{1}{2},-\frac{1}{2},-\frac{1}{2},-\frac{1}{2},-\frac{1}{2},-\frac{1}{2},\frac{1}{2},\frac{1}{2})$	0	$E_6\times\mathrm{SU}(2)\times\mathrm{U}(1)\|\mathrm{SU}(7)\times\mathrm{U}(1)^2$
48	$(-1,-1,0,0,0,0,0,0)(0,0,0,0,0,0,0,0)$	$-\frac{1}{2}$	$E_6\times\mathrm{U}(1)^2\|\mathrm{SO}(14)\times\mathrm{U}(1)$
49	$(-1,-1,0,0,0,0,0,0)(0,0,0,0,0,-2,0,0)$	$-\frac{1}{2}$	$E_6\times\mathrm{U}(1)^2\|\mathrm{SO}(14)\times\mathrm{U}(1)$
50	$(-1,-1,0,0,0,0,0,0)(-1,-1,-1,0,0,0,0,1)$	-1	$E_6\times\mathrm{U}(1)^2\|\mathrm{SO}(8)\times\mathrm{SU}(4)\times\mathrm{U}(1)$
51	$(-1,0,0,0,0,0,1,0)(-\frac{3}{2},-\frac{1}{2},-\frac{1}{2},\frac{1}{2},\frac{1}{2},\frac{1}{2},\frac{1}{2},\frac{1}{2})$	-1	$\mathrm{SO}(10)\times\mathrm{SU}(2)\times\mathrm{U}(1)^2\|\mathrm{SU}(7)\times\mathrm{U}(1)^2$
52	$(-1,0,1,0,0,0,0,0)(0,0,0,0,0,0,0,0)$	0	$\mathrm{SO}(10)\times\mathrm{U}(1)^3\|\mathrm{SO}(14)\times\mathrm{U}(1)$
53	$(-1,0,1,0,0,0,0,0)(0,0,0,0,0,-2,0,0)$	0	$\mathrm{SO}(10)\times\mathrm{U}(1)^3\|\mathrm{SO}(14)\times\mathrm{U}(1)$
54	$(-1,0,1,0,0,0,0,0)(-1,-1,-1,0,0,0,0,1)$	$-\frac{1}{2}$	$\mathrm{SO}(10)\times\mathrm{U}(1)^3\|\mathrm{SO}(8)\times\mathrm{SU}(4)\times\mathrm{U}(1)$
55	$(0,0,0,-1,0,0,1,0)(-\frac{3}{2},-\frac{1}{2},-\frac{1}{2},\frac{1}{2},\frac{1}{2},\frac{1}{2},\frac{1}{2},\frac{1}{2})$	$-\frac{1}{2}$	$\mathrm{SU}(6)\times\mathrm{SU}(2)^2\times\mathrm{U}(1)\|\mathrm{SU}(7)\times\mathrm{U}(1)^2$
56	$(0,-1,1,0,0,0,0,0)(-\frac{3}{2},-\frac{1}{2},-\frac{1}{2},\frac{1}{2},\frac{1}{2},\frac{1}{2},\frac{1}{2},\frac{1}{2})$	$-\frac{1}{2}$	$E_6\times\mathrm{SU}(2)\times\mathrm{U}(1)\|\mathrm{SU}(7)\times\mathrm{U}(1)^2$
57	$(-1,-1,-1,0,0,0,0,1)(-\frac{1}{2},-\frac{1}{2},-\frac{1}{2},-\frac{1}{2},-\frac{1}{2},-\frac{1}{2},\frac{1}{2},\frac{1}{2})$	-1	$\mathrm{SO}(10)\times\mathrm{SU}(2)\times\mathrm{U}(1)^2\|\mathrm{SU}(7)\times\mathrm{U}(1)^2$
58	$(-1,-1,0,-1,0,0,0,1)(-1,0,0,0,0,0,1,0)$	-1	$\mathrm{SU}(6)\times\mathrm{SU}(2)\times\mathrm{U}(1)^2\|\mathrm{SO}(12)\times\mathrm{U}(1)^2$
59	$(-1,-1,0,-1,0,0,0,1)(0,-1,0,0,0,0,1,0)$	$-\frac{1}{2}$	$\mathrm{SU}(6)\times\mathrm{SU}(2)^2\times\mathrm{U}(1)\|\mathrm{SO}(10)\times\mathrm{SU}(2)^2\times\mathrm{U}(1)$
60	$(-1,0,0,-1,-1,0,0,1)(-\frac{1}{2},-\frac{1}{2},-\frac{1}{2},-\frac{1}{2},-\frac{1}{2},-\frac{1}{2},\frac{1}{2},\frac{1}{2})$	$-\frac{1}{2}$	$\mathrm{SU}(6)\times\mathrm{SU}(2)^2\times\mathrm{U}(1)\|\mathrm{SU}(7)\times\mathrm{U}(1)^2$
	$V_{4,f}$: $(2,1,1,0,0,0,0,0)(2,2,2,0,0,0,0,0)$		
61	$(0,0,0,0,0,0,0,0)(-\frac{1}{2},-\frac{1}{2},-\frac{1}{2},-\frac{1}{2},-\frac{1}{2},-\frac{1}{2},\frac{1}{2},\frac{1}{2})$	$-\frac{1}{2}$	$E_6\times\mathrm{SU}(2)\times\mathrm{U}(1)\|\mathrm{SU}(5)\times\mathrm{SU}(3)\times\mathrm{U}(1)^2$
62	$(-1,-1,0,0,0,0,0,0)(0,0,0,0,0,0,0,0)$	$-\frac{1}{2}$	$E_6\times\mathrm{U}(1)^2\|\mathrm{SO}(10)\times\mathrm{SU}(4)$
63	$(-1,-1,0,0,0,0,0,0)(0,0,0,0,0,-2,0,0)$	$-\frac{1}{2}$	$E_6\times\mathrm{U}(1)^2\|\mathrm{SO}(10)\times\mathrm{SU}(4)$
64	$(-1,-1,0,0,0,0,0,0)(-1,-1,-1,0,0,0,0,1)$	-2	$E_6\times\mathrm{U}(1)^2\|\mathrm{SO}(8)\times\mathrm{SU}(4)\times\mathrm{U}(1)$
65	$(-1,-1,0,0,0,0,0,0)(-1,-1,0,-1,0,0,0,1)$	$-\frac{3}{2}$	$E_6\times\mathrm{U}(1)^2\|\mathrm{SU}(4)\times\mathrm{SU}(2)^4\times\mathrm{U}(1)$
66	$(-1,0,0,0,0,0,1,0)(-\frac{3}{2},-\frac{1}{2},-\frac{1}{2},\frac{1}{2},\frac{1}{2},\frac{1}{2},\frac{1}{2},\frac{1}{2})$	$-\frac{3}{2}$	$\mathrm{SO}(10)\times\mathrm{SU}(2)\times\mathrm{U}(1)^2\|\mathrm{SU}(5)\times\mathrm{SU}(3)\times\mathrm{U}(1)^2$
67	$(-1,0,1,0,0,0,0,0)(0,0,0,0,0,0,0,0)$	0	$\mathrm{SO}(10)\times\mathrm{U}(1)^3\|\mathrm{SO}(10)\times\mathrm{SU}(4)$
68	$(-1,0,1,0,0,0,0,0)(0,0,0,0,0,-2,0,0)$	0	$\mathrm{SO}(10)\times\mathrm{U}(1)^3\|\mathrm{SO}(10)\times\mathrm{SU}(4)$
69	$(-1,0,1,0,0,0,0,0)(-1,-1,-1,0,0,0,0,1)$	$-\frac{3}{2}$	$\mathrm{SO}(10)\times\mathrm{U}(1)^3\|\mathrm{SO}(8)\times\mathrm{SU}(4)\times\mathrm{U}(1)$
70	$(-1,0,1,0,0,0,0,0)(-1,-1,0,-1,0,0,0,1)$	-1	$\mathrm{SO}(10)\times\mathrm{U}(1)^3\|\mathrm{SU}(4)\times\mathrm{SU}(2)^4\times\mathrm{U}(1)$
71	$(0,0,0,-1,0,0,1,0)(-\frac{3}{2},-\frac{1}{2},-\frac{1}{2},\frac{1}{2},\frac{1}{2},\frac{1}{2},\frac{1}{2},\frac{1}{2})$	-1	$\mathrm{SU}(6)\times\mathrm{SU}(2)^2\times\mathrm{U}(1)\|\mathrm{SU}(5)\times\mathrm{SU}(3)\times\mathrm{U}(1)^2$
72	$(0,-1,1,0,0,0,0,0)(-\frac{3}{2},-\frac{1}{2},-\frac{1}{2},\frac{1}{2},\frac{1}{2},\frac{1}{2},\frac{1}{2},\frac{1}{2})$	-1	$E_6\times\mathrm{SU}(2)\times\mathrm{U}(1)\|\mathrm{SU}(5)\times\mathrm{SU}(3)\times\mathrm{U}(1)^2$
73	$(-1,-1,-1,0,0,0,0,1)(-\frac{1}{2},-\frac{1}{2},-\frac{1}{2},-\frac{1}{2},-\frac{1}{2},-\frac{1}{2},\frac{1}{2},\frac{1}{2})$	$-\frac{3}{2}$	$\mathrm{SO}(10)\times\mathrm{SU}(2)\times\mathrm{U}(1)^2\|\mathrm{SU}(5)\times\mathrm{SU}(3)\times\mathrm{U}(1)^2$
74	$(-1,-1,0,-1,0,0,0,1)(-1,-1,0,0,0,0,0,0)$	$-\frac{3}{2}$	$\mathrm{SU}(6)\times\mathrm{SU}(2)\times\mathrm{U}(1)^2\|\mathrm{SO}(10)\times\mathrm{SU}(2)^2\times\mathrm{U}(1)$
75	$(-1,-1,0,-1,0,0,0,1)(-1,0,0,0,0,0,1,0)$	-1	$\mathrm{SU}(6)\times\mathrm{SU}(2)\times\mathrm{U}(1)^2\|\mathrm{SO}(8)\times\mathrm{SU}(2)^2\times\mathrm{U}(1)^2$
76	$(-1,-1,0,-1,0,0,0,1)(0,0,0,-1,0,0,1,0)$	$-\frac{1}{2}$	$\mathrm{SU}(6)\times\mathrm{SU}(2)\times\mathrm{U}(1)^2\|\mathrm{SU}(4)^2\times\mathrm{SU}(2)^2$
77	$(-1,0,0,-1,-1,0,0,1)(-\frac{1}{2},-\frac{1}{2},-\frac{1}{2},-\frac{1}{2},-\frac{1}{2},-\frac{1}{2},\frac{1}{2},\frac{1}{2})$	-1	$\mathrm{SU}(6)\times\mathrm{SU}(2)^2\times\mathrm{U}(1)\|\mathrm{SU}(5)\times\mathrm{SU}(3)\times\mathrm{U}(1)^2$

M #	$V_{4,f}$:$(4,0,0,0,0,0,0,0)(3,1,0,0,0,0,0,0)$	M	Gauge Group
78	$(0,0,0,0,0,0,0,0)(-1,0,0,0,0,0,1,0)$	$-\frac{1}{2}$	$SO(16)\|SO(10)\times U(1)^3$
79	$(0,0,0,0,0,0,0,0)(-\frac{1}{2},\frac{1}{2},-\frac{1}{2},-\frac{1}{2},-\frac{1}{2},-\frac{1}{2},-\frac{1}{2},\frac{1}{2})$	0	$SO(16)\|SU(6)\times SU(2)\times U(1)^2$
80	$(-1,0,0,0,0,0,1,0)(-\frac{3}{2},-\frac{1}{2},-\frac{1}{2},\frac{1}{2},\frac{1}{2},\frac{1}{2},\frac{1}{2},\frac{1}{2})$	-2	$SO(12)\times SU(2)^2\|SU(6)\times SU(2)\times U(1)^2$
81	$(-1,0,0,0,0,0,1,0)(-1,0,-1,-1,0,0,0,1)$	$-\frac{3}{2}$	$SO(12)\times SU(2)^2\|SU(4)^2\times U(1)^2$
82	$(-\frac{1}{2},-\frac{1}{2},-\frac{1}{2},-\frac{1}{2},-\frac{1}{2},-\frac{1}{2},\frac{1}{2},\frac{1}{2})(-\frac{3}{2},-\frac{1}{2},-\frac{1}{2},\frac{1}{2},\frac{1}{2},\frac{1}{2},\frac{1}{2},\frac{1}{2})$	$-\frac{3}{2}$	$SU(8)\times U(1)\|SU(6)\times SU(2)\times U(1)^2$
83	$(-\frac{1}{2},-\frac{1}{2},-\frac{1}{2},-\frac{1}{2},-\frac{1}{2},-\frac{1}{2},\frac{1}{2},\frac{1}{2})(-1,0,-1,-1,0,0,0,1)$	-1	$SU(8)\times U(1)\|SU(4)^2\times U(1)^2$
84	$(0,0,0,0,0,-2,0,0)(-1,0,0,0,0,0,1,0)$	$-\frac{1}{2}$	$SO(14)\times U(1)\|SO(10)\times U(1)^3$
85	$(0,0,0,0,0,-2,0,0)(-\frac{1}{2},\frac{1}{2},-\frac{1}{2},-\frac{1}{2},-\frac{1}{2},-\frac{1}{2},-\frac{1}{2},\frac{1}{2})$	0	$SO(14)\times U(1)\|SU(6)\times SU(2)\times U(1)^2$
86	$(-\frac{3}{2},-\frac{1}{2},-\frac{1}{2},\frac{1}{2},\frac{1}{2},\frac{1}{2},\frac{1}{2},\frac{1}{2})(-1,0,0,0,0,0,1,0)$	-2	$SU(7)\times U(1)^2\|SO(10)\times U(1)^3$
87	$(-\frac{3}{2},-\frac{1}{2},-\frac{1}{2},\frac{1}{2},\frac{1}{2},\frac{1}{2},\frac{1}{2},\frac{1}{2})(-\frac{1}{2},\frac{1}{2},-\frac{1}{2},-\frac{1}{2},-\frac{1}{2},-\frac{1}{2},-\frac{1}{2},\frac{1}{2})$	$-\frac{3}{2}$	$SU(7)\times U(1)^2\|SU(6)\times SU(2)\times U(1)^2$
88	$(-1,-1,-1,0,0,0,0,1)(-1,0,0,0,0,0,1,0)$	$-\frac{3}{2}$	$SO(8)\times SU(4)\times U(1)\|SO(10)\times U(1)^3$
89	$(-1,-1,-1,0,0,0,0,1)(-\frac{1}{2},\frac{1}{2},-\frac{1}{2},-\frac{1}{2},-\frac{1}{2},-\frac{1}{2},-\frac{1}{2},\frac{1}{2})$	-1	$SO(8)\times SU(4)\times U(1)\|SU(6)\times SU(2)\times U(1)^2$
	$V_{4,f}$: $(2,0,0,0,0,0,0,0)(3,1,1,1,1,1,0,0)$		
90	$(0,0,0,0,0,0,0,0)(-1,0,0,0,0,0,1,0)$	$-\frac{1}{2}$	$SO(14)\times U(1)\|SU(6)\times SU(2)\times U(1)^2$
91	$(-1,0,0,0,0,0,1,0)(-\frac{1}{2},-\frac{3}{2},\frac{1}{2},\frac{1}{2},\frac{1}{2},\frac{1}{2},-\frac{1}{2},\frac{1}{2})$	$-\frac{1}{2}$	$SO(12)\times U(1)^2\|SU(8)\times U(1)$
92	$(-1,0,0,0,0,0,1,0)(-1,-1,-1,0,0,0,0,1)$	$-\frac{3}{2}$	$SO(12)\times U(1)^2\|SU(4)^2\times U(1)^2$
93	$(-\frac{1}{2},-\frac{1}{2},-\frac{1}{2},-\frac{1}{2},-\frac{1}{2},-\frac{1}{2},\frac{1}{2},\frac{1}{2})(0,0,0,0,0,0,0,0)$	0	$SU(7)\times U(1)^2\|SU(8)\times SU(2)$
94	$(-\frac{1}{2},-\frac{1}{2},-\frac{1}{2},-\frac{1}{2},-\frac{1}{2},-\frac{1}{2},\frac{1}{2},\frac{1}{2})(-1,0,0,1,-1,1,0,0)$	$-\frac{1}{2}$	$SU(7)\times U(1)^2\|SU(6)\times SU(2)^2\times U(1)$
95	$(-\frac{1}{2},-\frac{1}{2},-\frac{1}{2},-\frac{1}{2},-\frac{1}{2},-\frac{1}{2},\frac{1}{2},\frac{1}{2})(0,-1,-1,0,0,0,-1,1)$	$-\frac{1}{2}$	$SU(7)\times U(1)^2\|SU(4)^2\times SU(2)\times U(1)$
96	$(0,-1,0,0,0,0,1,0)(-\frac{1}{2},-\frac{3}{2},\frac{1}{2},\frac{1}{2},\frac{1}{2},\frac{1}{2},-\frac{1}{2},\frac{1}{2})$	0	$SO(10)\times SU(2)^2\times U(1)\|SU(8)\times U(1)$
97	$(0,-1,0,0,0,0,1,0)(-1,-1,-1,0,0,0,0,1)$	-1	$SO(10)\times SU(2)^2\times U(1)\|SU(4)^2\times U(1)^2$
98	$(0,0,0,0,0,-2,0,0)(-1,0,0,0,0,0,1,0)$	$-\frac{1}{2}$	$SO(14)\times U(1)\|SU(6)\times SU(2)\times U(1)^2$
99	$(-\frac{3}{2},-\frac{1}{2},-\frac{1}{2},\frac{1}{2},\frac{1}{2},\frac{1}{2},\frac{1}{2},\frac{1}{2})(-1,-1,0,0,0,0,0,0)$	$-\frac{3}{2}$	$SU(7)\times U(1)^2\|SU(6)\times SU(2)^2\times U(1)$
100	$(-\frac{3}{2},-\frac{1}{2},-\frac{1}{2},\frac{1}{2},\frac{1}{2},\frac{1}{2},\frac{1}{2},\frac{1}{2})(0,-1,0,0,0,1,0,0)$	$-\frac{1}{2}$	$SU(7)\times U(1)^2\|SU(6)\times SU(2)\times U(1)^2$
101	$(-\frac{3}{2},-\frac{1}{2},-\frac{1}{2},\frac{1}{2},\frac{1}{2},\frac{1}{2},\frac{1}{2},\frac{1}{2})(0,0,0,0,0,0,-1,1)$	$-\frac{1}{2}$	$SU(7)\times U(1)^2\|SU(8)\times SU(2)$
102	$(-1,-1,-1,0,0,0,0,1)(-1,0,0,0,0,0,1,0)$	-1	$SO(8)\times SU(4)\times U(1)\|SU(6)\times SU(2)\times U(1)^2$
M #	$V_{4,f}$:$(3,1,0,0,0,0,0,0)(1,1,1,1,1,1,1,-1)$	M	Gauge Group
103	$(0,0,0,0,0,0,0,0)(-\frac{1}{2},-\frac{1}{2},-\frac{1}{2},-\frac{1}{2},-\frac{1}{2},-\frac{1}{2},\frac{1}{2},\frac{1}{2})$	$-\frac{1}{2}$	$SO(12)\times SU(2)\times U(1)\|SU(7)\times U(1)^2$
104	$(0,0,0,0,0,0,0,0)(-\frac{1}{2},-\frac{1}{2},-\frac{1}{2},-\frac{1}{2},\frac{1}{2},\frac{1}{2},\frac{1}{2},\frac{1}{2})$	0	$SO(12)\times SU(2)\times U(1)\|SU(5)\times SU(3)\times U(1)^2$
105	$(-1,-1,0,0,0,0,0,0)(-\frac{1}{2},\frac{1}{2},\frac{1}{2},\frac{1}{2},\frac{1}{2},-\frac{3}{2},\frac{1}{2},-\frac{1}{2})$	$-\frac{1}{2}$	$SO(12)\times SU(2)\times U(1)\|SU(7)\times U(1)^2$
106	$(-1,-1,0,0,0,0,0,0)(-\frac{1}{2},-\frac{1}{2},-\frac{1}{2},-\frac{1}{2},\frac{1}{2},-\frac{3}{2},\frac{1}{2},\frac{1}{2})$	$-\frac{3}{2}$	$SO(12)\times SU(2)\times U(1)\|SU(5)\times SU(3)\times U(1)^2$
107	$(-1,0,0,0,0,0,1,0)(0,0,0,0,0,0,0,0)$	$-\frac{1}{2}$	$SO(10)\times U(1)^3\|SU(8)\times U(1)$
108	$(-1,0,0,0,0,0,1,0)(0,0,0,0,0,-2,0,0)$	-1	$SO(10)\times U(1)^3\|SU(8)\times U(1)$
109	$(-1,0,0,0,0,0,1,0)(-1,-1,-1,0,0,0,0,1)$	$-\frac{3}{2}$	$SO(10)\times U(1)^3\|SU(4)^2\times U(1)^2$
110	$(-1,1,0,0,0,0,0,0)(-\frac{1}{2},\frac{1}{2},\frac{1}{2},\frac{1}{2},\frac{1}{2},-\frac{3}{2},\frac{1}{2},-\frac{1}{2})$	0	$SO(12)\times SU(2)\times U(1)\|SU(7)\times U(1)^2$
111	$(-1,1,0,0,0,0,0,0)(-\frac{1}{2},-\frac{1}{2},-\frac{1}{2},-\frac{1}{2},\frac{1}{2},-\frac{3}{2},\frac{1}{2},\frac{1}{2})$	-1	$SO(12)\times SU(2)\times U(1)\|SU(5)\times SU(3)\times U(1)^2$
112	$(-\frac{1}{2},-\frac{1}{2},-\frac{1}{2},-\frac{1}{2},-\frac{1}{2},-\frac{1}{2},\frac{1}{2},\frac{1}{2})(-\frac{1}{2},\frac{1}{2},\frac{1}{2},\frac{1}{2},\frac{1}{2},-\frac{3}{2},\frac{1}{2},-\frac{1}{2})$	0	$SU(6)\times U(1)^3\|SU(7)\times U(1)^2$
113	$(-\frac{1}{2},-\frac{1}{2},-\frac{1}{2},-\frac{1}{2},-\frac{1}{2},-\frac{1}{2},\frac{1}{2},\frac{1}{2})(-\frac{1}{2},-\frac{1}{2},-\frac{1}{2},-\frac{1}{2},\frac{1}{2},-\frac{3}{2},\frac{1}{2},\frac{1}{2})$	-1	$SU(6)\times U(1)^3\|SU(5)\times SU(3)\times U(1)^2$
114	$(-\frac{1}{2},\frac{1}{2},-\frac{1}{2},-\frac{1}{2},-\frac{1}{2},-\frac{1}{2},-\frac{1}{2},\frac{1}{2})(0,0,0,0,0,0,0,0)$	0	$SU(6)\times SU(2)\times U(1)^2\|SU(8)\times U(1)$
115	$(-\frac{1}{2},\frac{1}{2},-\frac{1}{2},-\frac{1}{2},-\frac{1}{2},-\frac{1}{2},-\frac{1}{2},\frac{1}{2})(0,0,0,0,0,-2,0,0)$	$-\frac{1}{2}$	$SU(6)\times SU(2)\times U(1)^2\|SU(8)\times U(1)$
116	$(-\frac{1}{2},\frac{1}{2},-\frac{1}{2},-\frac{1}{2},-\frac{1}{2},-\frac{1}{2},-\frac{1}{2},\frac{1}{2})(-1,-1,-1,0,0,0,0,1)$	-1	$SU(6)\times SU(2)\times U(1)^2\|SU(4)^2\times U(1)^2$
117	$(0,0,-1,0,0,0,1,0)(-\frac{1}{2},\frac{1}{2},\frac{1}{2},\frac{1}{2},\frac{1}{2},-\frac{3}{2},\frac{1}{2},-\frac{1}{2})$	$\frac{1}{2}$	$SO(8)\times SU(2)^3\times U(1)\|SU(7)\times U(1)^2$
118	$(0,0,-1,0,0,0,1,0)(-\frac{1}{2},-\frac{1}{2},-\frac{1}{2},-\frac{1}{2},\frac{1}{2},-\frac{3}{2},\frac{1}{2},\frac{1}{2})$	$-\frac{1}{2}$	$SO(8)\times SU(2)^3\times U(1)\|SU(5)\times SU(3)\times U(1)^2$
119	$(0,0,0,0,0,-2,0,0)(-\frac{1}{2},-\frac{1}{2},-\frac{1}{2},-\frac{1}{2},-\frac{1}{2},-\frac{1}{2},\frac{1}{2},\frac{1}{2})$	$-\frac{1}{2}$	$SO(12)\times SU(2)\times U(1)\|SU(7)\times U(1)^2$
120	$(0,0,0,0,0,-2,0,0)(-\frac{1}{2},-\frac{1}{2},-\frac{1}{2},-\frac{1}{2},\frac{1}{2},\frac{1}{2},\frac{1}{2},\frac{1}{2})$	0	$SO(12)\times SU(2)\times U(1)\|SU(5)\times SU(3)\times U(1)^2$
121	$(-\frac{3}{2},-\frac{1}{2},-\frac{1}{2},\frac{1}{2},\frac{1}{2},\frac{1}{2},\frac{1}{2},\frac{1}{2})(0,0,0,0,-1,-1,0,0)$	$-\frac{3}{2}$	$SU(6)\times SU(2)\times U(1)^2\|SU(6)\times SU(2)\times U(1)^2$
122	$(-\frac{3}{2},-\frac{1}{2},-\frac{1}{2},\frac{1}{2},\frac{1}{2},\frac{1}{2},\frac{1}{2},\frac{1}{2})(-1,0,0,0,0,0,1,0)$	-1	$SU(6)\times SU(2)\times U(1)^2\|SU(6)\times SU(2)\times U(1)^2$
123	$(-\frac{3}{2},\frac{1}{2},-\frac{1}{2},-\frac{1}{2},\frac{1}{2},\frac{1}{2},\frac{1}{2},\frac{1}{2})(-\frac{1}{2},-\frac{1}{2},-\frac{1}{2},-\frac{1}{2},-\frac{1}{2},-\frac{1}{2},\frac{1}{2},\frac{1}{2})$	$-\frac{3}{2}$	$SU(6)\times U(1)^3\|SU(7)\times U(1)^2$
124	$(-\frac{3}{2},\frac{1}{2},-\frac{1}{2},-\frac{1}{2},\frac{1}{2},\frac{1}{2},\frac{1}{2},\frac{1}{2})(-\frac{1}{2},-\frac{1}{2},-\frac{1}{2},-\frac{1}{2},\frac{1}{2},\frac{1}{2},\frac{1}{2},\frac{1}{2})$	-1	$SU(6)\times U(1)^3\|SU(5)\times SU(3)\times U(1)^2$
125	$(-1,-1,-1,0,0,0,0,1)(-\frac{1}{2},-\frac{1}{2},-\frac{1}{2},-\frac{1}{2},-\frac{1}{2},-\frac{1}{2},\frac{1}{2},\frac{1}{2})$	$-\frac{3}{2}$	$SO(8)\times SU(2)^3\times U(1)\|SU(7)\times U(1)^2$
126	$(-1,-1,-1,0,0,0,0,1)(-\frac{1}{2},-\frac{1}{2},-\frac{1}{2},-\frac{1}{2},\frac{1}{2},\frac{1}{2},\frac{1}{2},\frac{1}{2})$	-1	$SO(8)\times SU(2)^3\times U(1)\|SU(5)\times SU(3)\times U(1)^2$
127	$(-1,0,-1,-1,0,0,0,1)(0,0,0,0,-1,-1,0,0)$	-1	$SU(4)^2\times U(1)^2\|SU(6)\times SU(2)\times U(1)^2$
128	$(-1,0,-1,-1,0,0,0,1)(-1,0,0,0,0,0,1,0)$	$-\frac{1}{2}$	$SU(4)^2\times U(1)^2\|SU(6)\times SU(2)\times U(1)^2$

M #	$V_{4,f}$: $(2,2,2,0,0,0,0,0)(3,1,1,1,1,1,0,0)$	M	Gauge Group
129	$(0,0,0,0,0,0,0,0)(-1,0,0,0,0,0,1,0)$	$-\frac{1}{2}$	SO(10)×SU(4)|SU(6)×SU(2)×U(1)^2
130	$(-1,-1,0,0,0,0,0,0)(-\frac{1}{2},-\frac{3}{2},\frac{1}{2},\frac{1}{2},\frac{1}{2},\frac{1}{2},-\frac{1}{2},\frac{1}{2})$	-1	SO(10)×SU(2)^2×U(1)|SU(8)×U(1)
131	$(-1,-1,0,0,0,0,0,0)(-1,-1,-1,0,0,0,0,1)$	-2	SO(10)×SU(2)^2×U(1)|SU(4)^2×U(1)^2
132	$(-1,0,0,0,0,0,1,0)(-\frac{1}{2},-\frac{3}{2},\frac{1}{2},\frac{1}{2},\frac{1}{2},\frac{1}{2},-\frac{1}{2},\frac{1}{2})$	$-\frac{1}{2}$	SO(8)×SU(2)^2×U(1)^2|SU(8)×U(1)
133	$(-1,0,0,0,0,0,1,0)(-1,-1,-1,0,0,0,0,1)$	$-\frac{3}{2}$	SO(8)×SU(2)^2×U(1)^2|SU(4)^2×U(1)^2
134	$(-\frac{1}{2},-\frac{1}{2},-\frac{1}{2},-\frac{1}{2},-\frac{1}{2},-\frac{1}{2},\frac{1}{2},\frac{1}{2})(0,0,0,0,0,0,0,0)$	$-\frac{1}{2}$	SU(5)×SU(3)×U(1)^2|SU(8)×SU(2)
135	$(-\frac{1}{2},-\frac{1}{2},-\frac{1}{2},-\frac{1}{2},-\frac{1}{2},-\frac{1}{2},\frac{1}{2},\frac{1}{2})(-1,0,0,1,-1,1,0,0)$	-1	SU(5)×SU(3)×U(1)^2|SU(8)×SU(2)
136	$(-\frac{1}{2},-\frac{1}{2},-\frac{1}{2},-\frac{1}{2},-\frac{1}{2},-\frac{1}{2},\frac{1}{2},\frac{1}{2})(0,-1,-1,0,0,0,-1,1)$	-1	SU(5)×SU(3)×U(1)^2|SU(4)^2×SU(2)×U(1)
137	$(0,0,0,-1,0,0,1,0)(-\frac{1}{2},-\frac{3}{2},\frac{1}{2},\frac{1}{2},\frac{1}{2},\frac{1}{2},-\frac{1}{2},\frac{1}{2})$	0	SU(4)^2×SU(2)^2|SU(8)×U(1)
138	$(0,0,0,-1,0,0,1,0)(-1,-1,-1,0,0,0,0,1)$	-1	SU(4)^2×SU(2)^2|SU(4)^2×U(1)^2
139	$(0,0,0,0,0,-2,0,0)(-1,0,0,0,0,0,1,0)$	$-\frac{1}{2}$	SO(10)×SU(4)|SU(6)×SU(2)×U(1)^2
140	$(-\frac{3}{2},-\frac{1}{2},-\frac{1}{2},\frac{1}{2},\frac{1}{2},\frac{1}{2},\frac{1}{2},\frac{1}{2})(-1,-1,0,0,0,0,0,0)$	-2	SU(5)×SU(3)×U(1)^2|SU(6)×SU(2)^2×U(1)
141	$(-\frac{3}{2},-\frac{1}{2},-\frac{1}{2},\frac{1}{2},\frac{1}{2},\frac{1}{2},\frac{1}{2},\frac{1}{2})(-1,0,0,0,0,1,0,0)$	$-\frac{3}{2}$	SU(5)×SU(3)×U(1)^2|SU(4)^2×SU(2)×U(1)
142	$(-\frac{3}{2},-\frac{1}{2},-\frac{1}{2},\frac{1}{2},\frac{1}{2},\frac{1}{2},\frac{1}{2},\frac{1}{2})(0,0,0,0,0,0,-1,1)$	-1	SU(5)×SU(3)×U(1)^2|SU(8)×SU(2)
143	$(-1,-1,-1,0,0,0,0,1)(-1,0,0,0,0,0,1,0)$	-2	SO(8)×SU(4)×U(1)|SU(6)×SU(2)×U(1)^2
144	$(-1,-1,0,-1,0,0,0,1)(-1,0,0,0,0,0,1,0)$	$-\frac{3}{2}$	SU(4)×SU(2)^4×U(1)|SU(6)×SU(2)×U(1)^2

Table D.3: The 144 models that have the chance of being modular invariant by adding a lattice vector such that the mismatch $M = 2(V_2 \cdot V_4 - v_2 \cdot v_4)$ is exactly 0 mod 2. M is shown in the third column. The first column gives the model number while the second gives the compatible V_2 shift vector to $V_{4,f}$ which is always given in the first line of each subtable. Note that the shifts are multiplied by their order!

Bibliography

[1] K. Becker, M. Becker, J. H. Schwarz, "String theory and M-theory: A modern introduction," Cambridge, UK: Cambridge Univ. Pr. (2007) 739 p.

[2] D. Lust, S. Theisen, Lect. Notes Phys. **346** (1989) 1-346.

[3] F. Ploger, S. Ramos-Sanchez, M. Ratz and P. K. S. Vaudrevange, "Mirage Torsion," JHEP **0704** (2007) 063 [arXiv:hep-th/0702176].

[4] N. Jacobson, "Lie Algebras". Wiley Interscience, New York, London, 1962.

[5] O. Lebedev, H. P. Nilles, S. Raby, S. Ramos-Sanchez, M. Ratz, P. K. S. Vaudrevange, A. Wingerter, "A Mini-landscape of exact MSSM spectra in heterotic orbifolds," Phys. Lett. **B645** (2007) 88-94. [hep-th/0611095].

[6] O. Lebedev, H. P. Nilles, S. Ramos-Sanchez, M. Ratz, P. K. S. Vaudrevange, "Heterotic mini-landscape. (II). Completing the search for MSSM vacua in a Z(6) orbifold," Phys. Lett. **B668** (2008) 331-335. [arXiv:0807.4384 [hep-th]].

[7] A. Wingerter, "Aspects of Grand Unification in Higher Dimensions," JHEP **0704** (2007) 063 (http://thp.uni-bonn.de/nilles/)

[8] L. J. Dixon, J. A. Harvey, C. Vafa, E. Witten, "Strings on Orbifolds," Nucl. Phys. **B261** (1985) 678-686.

[9] L. J. Dixon, J. A. Harvey, C. Vafa, E. Witten, "Strings on Orbifolds. 2.," Nucl. Phys. **B274** (1986) 285-314.

[10] L. E. Ibanez, H. P. Nilles, F. Quevedo, "Orbifolds and Wilson Lines," Phys. Lett. **B187** (1987) 25-32.

[11] K. -j. Takahashi, "Heterotic orbifold models on Lie lattice with discrete torsion," JHEP **0703** (2007) 103. [hep-th/0702025].

[12] Y. Katsuki, Y. Kawamura, T. Kobayashi, Y. Ono, K. Tanioka. N. Ohtsubo, "Z4 and Z6 orbifold models," Phys. Lett. **B218** (1989) 169-175.

[13] D. K. M. Peña, "Master Thesis: Towards realsitic spectra in $\mathbb{Z}_2 \times \mathbb{Z}_4$ orbifold models ," (2011) (http://thp.uni-bonn.de/nilles/).

[14] P. K. S. Vaudrevange, “Geometrical Aspects of Heterotic Orbifolds,”

[15] M. Blaszczyk, S. G. Nibbelink, M. Ratz, F. Ruehle, M. Trapletti and P. K. S. Vaudrevange, “A Z2xZ2 standard model,” Phys. Lett. B **683** (2010) 340 [arXiv:0911.4905 [hep-th]].

[16] H. M. Lee, S. Raby, M. Ratz, G. G. Ross, R. Schieren, K. Schmidt-Hoberg and P. K. S. Vaudrevange, “A unique $\mathbb{Z}_4^R$ symmetry for the MSSM,” Phys. Lett. B **694** (2011) 491 [arXiv:1009.0905 [hep-ph]].

[17] H. M. Lee, S. Raby, M. Ratz, G. G. Ross, R. Schieren, K. Schmidt-Hoberg and P. K. S. Vaudrevange, “Discrete R symmetries for the MSSM and its singlet extensions,” Nucl. Phys. B **850** (2011) 1 [arXiv:1102.3595 [hep-ph]].

[18] K. Nakamura et al. (Particle Data Group), J. Phys. G 37, 075021 (2010)

[19] S. Dimopoulos, S. Raby and F. Wilczek, “Supersymmetry And The Scale Of Unification,” Phys. Rev. D **24** (1981) 1681.

[20] H. P. Nilles, “Supersymmetry, Supergravity and Particle Physics,” Phys. Rept. **110**, 1-162 (1984).

[21] M. B. Green, J. H. Schwarz, E. Witten, “Superstring Theory. Vol. 1: Introduction,” Cambridge, Uk: Univ. Pr. (1987) 469 P. (Cambridge Monographs On Mathematical Physics).

[22] R. Slansky, “Group Theory for Unified Model Building,” Phys. Rept. **79** (1981) 1-128.

[23] J. Polchinski, “String theory. Vol. 2: Superstring theory and beyond,” *Cambridge, UK: Univ. Pr. (1998) 531 p*

[24] B. R. Greene, “String theory on Calabi-Yau manifolds,” [hep-th/9702155].

[25] J. Erler, A. Klemm, “Comment on the generation number in orbifold compactifications,” Commun. Math. Phys. **153** (1993) 579-604. [hep-th/9207111].

[26] S. G. Nibbelink, D. Klevers, F. Ploger, M. Trapletti, P. K. S. Vaudrevange, “Compact heterotic orbifolds in blow-up,” JHEP **0804** (2008) 060. [arXiv:0802.2809 [hep-th]].

[27] M. Blaszczyk, S. G. Nibbelink, F. Ruehle, M. Trapletti, P. K. S. Vaudrevange, “Heterotic MSSM on a Resolved Orbifold,” JHEP **1009** (2010) 065. [arXiv:1007.0203 [hep-th]].

[28] K. -S. Choi, J. E. Kim, “Quarks and leptons from orbifolded superstring,”

[29] J. H. Conway, R. T. Curtis, S. P. Norton, R. A. Parker, R. A. Wilson, “Atlas of finite groups,” Clarendon Press, Oxford 1985.

[30] T. Kobayashi, S. L. Parameswaran, S. Ramos-Sanchez, I. Zavala, "Revisiting Coupling Selection Rules in Heterotic Orbifold Models," [arXiv:1107.2137 [hep-th]].

[31] P. K. S. Vaudrevange,"Diploma Thesis: Geometrical Aspects of Heterotic Orbifolds,"(2004)

[32] Y. Katsuki, Y. Kawamura, T. Kobayashi, N. Ohtsubo, Y. Ono, K. Tanioka, "Tables Of Z(n) Orbifold Models,"

[33] M. Dine, N. Seiberg, E. Witten, "Fayet-Iliopoulos Terms in String Theory," Nucl. Phys. **B289** (1987) 589.

I hereby certify that the work presented here was accomplished by myself and without the use of illegitimate means or support, and that no sources and tools were used other than those cited.

Bonn, ____________________ Date

____________________ Signature